The Lectin Pathway of Complement Activation in Cerebral Ischaemia and Reperfusion Injury

Thesis submitted for the degree of Doctor of Philosophy

at the University of Leicester

by

Elvina Chrysanthou

Medical Research Council, Toxicology Unit

and

Department of Infection, Immunity and Inflammation

University of Leicester

2013

Statement of originality

This accompanying thesis submitted for the degree of PhD entitled "The lectin pathway of complement activation in cerebral ischaemia and reperfusion injury" is based on work conducted by the author at the University of Leicester mainly during the period between September 2008 and March 2013.

All the work recorded in this thesis is original unless otherwise acknowledged in the text or by references.

None of the work has been submitted for another degree in this or any other university.

Signed: Date:

The lectin pathway of complement activation in cerebral ischaemia

and reperfusion injury.

Elvina Chrysanthou

Abstract

The complement system constitutes a critical component of the innate immune response. The lectin pathway is one of the three activation pathways of the complement activation cascade that can recognise and respond to structures on oxygen deprived cells and contribute to ischaemia and reperfusion injury (IRI). Cerebral IRI mediated inflammation is known to be responsible for secondary damage in the penumbra region surrounding the initial area of infarct and the prevention of IRI-mediated secondary damage provides an attractive target for therapeutic intervention. Mannose binding lectin associated serine protease 2 (MASP-2) is the key effector enzyme of the lectin pathway, since depletion of this enzyme completely ablates lectin pathway function or activity. This study assessed the impact of MASP-2 deficiency on cerebral IRI and to what extent MASP-2 targeting can reduce the secondary inflammatory damage following an ischaemic insult.

The 3 vessel occlusion (3-VO) model of stroke was found to be the most appropriate model to use in this study, as it was shown to have a lower degree of variability than the middle cerebral artery occlusion (MCAO) stroke model. TTC staining revealed that MASP-2 -/- mice were significantly protected from cerebral damage, showing statistically significant smaller infarct sizes when compared to age and sex matched wild type controls. MASP-2 deficient mice showed reduced C3 deposition and a lower degree of astrocytic activation in brain sections from mice undergoing 3-VO and showed higher mRNA abundance of anti-inflammatory mediators (such as IL-10) and lower abundance of pro-inflammatory mediators (such as MIP-2) when compared to wild type control mice.

Subsequently, a recombinant inhibitory anti-MASP-2 antibody, AbD04211, a murine specific MASP-2 inhibitor, was assessed for the therapeutic utility of MASP-2 inhibition in the 3-VO cerebral IRI model of stroke. The results revealed that the use of MASP-2 inhibitors at a dose of 5mg/kg of body weight achieved a statistically significant protective effect, with infarct sizes reduced by up to 30% in the anti-MASP-2 treated animals.

Acknowledgements

Firstly I would like to give my sincere thanks to my supervisor Dr Dr Wilhelm Schwaeble and Prof Pierluigi Nicotera for giving me the opportunity to carry out this research journey. I would like to express my very great appreciation and gratitude especially to Wilhelm for his valuable expert guidance, support and encouragement during these years. His enthusiastic approach and excitement towards science has been positively pushing me to do better. The inspiration from my second supervisor, Dr Edward Bampton could not be missing. His constant smile, patience and understanding in the ups and downs faced in this project, have really kept me going and I cannot really thank you enough. This thesis could not have been possible without your great scientific guidance and training especially in performing the 3-Vessel Occlusion stroke model and immunohistochemistry. I feel blessed that I had two great supervisors keeping me motivated and having my back whenever needed.

I am particularly grateful for the assistance given by Dr Claire Gibson who kindly showed me the MCAO stroke model and allowed me to use her equipment in surgeries. I would like to thank David Read for his help in imaging and microscopy, Dr Lucia Pinon for guiding me in the perfusions and fixations and Jenny Edwards for guidance in cryostat sectioning. I must also thank all past and present members of the 231 lab, namely, Azam, Kashif, Anna, Bayad, Sadam, Ahmed, Samy, Ameen, Saleh, Ali, Mutaib and especial thanks and gratitude to Youssif, Hany and Nick for guiding and assisting me patiently whenever I needed them. Your friendly created atmosphere surely supported me daily. Asha, Dalbir and Chris thanks for being around.

Thanks to Medical Research Council for funding my PhD and OMEROS Corporation (Seatle) for their MASP-2 inhibitory antibody supplies.

I was lucky enough to have great friends who kept me sane throughout this period. George, Christiana, Panayiotis and Elena thank you for this. Last but not least I would deeply like to thank and express my love towards my beloved parents, my brother Andreas, my sister Maria, my dearest friends Eleni, Nektaria, Sofia and Clio and my unique cousins Iphigenia, Natasa and Anna who have always been supporting me with their love, patience and a kind ear to listen.

Table of Contents

Table of Figures

Table of Tables

List of Abbreviations

3-VO	3 Vessel Occlusion
aHUS	atypical Haemolytic Uraemic Syndrome
AMD	Age Macular Degeneration
AMPA	α-amino-3-hydroxy-5-methyl-4isoxazole propionic acid
AP	Alternative Pathway
APC	Antigen Presenting Cell
ATP	Adenosine Triphosphate
BBB	Blood Brain Barrier
BBS	Barbital Buffer Saline
BSA	Bovine Serum Albumin
C1 INH	C1 Inhibitor
C4BP	C4-binding Protein
CBF	Cerebral Blood Flow
CCA	Common Carotid Artery
CCP	Complement Control Protein
CL-11	Collectin-11
CP	Classical Pathway
CPN	Carboxypeptidase N
CR	Complement Receptor
CRD	Carbohydrate Recognition Domain
CT	Computer Tomography
CUB	Complement C1r/C1s, Uegf and Bone morphogenic protein 1
DAF	Decay Accelerating Factor
ECA	External Carotid Artery
EGF	Epidermal Growth Factor-like domain
GFAP	Glial Fibrillary Acidic Protein
HIF-1	Hypoxia Transcription Factor 1
Iba1	Ionised Calcium Adaptor Molecule 1
ICA	Internal Carotid Artery
ICAM	Intercellular Adhesion Molecule
Ig	Immunoglobulin

IL-10	Interleukin 10
IRI	Ischaemia Reperfusion Injury
LEA	Lectin Effector Arm
LP	Lectin Pathway
mAb	Monoclonal Antibody
MAC	Membrane Attack Complex
MAdCAM	Mucosal Addressin
MASP	Mannose Binding Lectin Associated Serine Protease
MBL	Mannose Binding Lectin
MCAO	Middle Cerebral Artery Occlusion
MCP	Membrane Co-factor Protein
MIP-2	Macrophage Inflammatory Protein 2
MMP	Matrix Metalloproteinase
MRI	Magnetic Resonance Imaging
NMDA	N-methyl-D-aspartic Acid
NMHC-II	Non-muscle Myosin H Chain type II
NO	Nitric Oxide
PAMPs	Pathogen Associated Molecular Patterns
PBS	Phosphate Buffer Saline
PcomA	Posterior Communicating Artery
PCR	Polymerase Chain Reaction
PECAM	Platelet Endothelial Cell Adhesion Molecule
PNH	Paroxysmal Nocturnal Haemoglobinuria
rhMBL	Recombinant Human MBL
ROS	Reactive Oxygen Species
rTPA	Recombinant Tissue Plasminogen Activator
SCR	Short Complement Regulator
sCR1	Soluble Complement Receptor 1
SEM	Standard Error of the Mean
TBS	Tris Buffer Saline
TIA	Transient Ischaemic Attack
TNF-α	Tumour Necrosis Factor α
TTC	2, 3, 5- Triphenyltetrazolium Chloride
VCAM	Vascular Cell Adhesion Molecule

Chapter 1: Introduction

> "Men ought to know that from nothing else but the brain come joys, delights, laughter and sports, and sorrows, griefs, despondency, and lamentations. And by this, in an especial manner, we acquire wisdom and knowledge, and see and hear, and know what are foul and what are fair, what are bad and what are good, what are sweet, and what unsavoury... By this we distinguish objects of relish and disrelish... And by the same organ we become mad and delirious... In these ways I am of the opinion that the brain exercises the greatest power in the man"

Using the words of the "father of medicine" Hippocrates on 400 BC, in 'On the Sacred Disease', the importance of a healthy brain in our entire being is emphasised. Hence, any mental disorder, traumatic brain injury, neurodegenerative disorders or the sudden event of stroke which can irrevocably alter the behaviour, skills and abilities of the person, deserve especial attention in the search for therapies which can promote a better recovery.

1.1 Stroke

Stroke, resulting in brain damage following an ischaemic insult, is the second leading cause of death leaving surviving patients with subsequent variable disabilities worldwide (Murray & Lopez 1997, Donnan *et al.* 2008, Brouns & De Deyn 2009). Hypertension is the main cause leading to a stroke incident, with obesity, atherosclerosis and old age as critical risk factors. People who develop the following symptoms are usually experiencing a stroke incident (Longmore *et al.* 2010):

- The face, and particularly the eye or mouth may have dropped unilaterally and the patient is unable to smile.
- The person may develop dysphasia (impairment in communication) or may not be able to speak at all or his/her speech may be slurred or garbled.
- The arms may appear to be weak or numb preventing the person from lifting them or develop hemiplegia.

There are two types of stroke, an ischaemic stroke (also called white stroke) following a thrombotic or an embolic (occlusion of a cerebral vessel by settlement of a thrombus that was formed in a different origin) occlusion of a cerebral vessel and the haemorrhagic stroke. Haemorrhagic strokes, including perimesencephalic and subarachnoid haemorrhage, are usually caused by hypertension and the subsequent rupture and bleeding of blood vessels (Donnan *et al.* 2008). Transient ischaemic attack (TIA) is considered to be a milder form of an ischaemic stroke, as the occluding event lasts from minutes up to an hour and the symptoms resolve within 24 hours. A real diagnostic distinction between the different types of stroke following an event is critical for the treatment. This is why patients presenting with stroke symptoms go through

computer tomography (CT) scans or magnetic resonance imaging (MRI) scans. Ischaemic strokes comprise the majority of stroke incidences, while haemorrhagic strokes account for only 10% of the clinical cases. However, the focus of this project is ischaemic stroke. This results in exposing the occluded cerebral area to oxygen and glucose deprivation in a gradient like format, depending on site of the clot infarction. To describe tissue oxygen and glucose deprivation, the term ischaemia will be used while for correct blood supply the term perfusion will be used; where blood supply returns following ischaemia, the terms used will be reperfusion. Ischaemia itself is a highly stressful condition for the cells; however, subsequent reperfusion may contribute to severe inflammatory conditions, leading to significant tissue injury described by the term ischaemia and reperfusion injury (IRI). The events following ischaemia and reperfusion in stroke will be discussed in more detail to examine our current understanding of the pathology of the disease.

In general, ischaemia and reperfusion cause a series of intracellular and extracellular alterations that will be discussed in more detail later. Alterations in cell membrane morphology following ischaemia are recognised by the immune system and lead to secondary tissue damage (Zhang *et al.* 2006) and a main contributor to this secondary damage is the complement system (Gorsuch *et al.* 2012). In terms of intracellular alterations mitochondrial dysfunction, generation of reactive oxygen species and upregulation of hypoxia transcription factors have crucial roles in promoting tissue damage (Zhang *et al.* 2006). Hypoxia inducible factor 1 (HIF-1) is one of the main oxygen regulated hypoxia transcription factors that regulates hypoxia inducible genes. In acute cerebral ischaemia, HIF-1α is thought to mediate apoptosis and brain damage and its inhibition by siRNA is neuroprotective (Chen *et al.* 2009). However, the role of

HIF-1 is dependent upon the severity and duration of ischaemia, whereby it can have either pro-apoptotic or pro-survival functions (Halterman & Federoff 1999). This is a limiting factor in using HIF-1 as a target for therapeutics and a therapeutic approach which focuses on restraining secondary damage caused by the complement system could be a promising alternative.

1.2 Immune system and inflammation overview

As this thesis is focused on tissue damage following an ischaemic stroke from an immunological point of view a brief overview of the immune system is introduced here. The immune system is the powerful multifunctional defence system in an organism that, upon identification of a foreign antigen or abnormal host cell phenotype (i.e. tumour or an ischaemic cell) which would potentially be harmful to the organism, becomes activated and initiates a series of biological processes to eliminate the initial cause of activation. As a result of this activation, the "battlefield" of action of the immune system is characterised by inflammation which has the characteristic signs of redness, warmness and swelling. These characteristics are due to the increase in blood flow, activation of the complement system and the subsequent recruitment and action of immune cells at the site of need. In general, inflammation is necessary for the elimination and clearance of invading microorganisms; therefore immunodeficiency leads to pathological conditions where the immune system is unable to clear infection. Furthermore, uncontrolled or excessive activation of the immune system also leads to a pathological condition called autoimmunity whereby the immune system leads to uncontrolled self cell damage.

The immune action is characterised by the innate and adaptive (or acquired) immune response that are each mediated by interactive humoral and cell-mediated responses. The cell mediated responses are the responses of the immune system that involve the recruitment and activation of different types of white blood cells (or leukocytes) depending on the progression of inflammation. The humoral responses involve all the other characteristic mediators in an immune response, from chemical involvement of cytokines, chemokines, anaphylatoxins and complement proteins to physical barriers like low pH in the stomach.

The innate immune response is the first line of defence. In contrast to the adaptive immune response, the innate immune response lacks any immunological memory such as the generation of antibodies which is mounting a response to a previously exposed antigen. Invading microorganisms pass through several stages of defence mechanisms until they are eliminated. The first innate defence comes from physical barriers like the skin, mucus membranes or low pH in the stomach. Once an invading microorganism overcomes these barriers and enters the body the innate immune response is triggered. Its specificity its lower compared to the adaptive immune response, but essential for the limitation of an infection while being selective enough to discriminate self from non-self cells. The main cellular players in the innate immune response are phagocytes like neutrophils and macrophages (Silva 2009). The recruitment of these cells at the site of inflammation facilitates the clearance of opsonised pathogenic bacteria, dead cells and cellular debris by phagocytosis (Fleischmann *et al.* 1986, Hochreiter-Hufford & Ravichandran 2013). In addition, activated neutrophils and macrophages are capable of producing reactive oxygen species (ROS), secrete cytokines and chemokines (i.e. IL-6, IL-1, TNF-α) as well as being recruited by them (Gosset *et al.* 1999) and produce

proteases (Pham 2006) important in mediating and promoting inflammation. It should be taken into consideration, however, that excess inflammation in some cases (which is promoted by infiltration of leukocytes (as in the case of stroke)) could lead to further tissue damage. Within all this, the complement system is a vital component of the innate immune response as it recognises foreign material and initiates general inflammatory reactions via the activation of the complement cascades and in addition forms a critical link with the adaptive immune response. The complement system and its role in inflammation will be described in more detail later. The main cellular entities of the adaptive immune response are the B and T cells (cytotoxic T cells, helper T cells, memory T cells and regulatory T cells). Upon antigen presentation on antigen presenting cells (macrophages, dendritic cells, B cells) via MHC class II molecules, T helper cells and B cells get activated. B cells are activated and differentiate into plasma cells to produce antigen specific antibodies that target pathogenic cells, while T cells, among their other functions, secrete several chemokines (i.e. TNF-α and interleukins) that attract other immune cells to the site of infection.

1.3 Events in cerebral ischaemia and reperfusion injury (Ischaemic stroke)

As mentioned above, when a blood vessel is occluded, oxygen deprivation occurs in a gradient like manner, having the cells that are exposed less to hypoxia, being at a more distant location (from the origin of the thrombus obstruction point). This leads to the generation of the core which is comprised by cells irreversibly dying by necrosis and the penumbra region in the brain which is likely the apoptotic salvageable area. The core is typically characterised by cells irreversibly dying as a result of necrosis while

the penumbra is comprised by salvageable tissue In the centre of hypoxia, where blood flow is severely occluded (blood flow less than 25%), the cells are irreversibly stressed and are driven into necrosis, mainly due to total cellular bioenergetic failure and proteolysis (Brouns & De Deyn 2009, Paciaroni *et al.* 2009). Surrounding cells are also affected leading to irreversible cell damage. The formation of this cellular necrotic region after acute ischaemic stroke characterises the core. Cells around the core form the penumbra region. This area comprises cells that are also affected by ischaemia, thereby having reduced physiological and metabolic function, but that are not irreversibly damaged, possibly due to blood supply coming from collateral circulation. However, over the period of time this will not be sufficient to maintain cellular survival, especially neuronal survival, due to the high demand of glucose consumption in the brain and insufficient levels of oxygen for ATP production, leading to extensive brain damage. When the ischaemic episode is shortened or inhibition of the ongoing ischaemic events following ischaemia takes place, the cells can recover and escape necrosis and apoptosis (Brouns & De Deyn 2009, Paciaroni *et al.* 2009). Thus the major therapeutic strategy is to try to support the recovery of penumbra cells in order to reduce brain damage after stroke.

The events following ischaemia that lead to tissue damage are cellular bioenergetic failure, excitotoxicity, oxidative stress, blood-brain barrier (BBB) dysfunction, ischaemia-induced microvascular injury, haemostatic activation and finally post-ischaemic inflammation (Brouns & De Deyn 2009) (see figure 1.1) which is particularly increased during reperfusion.

1.3.1 Ischaemia leads to bioenergetic failure

Brain cell metabolism is dependent on high levels of oxygen and glucose and the brain accounts for 25% of basal metabolism (Lee *et al.* 2000); therefore any complete deprivation (of oxygen and glucose) for a duration of only 5 minutes could be sufficient enough to cause severe damage (Choi & Rothman 1990, Rossi *et al.* 2007). Neurons in particular are extremely sensitive to oxygen and glucose deprivation and are highly dependent on oxygen and glucose supplies in circulating blood, as they lack any glucose stores, whereas astrocytes have glycogen stores enabling them to be less susceptible to ischaemia (Rossi *et al.* 2007).

Deprivation of glucose and especially oxygen leads to reduced adenosine triphosphate (ATP) production through glycolysis and oxidative phosphorylation leading subsequently to bioenergetic failure (Rossi *et al.* 2007). As a result of ATP loss, energy dependent ion transport pumps, especially Na^+-K^+ ATPases (also known as sodium potassium pumps which are responsible for maintaining the resting action potential) present throughout the neuronal axons, are not energetically supported. Therefore their activity fails, leading to loss of ion gradients and membrane depolarization (caused by Na^+ influx through sodium channels) of neurons and glial cells (Katsura *et al.* 1994, Martin *et al.* 1994, Brouns & De Deyn 2009).

1.3.2 Excitotoxic damage of cells following ischaemia

Furthermore, as a result of ischaemia, excess release of neurotransmitters in the extracellular space, notably glutamate, which is thereby neurotoxic, leads to over activation of neurotransmitter receptors (α-amino-3-hydroxy-5-methyl-4isoxazole

propionic acid (AMPA), kainate and N-methyl-D-aspartic acid (NMDA)-type glutamate receptors) and activation of calcium channels. This leads to Na^+, Cl^- and Ca^{2+} ion influx and K^+ efflux and therefore membrane depolarisation (Meldrum *et al.* 1985, Dirnagl *et al.* 1999, Rossi *et al.* 2000, Chen *et al.* 2008, Brouns & De Deyn 2009, Brouns & De Deyn 2009). The activity of the uncontrolled neurotransmitter release and the increased influx of calcium ions in cells results in excitotoxic damage of brain cells.

Intracellular and mitochondrial overload of calcium can also act as a mediator in the expression of genes mediating inflammatory reactions, generation of ROS (especially after reperfusion) like superoxide, hydroxyl and nitric oxide (NO via NO synthase), as well as activation of proteases (i.e. endonucleases and matrix metalloproteinase-9) (Chan 2001, Kelly *et al.* 2008, Brouns & De Deyn 2009) leading to cell death either by necrosis or apoptosis of brain cells. Infiltrating leukocytes (macrophages, neutrophils), during reperfusion, as well as microglia in the ischaemic brain mediate further production of ROS. ROS are detrimental to cells and mediate cellular damage through damaging essential macromolecules (i.e. lipids, proteins, DNA) via lipid peroxidation, protein and DNA oxidation (Hall & Braughler 1989, Chan 2001) as well as affecting DNA repair enzymes (Chan 2001). ROS mediated tissue damage in brain is thought also to be through delocalisation of protein bound iron (Lundgren *et al.* 1991). In addition to that, ROS production affects mitochondrial cytochrome C release, leading to apoptosis and DNA fragmentation (Chan 2001).

Intracellular acidification is also observed following ischaemia contributing to cell damage. As a result of oxygen depletion and absence of oxidative phosphorylation, glycolysis persists, and eventually accumulates protons and lactate within the cells

causing the deleterious intracellular acidification (Silver *et al.* 1997, Rossi *et al.* 2007). As many enzymes and biological processes are dependent on a balanced pH, disruption of this leads to cell stress and failure.

1.3.3 Oedema

Following ischaemia and reperfusion injury in the brain there is increased permeability of the BBB due to its destruction. This contributes to osmotic imbalance and oedema is observed, which is also a factor contributing to cell loss and tissue damage in stroke. The cytotoxic oedema occurs as a result of bioenergetic failure and the increased influx of Na^+ and Cl^- in neuronal and astrocytic cells, which changes the ionic gradient inside and outside the cells, as it was previously described. The intracellular influx of these ions in neurons and astrocytes drives water infiltration within cells resulting in cellular swelling and reduction of the extracellular space (Liang *et al.* 2007). The aquaporin water channels (i.e. aquaporin 4) present in the brain are also involved in this water infiltration (King & Agre 1996). Cellular swelling and the resulting cytoskeletal alterations lead to cell death, which in this case is called oncosis (Liang *et al.* 2007).

Cytotoxic oedema doesn't result in brain swelling while vasogenic oedema does (Liang *et al.* 2007). Secondary damage of the brain tissue is extended following reperfusion and BBB breakdown (which will be discussed later in more detail). The increased permeability of the BBB and the change in the ionic gradient (from cytotoxic oedema) in the extracellular spaces drives sodium ion flux from the intravascular space to the extracellular space (ionic oedema). This in turn drives water infiltration from the intravascular endothelial cells of the vessels space to the extravascular (vasogenic oedema). The water infiltration is further increased by the loosening of the tight

junctions of the BBB which allows protein rich fluid (i.e. albumin) to pass from the endothelial cells of the capillaries in the brain's extracellular space, resulting in brain swelling and increase in the intracranial pressure (Kahle *et al.* 2009).

1.3.4 Inflammation mediates cellular damage in stroke

As mentioned before, in contrast to other organs, the brain is selectively protected by the blood-brain barrier (BBB). This is formed by astrocytes and endothelial cells closely apposed by tight junctions. Some of the tight junction proteins holding endothelial cells together include occludin and claudin-5 (Rosenberg & Yang 2007). During stroke, and particularly after reperfusion, the BBB becomes damaged and leaky, facilitating the entry of macromolecular proteins, leukocytes and subsequent release of inflammatory mediators (cytokines, chemokines) that lead to further tissue damage. The activation of complement in the ischaemic tissue, as discussed later on in more detail, is an important contributor in promoting inflammation, the recruitment of leukocytes and secondary damage of the tissue during reperfusion. This secondary damage as a result of prolonged inflammation is especially detrimental to neurons as these cells are unable to regenerate once damaged (Horner & Gage 2000).

1.3.5 Blood brain barrier disruption

The blood brain barrier has a biphasic opening following reperfusion (Rosenberg & Yang 2007). The initial transient opening of the BBB takes place around 2 hours after the onset of ischaemia (Hamann *et al.* 1995). The permeability of BBB is initiated by dissolution of the basal lamina via loss of the integrin matrix attachments of astrocytes

and endothelial cells (D'Ambrosio *et al.* 2001) as well as by the loss of tight junction proteins (i.e. occludin and claudin-5) by the activity of the metalloproteinase enzyme, gelatinase A (matrix metallopreinase protein-2; MMP-2) (Rosenberg & Yang 2007). The extended inflammatory reactions lead to further blood vessel damage resulting in the second opening of the BBB between 24 to 48 h, occurring by the activity of the metalloproteinases, gelatinase B (matrix metallopreinase protein-9; MMP-9) and stromelysin-1 (matrix metallopreinase protein-3; MMP-3). The activity and increased abundance of these metalloproteinases is also associated with their secretion by infiltrated leukocytes (i.e. neutrophils) or microglia (Rosenberg & Yang 2007).

Mediating the entry of leukocytes in the brain parenchyma are leukocyte endothelial cell adhesion molecules (selectins and integrins) which become upregulated as a result of ischaemia (Lee *et al.* 2000) and the action of cytokines. Intercellular adhesion molecules 1 and 2 (ICAM-1 and ICAM-2), vascular cell adhesion molecule 1 (VCAM-1), platelet endothelial cell adhesion molecule-1 (PECAM-1) and the mucosal addressin (MAdCAM-1) are adhesion molecules mediating firm attachment and transmigration of leukocytes in the brain parenchyma (Frijns & Kappelle 2002). ICAM-1 expression becomes upregulated via the activity of cytokines (Frijns & Kappelle 2002) and neutrophils and macrophages are thought to be the main infiltrating leukocytes involved in brain damage after stroke (Matsuo *et al.* 1994, D'Ambrosio *et al.* 2001). The importance of ICAM-1 in brain IRI is demonstrated using ICAM-1 deficient mice. Those mice showed a significantly reduced degree of ischaemic infarction (Connolly *et al.* 1996).

1.3.6 Haemostatic activation and the "no-reflow phenomenon"

Prolonged ischaemia and subsequent endothelial cell injury during reperfusion could also lead to activation of platelets and the coagulation cascade in the microvasculature (Zeller *et al.* 1999). The adherence (as a result of fibrin clot formation) of platelets and endothelial cells together with the recruited leukocytes like neutrophils (especially after BBB disruption), could obstruct the capillaries and blood flow, a consequence called the "no-reflow phenomenon" which subsequently could lead to infarct expansion (Chong *et al.* 2001, Zeller *et al.* 2005, Brouns & De Deyn 2009).

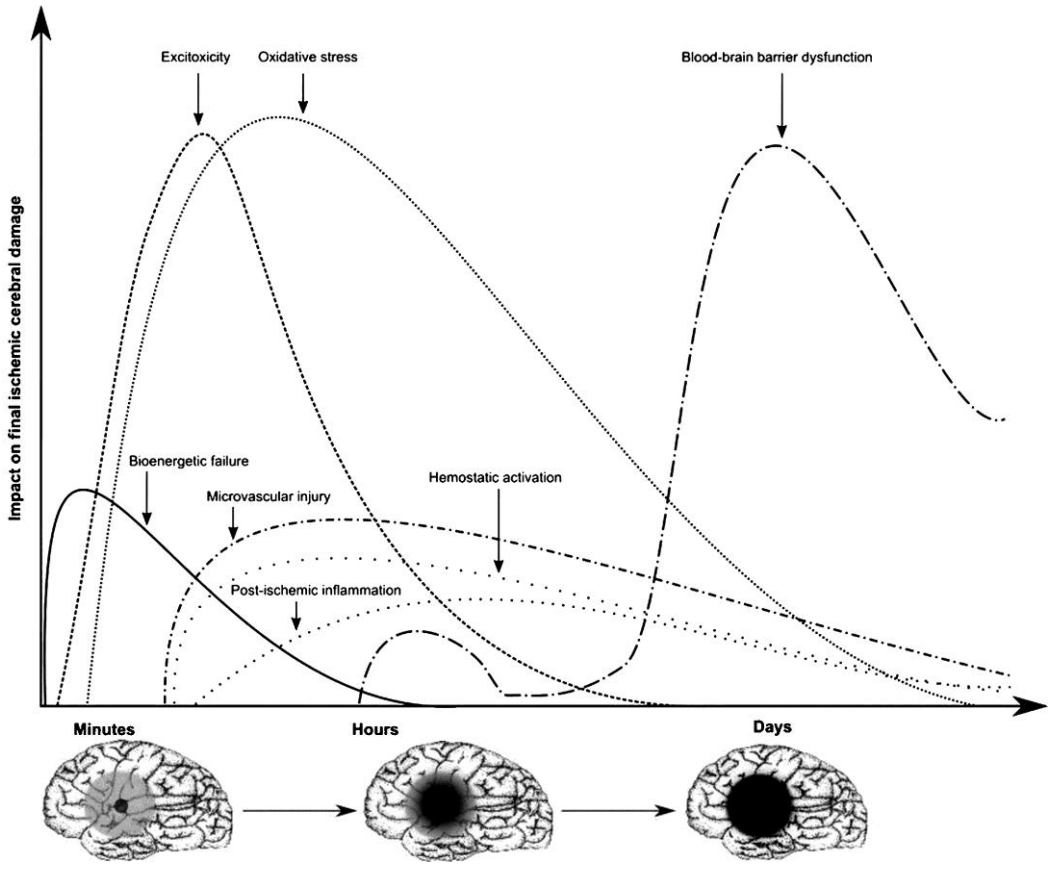

Figure 1.1: Time course of events in brain damage

Time course of events leading to increasing brain damage within the core and the penumbra region. The events driving brain cell damage after stroke are bioenergetic failure, excitotoxicity and oxidative stress. These are the first responses after stroke initiating within minutes. Microvascular injury, hemostatic activation and post-ischemic inflammation follow and finally after hours and days the blood brain barrier is damaged leading to further brain injury. Source: R. Brouns, R. 2009.

1.4 The complement system

The events mediating cerebral ischaemia and reperfusion injury have been previously described. Since, however, this thesis focuses on the role of the complement system in cerebral IRI, a closer overview of the complement cascade is essential. The complement system consists of more than 30 serum and cell surface proteins (Whaley & Schwaeble 1997) and although it is part of the innate immune response, it also mediates in adaptive immune responses (Dunkelberger & Song 2010). In the 1890s, Jules Bordet first described complement as a heat labile component in serum that was able to lyse bacteria as well as to 'complement' the antibacterial properties of antibodies; hence the name (Dunkelberger & Song 2010, Schmalstieg & Goldman 2010). Since then, the complement system has been widely studied and research is still evolving.

As an effective system of the immune response it is involved in initiating and coordinating numerous active inflammatory reactions. Within these inflammatory reactions the complement system is a mediator in the opsonisation (targeting for phagocytosis) of bacteria (via i.e. C1q, C3b, iC3c, C4b) and subsequent phagocytosis through interactions with cellular receptors on phagocytes (Complement receptors type 1 (CR1), type 2 (CR2), type 3 (CR3) and type 4 (CR4)) (Wagner & Frank 2010), chemotaxis (C3a, C4a, and C5a), generation of anaphylatoxins (i.e. C3a and C5a), direct killing by cell lysis via the insertion of the membrane attack complex (MAC) in the cellular membrane lipid bilayer (Podack *et al.* 1982) and clearance of cell debris and apoptotic cells (van Beek *et al.* 2003, Wallis 2007). Complement is also involved in the increased vascular permeability aiding leukocyte adhesion on endothelial cells during inflammation especially by the activity of C5a and C3a (Williams 1983). The

involvement of complement in mediating leukocyte activation and recruitment at the site of damage or infection makes complement critically important, while leukocytes will be the cells that will initiate the secretion of more pro-inflammatory mediators like TNF-α and IL-1β and generate and secrete ROS, as well as anti-inflammatory mediators like IL-10. Finally, in adaptive immune responses, complement proteins mediate activity through interactions with follicular dentritic cells and B cells in promoting B-cell memory, as well as mediating the generation of specific antibodies (Barrington *et al.* 2002, Le Friec & Kemper 2009). Moreover, complement is able to modulate T cell responses by interacting with antigen presenting cell (APC) complement receptors as well as through opsonisation of antigen, thereby facilitating optimal T cell activation (Zhou *et al.* 2006, Le Friec & Kemper 2009, Kwan *et al.* 2012). The complement system is activated via three activation pathways (Phillips *et al.* 2009). These are the classical pathway (CP), the alternative pathway (AP) and finally the lectin pathway (LP) of complement activation. This latter pathway and its role in promoting tissue damage following cerebral IRI is the focus of this thesis (see figure 1.2). In general, all three activation pathways excluding the initial activation step, converge on the formation of a C3 and a C5 convertase as well as the formation of the membrane attack complex (MAC) on the targeted surface. In the course of these reactions other reactive complement components are generated, acting as anaphylatoxins and chemoattractants.

1.4.1 The classical pathway

Of the three activation pathways the classical is the only antibody dependent activation pathway. The C1 complex of the classical pathway is responsible for the activation of the cascade. The C1 complex consists of C1q and homodimers of both C1r and C1s,

which are serine proteases. C1q is the recognition subcomponent of the classical pathway and is able to recognise an antigen within an immune complex by interaction with the Fc regions of antibodies (IgM and IgG) on infected, microbial, necrotic and apoptotic cells (Thiel *et al.* 2000, Schwaeble *et al.* 2002, Phillips *et al.* 2009). After the recognition event, the serine protease C1r in the C1 complex becomes autoactivated and subsequently activates another serine protease, C1s, that will later on initiate the complement cascade (Phillips *et al.* 2009). The subsequent complement cleavage events lead to the generation of C3 (C4b2a) and C5 (C4b2a) convertases, the active enzymes of the complement cascade, that are responsible for the generation of mediators of inflammation, as well as the initiation of the terminal pathway leading to the generation and insertion of the membrane attack complex (MAC) C5b-9 within the cell wall of "targeted" cells (Schwaeble *et al.* 2002). The MAC acts like a pore on cellular membranes leading to cell death. Beside the activation route, the events that follow the activation of the classical complement cascade are similar to that following lectin pathway activation. These will be described in more detail later on when describing the molecular events leading to the activation via the lectin pathway, the focus of this project.

1.4.2 The alternative pathway

Until recently, the alternative pathway was considered to be initiated by slow spontaneous hydrolysis of C3 to form C3 (H2O) (Phillips *et al.* 2009) and to generate a C3 convertase (C3 (H2O) Bb or C3bBb) on the surface of microbial cells (or other activating surfaces) that will cleave circulating C3 into C3b and C3a (Farries *et al.* 1988). C3b remains bound on the activating surface while C3a is released in plasma

and acts as an anaphylatoxin. The formation of the alternative pathway C3 convertase is mediated by the involvement of factor B and factor D. The alternative pathway provides an amplification loop of the complement activation cascade, as factor B can bind C3b (C3bB) to form further C3 convertase (C3bBb) upon factor D mediated cleavage of C3b bound factor B (Farries *et al.* 1988, Muller-Eberhard 1988). Properdin, the only known positive regulator of complement, mediates the stabilisation of this convertase (Wirthmueller *et al.* 1997, Schwaeble & Reid 1999). Recent studies indicated that components of the lectin pathway may also be involved in the activation of the alternative pathway. These studies were initiated by the observation that MASP-1/3$^{-/-}$ double knockout mice had no detectable alternative pathway activity *in vitro* and this indicated that the serine protease of the lectin pathway, MASP-1, is important in activating the inactive zymogen form of factor D (Takahashi *et al.* 2008, Takahashi *et al.* 2010). Furthermore, the same group suggested with their *in vitro* studies that MASP-1 could activate MASP-3 on the surface of bacteria when in complex with MBL and that MASP-3 is able to activate factor B (Iwaki *et al.* 2011).

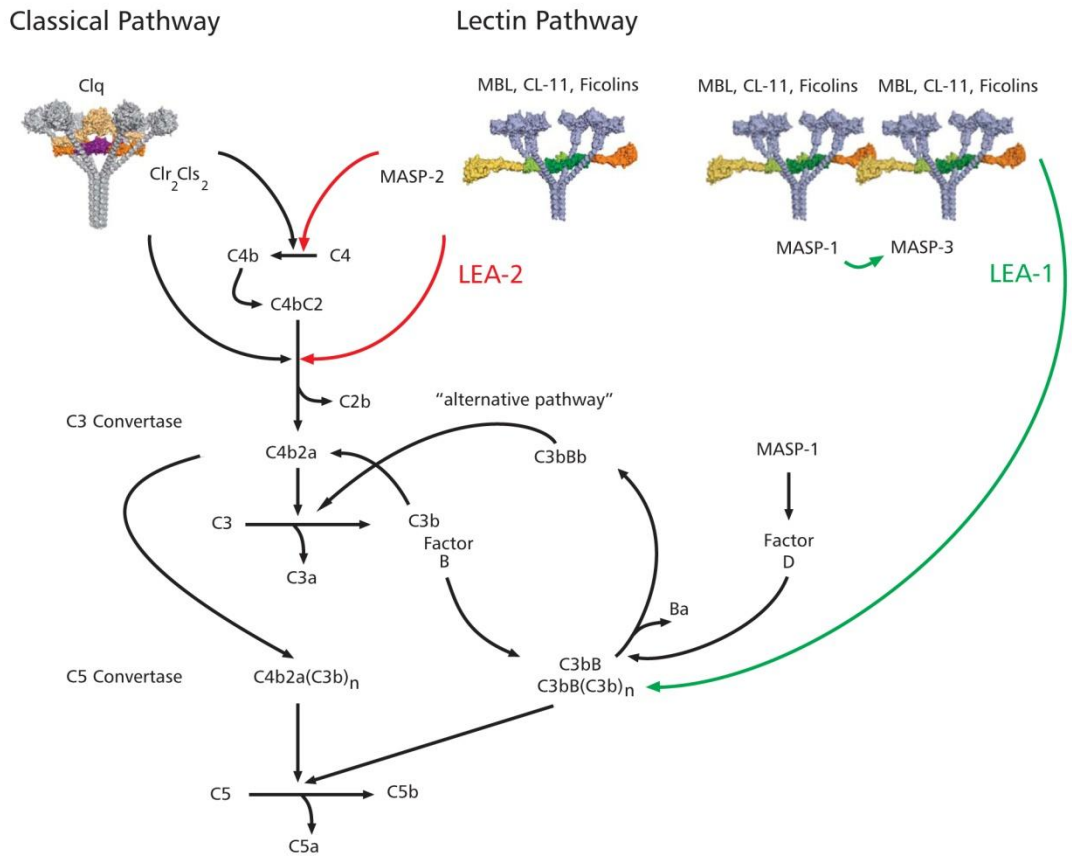

Figure 1.2: The Complement System

Complement activation by the classical, the lectin (Lectin effector arm 2, LEA-2, initiated by MASP-2 activity and the lectin effector arm, LEA-1, driven by MASP-1) and the alternative pathway. (Figure courtesy of Professor W. Schwaeble, University of Leicester UK).

1.5 The lectin pathway of complement activation

In evolutionary terms, the lectin pathway of complement activation seems to be the oldest of the three (Dodds 2002, Wallis 2007). In understanding the involvement of the lectin pathway of complement activation in ischaemia and reperfusion injury a detailed description of the whole cascade is necessary. The lectin pathway cascade is initiated by the activation of the lectin pathway activation complex in an antibody independent

manner. In humans, this comprises the carbohydrate recognition molecules lectin mannose binding lectin (MBL), ficolins and the recently described C-type lectin collectin-11 (CL-11), the serine proteases (MASP-1, MASP-2, MASP-3) and a non enzymatic protein called MAp19 or sMAP of unknown function (Schwaeble *et al.* 2002). Each carbohydrate recognition molecule associates only with one type of the MASP homodimers; either MASP-1, MASP-2 or MASP-3 (Schwaeble *et al.* 2002). Of the three serine proteases, mannose binding lectin associated serine protease 2 (MASP-2) has the key function in the activation of the complement cascade and is the effector enzyme of the lectin pathway by its ability to cleave both C4-bound C2 and C4. A MASP-2 deficient mouse colony has been generated to be used as a model of total lectin pathway deficiency, and indeed, in the absence of MASP-2 the lectin pathway activation complex was unable to initiate the cascade and therefore complete inhibition of the pathway was observed (Schwaeble *et al.* 2011). MASP-1 and MASP-3 are insufficient to initiate the cascade on their own (Gorsuch *et al.* 2012). However, MASP-1 facilitates in the formation of the C3 convertase (C4b2a) by cleaving C4-bound C2 but not C4 (Chen & Wallis 2004, Schwaeble *et al.* 2011, Gorsuch *et al.* 2012). The exact functional activity of MASP-3 is still not clear, although recent studies indicated that it could promote the formation of the alternative convertase by activating factor B (Iwaki *et al.* 2011). MASP-3 (unlike MASP-2) is unable to cleave C4 and C2 (Dahl *et al.* 2001, Rossi *et al.* 2001, Zundel *et al.* 2004).

The MASPs in the inactive form of a zymogen are circulating in serum in a complex with ficolins or MBL or CL-11 (Wallis *et al.* 2007). When the recognition subcomponents of the lectin pathway, MBL, CL-11 or serum ficolins bind to pathogen associated molecular patterns (PAMPs), such as carbohydrate structures and N-acetyl

groups on the surface of pathogens (including bacterial, viral, fungal pathogens) or oxygen deprived cells, they are capable of activating MASPs (Turner 1996), (Wallis 2007). MASP-2, upon activation, cleaves C4 and generates C4b that attaches to the surface of the cell. C4a is released and acts as an anaphylatoxin (Wallis *et al.* 2007). C2, upon binding to the already cell bound C4b and in the presence of MASP-2, becomes cleaved by MASP-2. Cleavage of C2 releases C2b into the serum and C2a remains bound to C4b forming a new enzyme called C3 convertase (C4b2a) (Rossi *et al.* 2001, Wallis *et al.* 2007). The C3 convertase that is bound to the cell surface can then cleave serum circulating C3 into C3a and C3b. C3a is released and C3b remains bound to the C3 convertase forming a new enzyme called C5 convertase. Circulating C5 is then cleaved by the enzyme into C5a (a 9kD peptide and anaphylatoxin which is released) and C5b. C5b remains bound on C5 convertase. Finally, C5b binds to C6, C7, C8 and C9 to form the membrane attack complex (MAC) that inserts itself in the cell surface leading to direct cell lysis. The lectin pathway protease in contrast to the classical pathway serine proteases, can still maintain its functional activity activating the complement cascade even in the absence of C4, by the C4 bypass mechanism, probably by direct cleavage of C3 by MASP-2 or MASP-1 (Matsushita & Fujita 1995, Schwaeble *et al.* 2011, Gorsuch *et al.* 2012).

1.6 Recognition molecules

1.6.1 Mannose binding lectin (MBL)

In humans, there is only one type of MBL while in rodents there are two types, the MBL-C and MBL-A, all synthesised primarily in the liver (Liu *et al.* 2001). MBL belongs to the protein family of collectins which is a subgroup of the C-type lectin

superfamily. The collectins are generally characterised by the presence of the Ca^{2+} dependent carbohydrate recognition domain as well as by the collagen-like domain (Selman & Hansen 2012). Three identical MBL polypeptide chains form a trimeric subunit, which associate with one another to form oligomers of MBL (Drickamer & Taylor 1993). Human MBL is primarily present in trimers and tetramers of subunits (although hexamers are found). High number oligomers have the highest activity in activating the complement cascade compared to dimers or single subunits (Lu *et al.* 1990, Wallis & Drickamer 1999, Teillet *et al.* 2005, Wallis 2007). Structurally MBL is composed of four domains (see figure 1.3). At the N-terminus MBL has a cysteine-rich domain, followed by a collagenous domain (which is the region where MBL associates with the CUB 1 and EGF like domains of MASPs), an α-helical coiled coil (or neck) domain and a globular C-terminal C-type carbohydrate-recognition domain (CRD) (Wallis *et al.* 2004, Wallis 2007). The subunits in MBL oligomers are held together at the N-terminal domain of the protein by interchain disulphide bonds (Wallis & Drickamer 1999, Wallis 2007). As mentioned before, MBL can discriminate invading microorganisms from host cells through the specificity of the CRD domains mainly on monosaccharides (e.g. mannose, fucose, N-acetylglucosamine) present on bacterial, fungal and parasitic cells, but that are uncommon on the terminal ends of mammalian oligosaccharides, glycoproteins and glycolipids (Wallis 2007).

1.6.2 Ficolins

The other recognition components of the lectin pathway are the ficolins. In human there are three types of ficolins namely L- ficolins, H-ficolins and M-ficolins while in mice there are two types namely ficolin A and ficolin B (Fujita *et al.* 2004). Ficolin B however, does not act as a recognition molecule for the lectin pathway as MASP-2 is

unable to bind with ficolin B and thus cannot activate the complement lectin pathway (Endo *et al.* 2005). Ficolins have binding specificity for N-acetylglucosamine and N-acetylgalactosamine and generally are able to recognise N-acetyl polysaccharides (Endo *et al.* 2005). The structure of ficolins is very similar to MBL, consisting of a small cysteine rich region at the N-terminal end, a collagen like region, a neck region and on their C-terminal end a fibrinogen like domain, which serves as the carbohydrate recognition domain and which also defines their binding specificity (see figure 1.3) (Fujita *et al.* 2004).

1.6.3 Collectin-11

Collectin-11 (CL-11 also known as collectin kidney 1, CL-K1) is the more recently described recognition molecule of the lectin pathway (Keshi *et al.* 2006). As does MBL, collectin CL-11 belongs to the protein family of collectins. As with MBL, the structure of CL-11 is comprised by an N terminal domain, a collagenous region, a neck region and finally the carbohydrate recognition domain (CRD) (Selman & Hansen 2012) and it is found to preferentially bind to L-fucose and D-mannose, while being able to interact with MASP-1 and MASP-3(Hansen *et al.* 2010). The main production organs in human for this recognition molecule are the adrenal glands, liver and kidneys (Hansen *et al.* 2010).

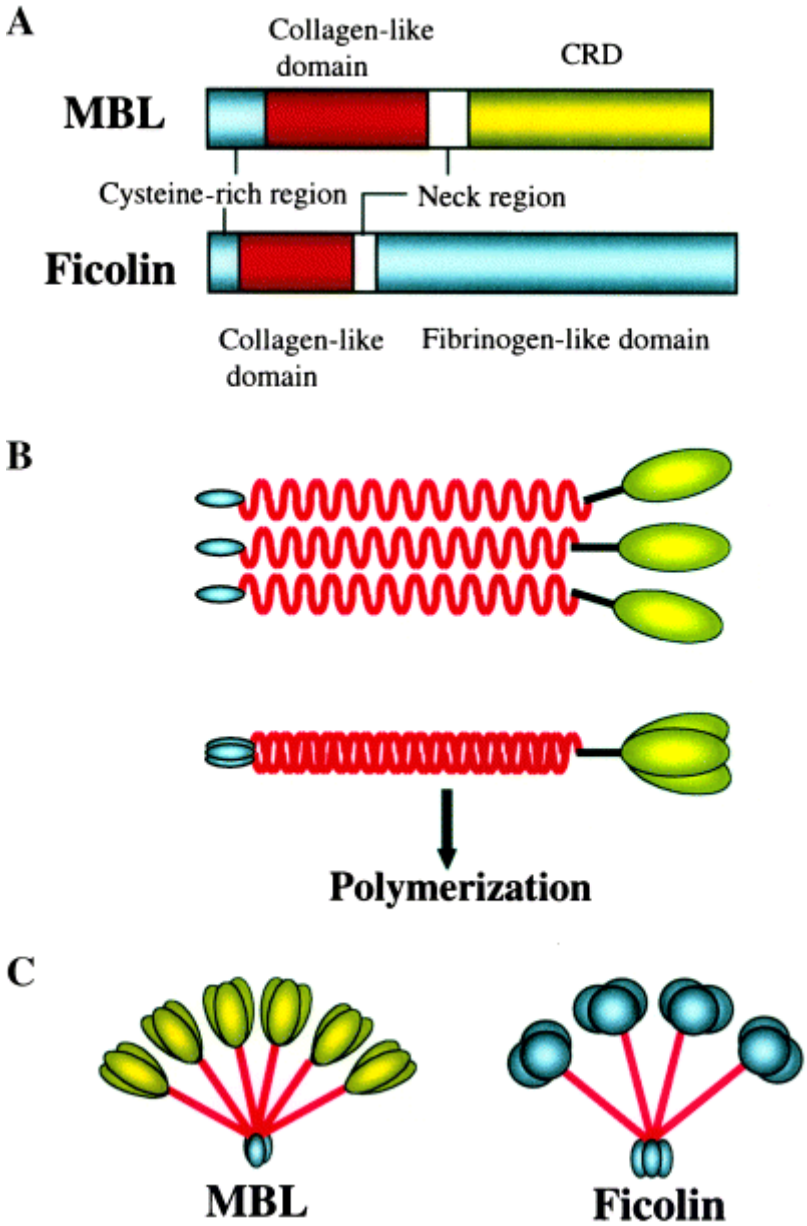

Figure 1.3: MBL and Ficolin structure

A) MBL and ficolin structure, B) Three identical polypeptide chains form an MBL subunit, C) Multiple subunits of MBL and ficolin associate with one another to form oligomers (The hexameric form of MBL and the tetrameric form of L-ficolin are shown). Figure taken from Fujita, T et al. 2004.

1.7 The mannan-binding lectin-associated serine proteases (MASPs)

Following the recognition subcomponents of the lectin pathway, the initiator enzymes of the lectin pathway, MASPs, are homologs of the C1s and C1r proteases of the classical pathway and share the same structural domains (Matsushita & Fujita 1992, Chen & Wallis 2004). MASP-1 and MASP-3 are encoded by the same gene, *MASP1/3*, located on chromosome 3q27-28 and are products of alternative splicing (Takada *et al.* 1995, Schwaeble *et al.* 2002) and the serine protease domains are present on their individual B chains (Schwaeble *et al.* 2002). MASP-2 and MAp19 are also products of alternative splicing of the same gene (*MASP-2*), located on chromosome 1p36.3-2 (Stover *et al.* 1999c, Schwaeble *et al.* 2002). The molecular masses calculated by western blotting of MASP-1, MASP-2, MASP-3 and Map19 are 90kDa, 74kDa, 94kDa and 19kDa, respectively (Stover *et al.* 1999c, Schwaeble *et al.* 2002). Structurally, MASPs consist of six domains (see figure 1.5 and 1.6). On the N terminal of the protein there is a CUB domain (complement C1r/C1s, Uegf and bone morphogenic protein 1) (Wallis *et al.* 2007), an epidermal growth factor-like domain (EGF), a second CUB domain (CUB2), two complement control protein domains (CCP1 and CCP2) or short complement regulators (SCRs) and finally, on the C-terminal of the protein the serine protease domain (Schwaeble *et al.* 2002). The CUB and EGF domains of MASPs are the domains that are responsible for the interaction of the enzyme with MBL and ficolins (Wallis & Dodd 2000) and the activation of the enzyme occurs via autolysis (with the exception of MASP-3 that does not autoactivate) at a single site within the linker region between the CCP-2 and serine protease domain. The activation of MASPs generates the heavy chain (also known as A chain) comprising the N-terminal site of the enzyme and the light chain (also known as B chain) comprising the

protease domain, while a disulphide bond keeps the protease domain attached to the N-terminal site of the enzyme after activation (Zundel *et al.* 2004, Wallis 2007). MAp19 has only the first two N-terminal domains of MASP-2 which are the CUB1 and EGF domains, as well as an additional four amino acids.

As mentioned before, MBL interacts with MASPs through its collagen-like domains. Currently it is thought that in the lectin pathway activation complex MASP dimers interact with MBL subunits in a manner such that each MASP protomer interacts with a separate MBL subunit, positioning the MASP CCP and protease domains in between MBL subunits. The binding of MBL on the surface of a pathogen leads to the alteration of the angle between the subunits and results in a conformational change in the interacting MASPs. This is followed by a subsequent autoactivation due to the cleavage within the linker region of one MASP protomer to the other (see figure 1.4). As a result the protease domains of MASPs are exposed to interact and cleave downstream complement components (i.e. C4 and C2) (Wallis 2007).

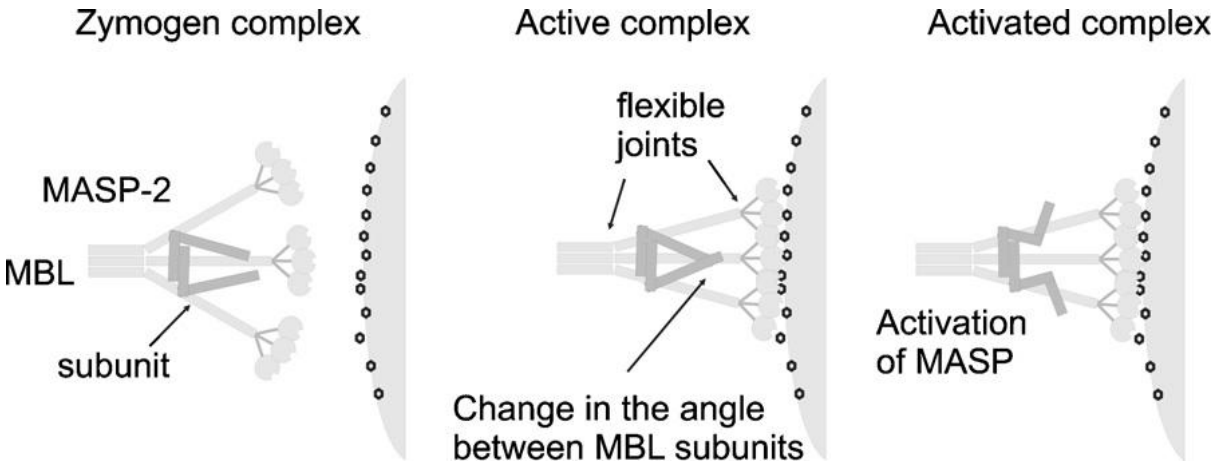

Figure 1.4: Activation of MASPs

Activation of MASP dimers through conformational changes upon binding of MBL to an activating surface (i.e. bacterial cell). Source: Wallis, R. 2007.

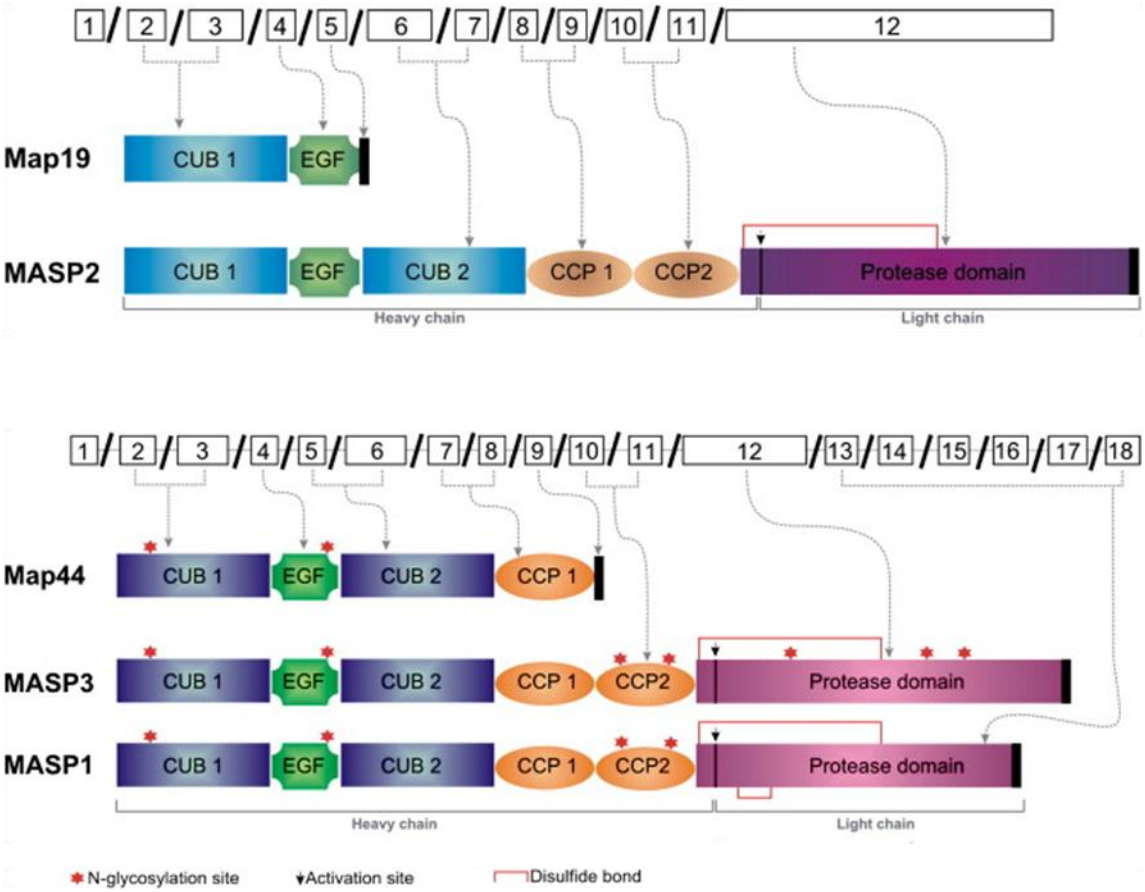

Figure 1.5: Genomic and protein organisation of MASP-1, MASP-2, MASP-3, Map19 and Map44. Figure modified from Yongqing *et. al.* (2012).

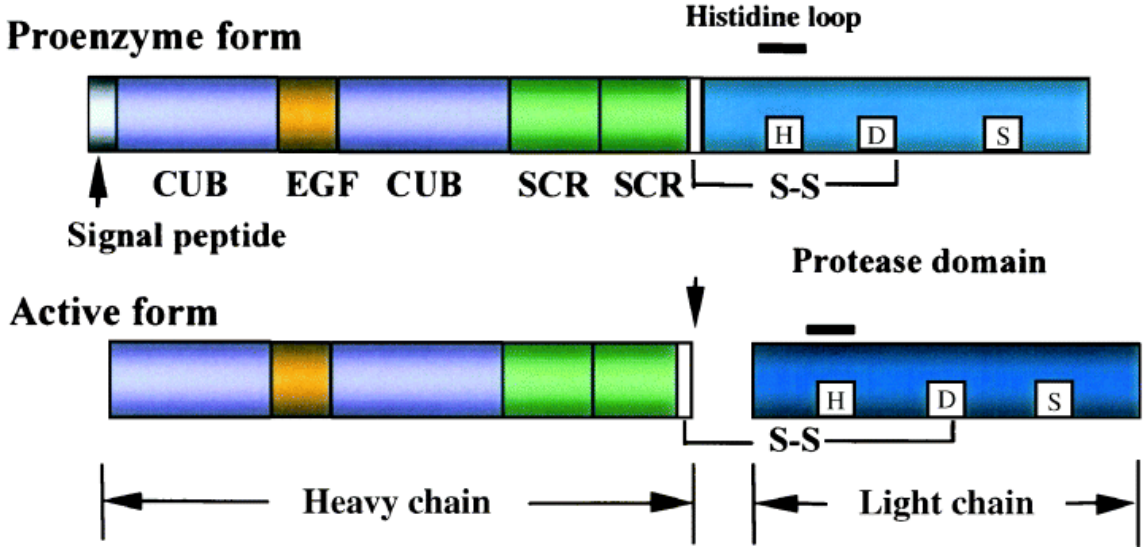

Figure 1.6: Structure of MASPs in their active and inactive form as presented in Fujita, T et al. (2004).

MASPs domains, showing in the protease domain the amino acids histidine (H), aspartic acid (D) and serine (S) which are important for the proteolytic activity of these enzymes.

1.8 Complement regulators

Unregulated complement activation would be catastrophic for the organism, both in health and disease and therefore the role of complement regulators is critical. The complement regulators are distinguished into two groups, one being the fluid-phase regulators and the other the cell membrane-bound regulators (see figure 1.7).

1.8.1 Fluid-phase regulators

The C1 inhibitor (C1 inh), also known as Serping1, is a serine protease inhibitor able to interfere with C1r and C1s activation in the C1 immune complex and consequently inhibits classical pathway initiation at low antigen-antibody affinities (Chen *et al.* 1998, Cicardi *et al.* 2005). Serping1 has also been reported to inhibit the lectin pathway serine proteases, MASP-1 and MASP-2 (Presanis *et al.* 2004). Besides complement regulation serpin1 can also inactivate serine proteases of the coagulation cascade (i.e. thrombin), of the contact system (i.e. kallikrein) and the fibrinolytic system (i.e. plasmin) (Cicardi *et al.* 2005, Wagner & Frank 2010).

Another fluid phase regulator is the protease factor I. Factor I inactivates the activated complement component C3b in the presence of the co-factor, factor H, whilst it inactivates C4b in the presence of the co-factor C4-binding protein (C4BP) (Seya *et al.* 1995). Inactivation of C3b by factor I leads to the C3b inactivated fragments, iC3b, C3c and C3dg. Binding of C4BP on C4b inhibits C4b-C2a binding, preventing the formation of the C3 convertase (Blom *et al.* 2004). Inactivation of the C4b by factor I leads to the inactivated complement C4b fragments iC4b, C4c and C4d.

Factor H is an important alternative pathway regulator the main activity of which, besides mediating C3b inactivation by factor I, is to destabilise and also accelerate the decay of the alternative pathway C3 convertase (C3bBb) and C5 convertase (C3bBb (C3b) n) (Pangburn *et al.* 2000, Wagner & Frank 2010). Factor H destabilises the C3 convertase by competitive binding to C3b which dislodges C3b from the convertase (C3bBb) (Wu *et al.* 2009). Factor H is important for the discrimination of self from non-self cells and therefore preventing autoimmunity. Binding of factor H, for example on sialic acid or glycosaminoglycans of host cells, inhibits alternative pathway activation on the surface of host cells (Pangburn *et al.* 2000, Wu *et al.* 2009). Carboxypeptidase N (CPN) is an inactivating regulator of the C3a and C5a anaphylatoxins (Bokisch & Muller-Eberhard 1970). Clusterin and vitronectin are also fluid-phase regulators, inhibiting MAC formation on the surface of host cells hence preventing cell lysis (Wagner & Frank 2010).

1.8.2 Cell membrane-bound regulators

The cell membrane-bound regulators of complement are present on the surface of a variety of cells i.e. erythrocytes and antigen presenting cells. These comprise the decay-accelerating factor (DAF, also known as CD55), the complement receptor 1 (CR1, also known as CD35), the membrane co-factor protein (MCP, also known as CD46) and CD59 (also known as protectin) (Wagner & Frank 2010). Like factor H, DAF, (found on erythrocytes and epithelial cells) regulates complement activation by accelerating the decay (dissociation of the convertases) of the C3 convertases (C3b2a and C3bBb) (see figure 1.7) (Lublin & Atkinson 1989). CR1 and MCP act as co-factors for the cleavage of C3b and C4b by factor I (Wagner & Frank 2010). CD59, is a

regulator of the MAC complex. CD59 binds the nascent MAC complex (C5b-8) inhibiting C9 polymerisation and subsequent pore formation on the surface of a cell (Lehto *et al.* 1997, Farkas *et al.* 2002).

1.8.3 Properdin

Properdin is the only known and essential positive regulator of the complement system. It is essential for alternative pathway activation as properdin depleted sera lack the ability to activate the alternative pathway (Schwaeble & Reid 1999). Properdin is produced by monocytes/macrophages, peripheral T lymphocytes and granulocytes (i.e neutrophils) (Wirthmueller *et al.* 1997) and acts as a positive regulator by stabilising the alternative pathway C3 and C5 convertases (Schwaeble & Reid 1999).

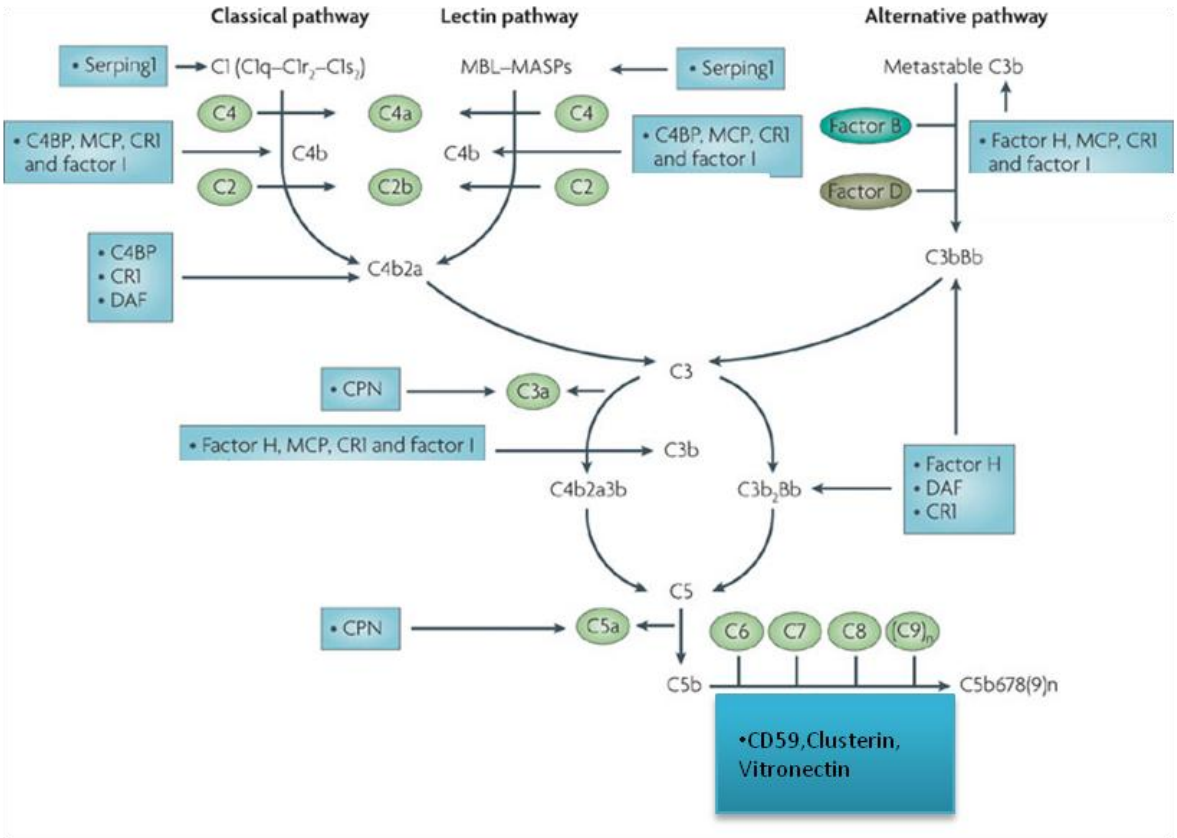

Figure 1.7: The regulators of the complement system.

Figure edited from Wagner and Frank (2010).

1.9 Complement deficiencies

As discussed before, the complement system is a powerful mediator in immune reactions and its many components are involved not only in a variety of inflammatory functions in order to clear any invading pathogens, but also in maintaining homeostasis by clearing necrotic and apoptotic cells and in the case of complement regulators, in controlling complement over-activation and preventing host cell targeting. Therefore, usually, complement deficiencies are involved with susceptibility to bacterial or fungal infections (i.e. C1, C4, C2, C3 mutations) (Wagner & Frank 2010, Goldberg *et al.* 2011,

Kainulainen *et al.* 2012) or result in autoimmune diseases (i.e. systemic lupus erythematosus) (Pradhan *et al.* 2012).

MASP-2 deficiency is uncommon. A MASP-2 mutation has been reported in which the MASP-2 gene had a mutation in the CUB 1 region of the enzyme whereby the aspartic acid was substituted in position 105 on the mature protein with glycine (D105G). While the CUB 1 domain of MASP-2 is responsible for MBL and ficolin binding, this amino acid substitution prevents the formation of the lectin pathway activation complex and thus the inability to induce lectin pathway activation (Stengaard-Pedersen *et al.* 2003). The particular patient was healthy at a young age, but later he was diagnosed with severe recurring pneumococcal pneumonia, ulcerative colitis, erythema multiforme bullosum and hypocomplementemia (Stengaard-Pedersen *et al.* 2003).

MBL deficiencies are more common in the population (i.e. around 30% of the population carry heterozygous mutations in MBL) than in MASP-2 and they are usually associated with upper respiratory infections and general susceptibility to bacterial infections (Ram *et al.* 2010, Wagner & Frank 2010).

Other examples of complement deficiencies associated with disease are paroxysmal nocturnal haemoglobinuria (PNH), which is a condition caused by CD59 deficiency causing unregulated MAC deposition on erythrocytes, while atypical haemolytic uraemic syndrome (aHUS) and age macular degeneration (AMD) are associated with factor H deficiencies causing unregulated alternative pathway activation (Klein *et al.* 2005, Lee *et al.* 2009, Wagner & Frank 2010, Risitano 2013).

1.10 Complement system and ischaemia and reperfusion injury

The complement system has been proven to be involved in ischaemia and reperfusion injury, mainly by studies made on knockout mice or via the use of complement inhibitors (Gorsuch *et al.* 2012). The exact alteration on the glycocalyx on oxygen deprived cells that leads to the activation of complement is still under investigation. Studies performed on intestinal and hindlimb IRI revealed a neo epitope (new antigen) that possibly mediates IRI in these models. This is a highly conserved region within the non-muscle myosin H chain type II (NMHC-II) A and C which seems to act as a target for a monoclonal natural IgM antibody involved in this IRI (Zhang *et al.* 2004, Zhang *et al.* 2006).

Other studies on IRI showed that mice completely deficient in antibodies (Rag (-/-)), were protected from intestinal IRI while reconstitution with monoclonal IgM (CM22) restored injury (Zhang *et al.* 2004). Although they thought that the classical pathway would be involved in inducing IRI, C1q (-/-) mice, lacking the classical activation pathway, were not protected from intestinal IRI, in contrast to MBL (-/-) mice; suggesting a more critical role for the lectin pathway in IRI (Zhang *et al.* 2006). In the same study, immunohistochemisty on MBL and IgM showed co-localisation. Experiments performed by the same group showed that IgM deposition on MBL knockouts, which were protected from IRI, was present at an early phase of reperfusion (15 min), but absent in the late phases, indicating that IgM in this model is unable to cause damage in the absence of MBL. Therefore, it was proposed that IgM mediates and enhances the binding of MBL on ischaemic cells, leading to the activation of the lectin pathway. At least *in vitro* it was proved that mouse MBL binds mouse IgM,

corroborating the previous results (Zhang *et al.* 2006). Furthermore, studies using knock out animals performed by M. Hart et al. in 2005 on gastrointestinal IRI further support that MBL and C2, but not C1q is involved in gut injury (Hart *et al.* 2005).

Moving on to studies on myocardial ischaemia and reperfusion injury (IRI), the lectin pathway of complement activation seems to be the key player involved in tissue injury and MASP-2 deficient mice are protected from both myocardial and gastrointestinal IRI (Schwaeble *et al.* 2011, Gorsuch *et al.* 2012). Classical pathway knockouts (C1q -/-) indicated no infarct protection, in contrast to MBL null mice that did (Walsh *et al.* 2005). In addition to that, examination of heart function based on ejection fraction percentage showed that the alternative pathway knockouts (factor D KO) and C1q knockouts were not protected from the left ventricular dysfunction in contrast to the MBL null mice that had a relevant protection compared to MBL null mice reconstituted with rhMBL (Recombinant human MBL) (Walsh *et al.* 2005).

Evidence of the involvement of the lectin pathway also in renal IRI is shown by Vries B. *et al.* in 2004. It was observed that MBL, one of the recognition molecules of the lectin pathway, was pre-deposited and also co-localised with complement components like C6, showing the role of the pathway in activating complement in IRI. Furthermore, post transplant IRI, resulting in a non-functional organ was accompanied by MBL deposition (de Vries *et al.* 2004). More interestingly MASP-2 deficient mice show a significant degree of protection in renal IRI (Gorsuch *et al.* 2012).

Through studies performed on C3 and C5 knockout mice, it was shown that they were protected from intestinal, renal and hindlimb IRI, showing that these complement

components are involved in tissue damage (Diepenhorst *et al.* 2009). C4 KO mice were protected in hindlimb IRI and C6 KO mice from renal IRI (Diepenhorst *et al.* 2009). In general complement deposition, like C3, C9 and the MAC complex, shows the involvement of the complement system in the pathology of ischaemia and reperfusion injury (D'Ambrosio *et al.* 2001).

1.11 Complement in the brain

The exact role of the complement system in cerebral ischaemia and reperfusion injury has not yet been clarified. Although liver is considered one of the important organs for complement biosynthesis (Whaley & Schwaeble 1997), the brain is also capable of biosynthesising most of the complement components and their activation and action is recorded in many neurological disorders like multiple sclerosis, schizophrenia and Alzheimer's disease (Huber *et al.* 2001, Mayilyan *et al.* 2006). Additionally, the complement system becomes activated in human stroke (Di Napoli 2001, De Simoni *et al.* 2004). Cells of the central nervous system that are capable of complement component biosynthesis are astrocytes, neurons and microglia (Thomas *et al.* 2000, D'Ambrosio *et al.* 2001). Complement receptors like the C5a receptor, CD88, are also found to be locally expressed in the brain by microglia, neurons and astrocytes (Crane *et al.* 2009). However, studies on the mRNA expression levels showed that MASP-2 mRNA was only detectable in liver tissue and was not present in the brain or other organs (Stover *et al.* 1999a). In contrast C1q is highly synthesised by activated microglia and its expression can be used as a marker of inflammation in the brain (Lynch *et al.* 2004). This observation was obtained after administration of 3-chloropropanediol which induces BBB breakdown (Lynch *et al.* 2004). The presence of

C1q in cell death areas in this model might indicate the involvement of the classical pathway in clearing cell debris after brain injury. This is further supported by unpublished observations where C1q deficient mice showed a bigger infarct size after middle cerebral artery occlusion, indicating that the classical pathway activation in the brain is neuroprotective and its absence leads to more tissue damage. This is in contradiction with a model of hypoxic-ischemic brain injury performed in neonatal mice whereby C1q deficient mice had a smaller infarct size compared to wild types (Ten *et al.* 2005). However, this model is less reliable when studying the effects of ischaemia and reperfusion injury after stroke in adults. Other studies were performed using C1 inhibitor (C1 INH), whereby infarct volume in the brains of mice was significantly reduced (De Simoni *et al.* 2004). However, among other anti-inflammatory reported activities, C1 inhibitor acts against serine proteases of the complement system and this includes not only the inhibition of C1q and C1s, but also the MASPs and the alternative pathway (De Simoni *et al.* 2004). Moreover, in the same studies, the effect of C1 INH was observed on C1q deficient mice. Given the still significant decrease in infarct size after administration of C1 INH, but the small non significant decrease of infarct size on C1q deficient mice compared to WTs, it appears that that C1 INH could still be neuroprotective via other C1q independent mechanisms. The lectin pathway therefore could be one of the possible targets of C1 INH leading to neuroprotection.

Furthermore it was shown that uncontrollable MAC formation is detrimental for cerebral injury. This was shown in CD59a deficient mice which had increased infarct sizes compared to wild type controls following transient cerebral ischemia using the MCAO stroke model.

Finally, the lectin pathway activation complex is believed to be triggered by the altered glycocalyx pattern on the surface of oxygen deprived cells (Schwaeble *et al.* 2011, Gorsuch *et al.* 2012). This ability makes the lectin pathway a promising target for investigation in the secondary damage of cells after an ischaemic stroke incidence and gives a new promising area of research. The involvement of the lectin pathway of complement activation in inducing tissue damage following cerebral IRI has been indeed proven in studies using MBL null mice as well as by using MBL inhibitors (Cervera *et al.* 2010, Orsini *et al.* 2012). In these studies it was shown that MBL depletion and inhibition is protective in cerebral IRI, conferring reduced infarct sizes in MBL deficient mice when compared to their wild type controls, while reduced infarct sizes were also observed when MBL inhibitors were administered even up to 24h after ischaemia when compared with their controls (Cervera *et al.* 2010, Orsini *et al.* 2012). This project aims to validate further the involvement of the lectin pathway in inducing tissue injury following cerebral IRI using MASP-2 deficiency and MASP-2 inhibition as a means of protection.

1.12 Available therapy

The only available therapeutic strategy for ischaemic stroke at the moment is via thrombolysis, whereby the blood supply to the infarcted area is restored to minimise the effects of ischaemia. Recombinant tissue plasminogen activator (rTPA) is the only thrombolytic drug used today, but is limited in its efficacy. TPA is only administered to patients after the confirmation of an ischaemic stroke and absence of any haemorrhagic events. This is necessary because administration of a thrombolytic in a haemorrhagic stroke would be detrimental due to increased haemorrhage. Moreover, this drug can

only be administered within three hours after the ischaemic event in trying to reduce the exposure of cells to hypoxia and thereby reducing further tissue damage. Administration after this time window would have no therapeutic event as maximal ischaemic damage occurs within 3 hours. The inflammatory reactions prolong the damaging events after the ischaemic signal. Targeting and minimising the damaging effects of inflammation would potentially offer reduced tissue damage. Identification of the involvement of mediators inducing damage in ischaemia and reperfusion injury, and ultimately inhibition of their activity, would be of high significance. Targeting inflammation could be one of the strategies that would potentially give a longer time window for administration of therapy and reduction of brain damage as more extensive inflammatory reactions take place even hours to days after the ischaemic event extending tissue damage.

1.13 Aims and objectives

The role of MASP-2 depletion and MASP-2 inhibition has not yet been examined in cerebral IRI and whether MASP-2 inhibition could be used to reduce tissue damage in the brain with a resultant better functional outcome has yet to be addressed. This research project aims to:

- establish to what extent the lectin pathway may contribute to the loss of CNS tissue by comparing the infarct volumes in MASP-2 deficient mice with the infarct sizes of MASP-2 sufficient mice in experimental models of transient cerebral ischaemia. The experimental models of stroke examined in this study were the middle cerebral artery occlusion (MCAO) stroke model and the 3-Vessel occlusion stroke model (3-VO).

- histologically assess cellular alterations as well as complement activation and deposition following transient cerebral ischaemia in wild type and MASP-2 deficient mice.

- quantify at the mRNA level any differences in markers of inflammation (i.e. cytokines) among wild type and MASP-2 deficient mice following ischaemia and reperfusion injury.

- assess the therapeutic potential of a transient inhibition of the lectin pathway activation using MASP-2 blocking antibodies administered in MASP-2 C57BL/6 sufficient mice.

Chapter 2: Materials and Methods

2.1 Subjects of study

For the purpose of this research *in vivo* based studies were performed on C57/Bl6 MASP-$2^{+/+}$ and MASP-$2^{-/-}$ mice at the age of 8 to 16 weeks old with a body weight of 18 to 35g. All procedures were conducted in accordance to the UK Animals (Scientific Procedures) Act, 1986.

2.2 Genotyping of MASP-$2^{-/-}$ mice:

2.2.1 Isolation of mouse genomic DNA

Genomic DNA was extracted and isolated from mouse ear snips according to the Promega wizard DNA Purification Kit. Mice ear snips were digested overnight at 55 OC using 250 µl nuclei lysis solution, 60 µl 0.5 M EDTA and 10 µl of 600 mAU/ml of proteinase K (Qiagen) with gentle shaking. Next day, 3µl of Rnase A solution (4mg/ml) was added and samples were incubated at 37°C for 15 min. Samples were left to cool and 100 µl of protein precipitation solution was added and mixed by vortexing at high speed for 20 seconds. The samples were chilled in ice for 5 minutes and the precipitated protein was removed by centrifugation at 3000 x g for 4 minutes. The clear supernatant containing DNA was removed carefully and transferred into 1.5 ml eppendorf tubes. 300 µl of room temperature isopropanol was added and mixed by inverting the tubes several times to precipitate the genomic DNA. The precipitated DNA was obtained by centrifugation at 10000 x g for 5 minutes at room temperature. 300 µl of 70% ethanol was used to wash the DNA pellet which was re-precipitated by centrifugation at 10000

x g for 5 minutes. The DNA pellet was air dried for 10-15 minutes and 50 µl of DNA re-hydration solution was added and incubated for overnight at 4°C. The prepared genomic DNA was then stored at 4°C.

Purified genomic DNA was used to identify MASP-2$^{-/-}$ from their wild type littermates using polymerase chain reaction (PCR) and the following primers:

Primer name	**Primer sequence**
M2screen_F1 (1)	5`-CAT CTA TCC AAG TTC CTC AGA-3`
Neo5_R1 (2)	5`-CTG ATC AGC CTC GAC TGT GC-3`
M2wto_R1 (3)	5`-AGC TGT AGT TGT CAT TTG CTT GA-3`

These primers can identify homozygous, heterozygous and wild type mice. The PCR reaction mixture consists of:

Reagents	**Volume**
Taq DNA polymerase (5U/µl, Thermo)	0.12 µl
Reaction buffer (10x, Thermo)	1.5 µl
dNTP mix (10mM, Promega)	0.3 µl
$MgCl_2$ (25mM, Thermo)	1.5 µl
M2screen_F1 (Eurofins)	1.5 µl
M2wto_R1 (Eurofins)	1.5 µl
Neo5_R1 (Eurofins)	1.5 µl
Nano pure water	6.08 µl
DNA (200ng/µl)	1 µl

The cycling program was run under the following conditions:

Step	**Temperature (°C)**	**Duration (s)**	**Step repeats**
Initial denaturation	95	90	1
Denaturation	95	30	35
Annealing	62	30	35
Elongation	72	30	35
Final elongation	72	300	1
	4	∞	

Amplification products were finally run on a 1% agarose gel.

2.3 Mouse models of cerebral stroke

2.3.1 Middle cerebral artery occlusion (MCAO) - Stroke model A'

Transient focal ischaemia for 60 min followed by 24 hours of reperfusion was induced using MCAO. Buprenorphine (Vetergesic) diluted in saline (0.1mg/kg) was pre-operatively administered to the animals as an analgesic as well as for hydrating operated mice. Initial anaesthesia was induced with a mixture of 3 L/min isofluorane followed by maintenance anaesthesia at 1 to 2 L/min. O_2 and N_2O levels were kept constant at 1L/min and 0.8L/min respectively. Body temperature was maintained at around 36°C using a heating blanket. Via a neck ventral incision, the right common carotid artery (CCA) and its branch, the external carotid artery (ECA), was revealed (see figure 2.1). A 6.0 silk suture was then used to occlude permanently the lower part of the CCA and ECA to prevent bleeding and false introduction of the filament into the ECA. A 0.083 mm thick filament (Drennan) with a thermomelting glue coated end was advanced in the internal carotid artery (ICA) directing the filament to the MCA for occlusion via an incision made in the CCA (Gibson *et al.* 2005). Blood flow measurement was monitored using Laser Doppler (Moor Instruments, UK) before and after introduction of ischaemia to ensure occlusion by the filament. These 2cm long filaments were manually glue coated and colour marked for 1cm at the front ends prior to surgery. The introduction distance from the CCA cut to the MCA was around 1 cm long hence the colour marking of the filaments. The MCA was transiently occluded for 1 h once laser Doppler recordings were reached ensuring MCA occlusion and the filament was retracted upon completion of the hour. Mice that did not meet the required levels of ischaemia (70% reduction in blood flow upon insertion of the filament) were excluded.

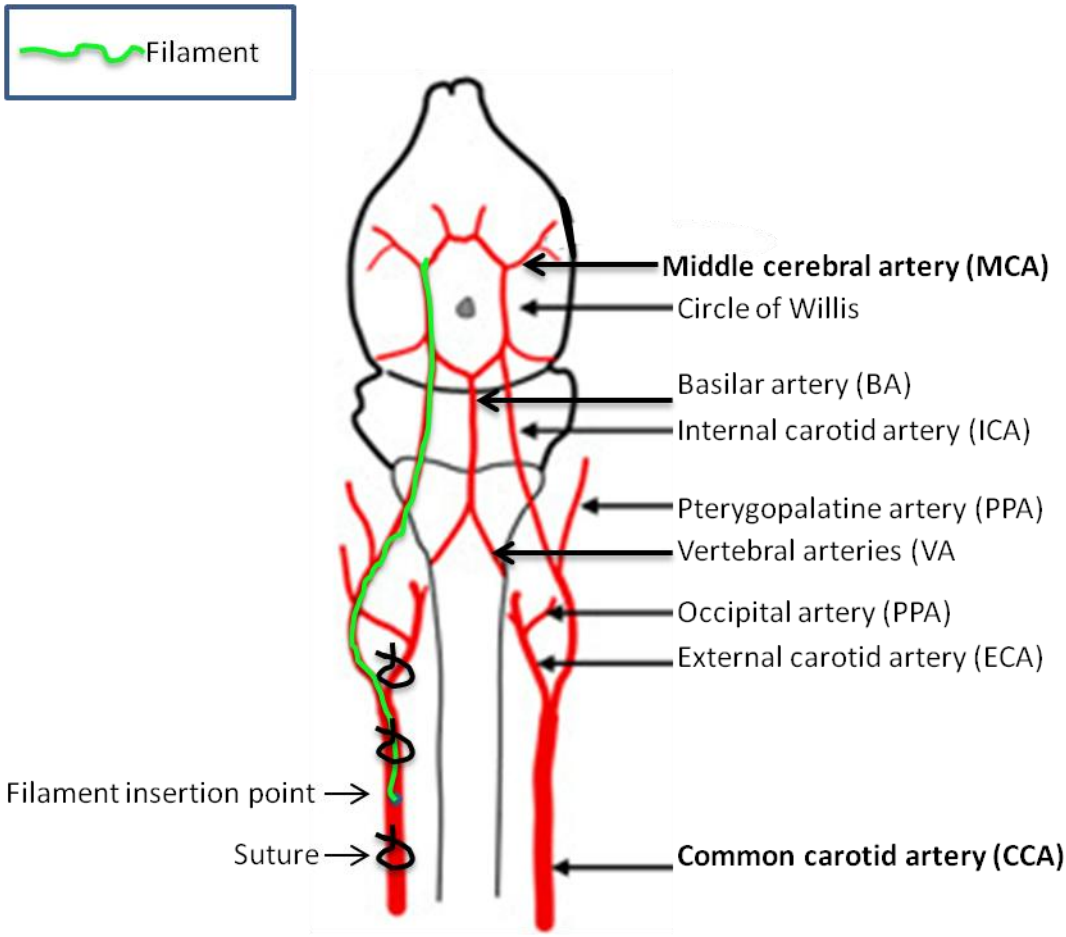

Figure 2.1: Diagram of the cerebrovascular anatomy in mouse showing the procedure that was used in the MCAO model of stroke.

The right common carotid artery (CCA) and its branch, the external carotid artery (ECA), were revealed. A silk suture was then used to occlude permanently the lower part of the CCA and ECA to prevent bleeding and false introduction of the filament into the ECA. The occluding filament was advanced in the internal carotid artery (ICA), directing the filament to the beginning of the MCA for occlusion via an incision made in the CCA. Upon cerebral blood flow decrease to 30% the ischaemic time was initiated and lasted for 1h. The filament was later on withdrawn allowing reperfusion. The diagram was modified from Engel et.al, 2011 (Engel *et al.* 2011).

2.3.2 Three vessel occlusion (3VO) surgery - Stroke model B'

The same anaesthesia protocol was used in this model as described for MCAO. As described by Yanamoto *et al.* 2003 (Yanamoto *et al.* 2003), via a ventral midline incision of the neck, the two common carotid arteries (CCA) were exposed followed by clamping of the left CCA using an aneurism clip (see figure 2.2). This reduces bleeding

during the procedure to cauterise the ipsilateral middle cerebral artery (MCA). Following the left CCA clipping, the left zygomatic arch was removed to enable access to the skull and the middle cerebral artery. A 1 mm thick burr hole was opened 1 mm superior–rostral to the foramen ovale to allow access to the MCA followed by its permanent cauterisation using a bipolar coagulator (Aura, Kirwan Surgical Products). Cauterisation was performed at the lateral edge of the left olfactory tract. After the MCA occlusion complete ischaemia was induced for 30 minutes by the clipping of the right CCA. During the ischaemic time the head wound was closed. After the termination of ischaemia both clips were removed allowing reperfusion for 24 h or for shorter time points depending on the study requirements. Sham operations performed included the whole procedure taking place without the dual common carotid artery occlusion and MCA cauterisation. Further test sham operations were performed to ensure that infarctions in the brain where induced by simultaneous CCA and MCA occlusions whereby both CCA were occluded for 30 min without MCA cauterisation as well as cauterisation of MCA without CCA occlusions.

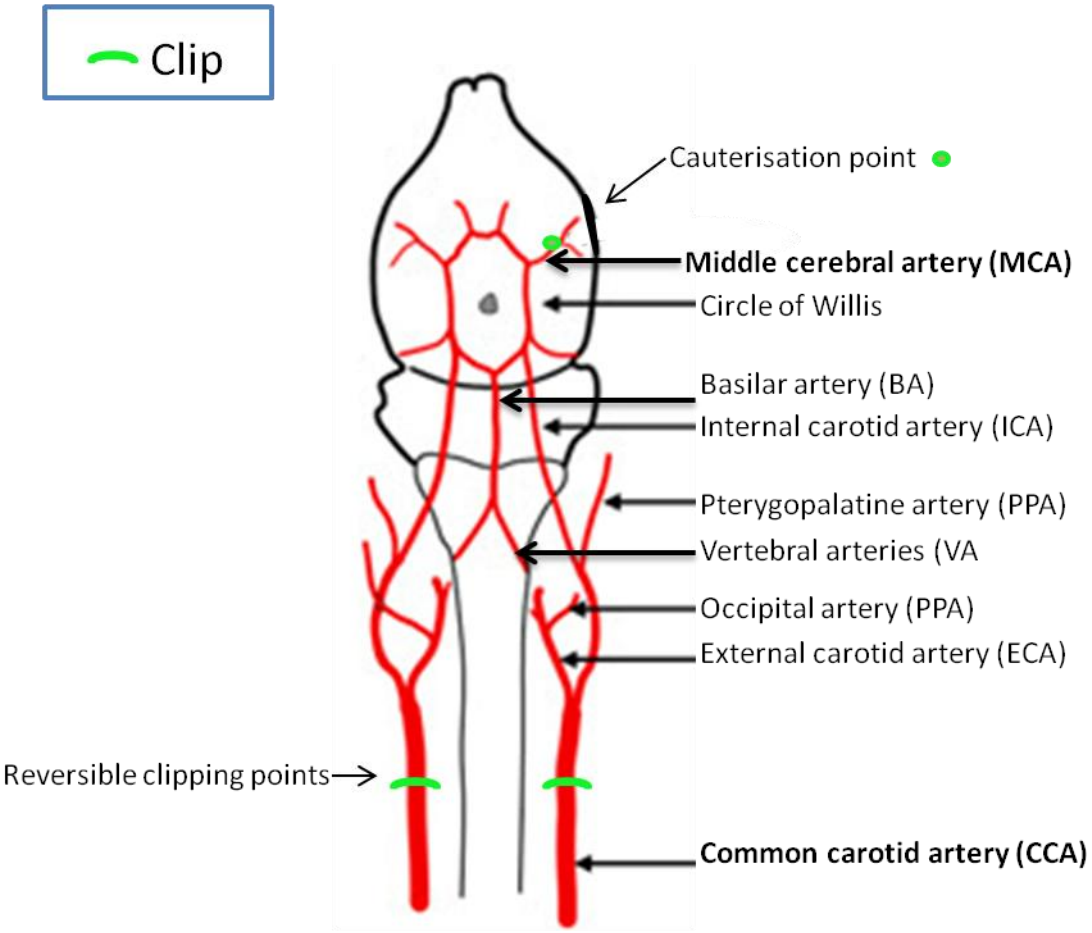

Figure 2.2: Diagram of the cerebrovascular anatomy in mouse showing the procedure that was used in the 3-VO model of stroke.

Following the left common carotid artery (CCA) clipping, the middle cerebral artery (on the ipsilateral site) was exposed and permanently cauterised at the lateral edge of the olfactory tract. The right CCA was immediately clipped and occluded, initiating the ischaemic time that lasted for 30 min. Upon completion of the ischaemic time the two CCA clips were removed allowing reperfusion for the desired period of time. The diagram was modified from Engel et.al, 2011 {{168 Engel,O. 2011}}.

2.4 Schedule 1 terminal procedures

Mice were culled by schedule 1 terminal procedures either by cervical dislocation or overdose of CO2. For the latter initiating concentrations of oxygen were set at 1 L/ml and CO2 at 0.3 L/ml each gradually decreasing or increasing respectively until death.

2.5 Infarct size measurements

After 24 h of reperfusion mice were killed via cervical dislocation and brains were removed and sliced into 1 mm thick slices using a pre-cooled brain matrix. Infarct size volume after ischaemia was measured using 2, 3, 5- Triphenyltetrazolium chloride (TTC), which is a metabolic cell indicator of mitochondrial activity (Bederson *et al.* 1986, Lin *et al.* 1993). Mitochondrial activity due to dehydrogenase enzymes is believed to reduce TTC into red formazan (Lippold 1982). Therefore, the red colouring in brain sections indicates the normal, non-infarcted tissue whereas non-coloured, white areas indicate the infarcted tissue which is metabolically compromised (Bederson *et al.* 1986). Brain sections were stained with 2% TTC in saline at room temperature for 30 minutes in the dark. Afterwards the sections were fixed in 10% formalin (Sigma) and stored in the dark at 4°C. Digital images were taken and analysed using IMAGE J software designed to calculate the infarct volume. The infarct volume was calculated in a way to avoid overestimation of the infarct area by oedema. This was done in each individual section having a lesion by dividing the measured infarct area by the oedema index. The latter was calculated by dividing the total volume of the hemisphere ipsilateral to the MCA by the area of the contralateral hemisphere (Yanamoto *et al.* 2003)The infarct sum from all the infarcted slides was then added up to give the total volume of infracted size.

Total Infarct size = sum from: Infarct area / (oedema index*) x 1mm (slide thickness)

***Oedema index= area of the ipsilateral hemisphere / contralateral hemisphere**

2.6 Neurological scoring

A 28 point neurological scale was used to assess neurological deficits in individual mice with higher scoring from the sum of the 7 individual tests would indicate worse neurological impairments (Figure 2.3) (Clark *et al.* 1998).

Scoring	**0**	**1**	**2**	**3**	**4**
Body symmetry (open bench top)	Normal	Slight asymmetry	Moderate asymmetry	Prominent asymmetry	Extreme asymmetry
Gait (open bench top)	Normal	Stiff, inflexible	Limping	Trembling, drifting, falling	Does not walk
Climbing (gripping surface, 45° angle)	Normal	Climbs with strain, limb weakness present	Holds onto slope, does not slip or climb	Slides down slope, unsuccessful effort to prevent fall	Slides immediately, no effort to prevent fall
Circling behaviour (open bench top)	Not present	Predominantly one-sided Turns	Circles to one side (not constantly)	Circles constantly to one side	Pivoting, swaying, or no Movement
Front limb symmetry (mouse suspended by its tail)	Normal	Light asymmetry	Marked asymmetry	Prominent asymmetry	Slight asymmetry, no body/limb movement
Compulsory circling (front limbs on bench, rear suspended by tail)	Not present	Tendency to turn to one side	Circles to one side	Pivots to one side sluggishly	Does not advance
Whisker response (light touch from behind)	Symmetrical response	Light asymmetry	Prominent asymmetry	Absent response ipsilaterally, diminished contralaterally	Absent proprioceptive response bilaterally

Figure 2.3: The 28 point neurological scoring system

The worse neurological deficits come with a higher scoring sum (Clark *et al.* 1998).

2.7 Tissue preparation for immunohistochemistry

2.7.1 Perfusion-fixation

Mice were anaesthetised for terminal procedures with 5 L/min of isofluorane and 1 L/min of oxygen. The chest was cut open revealing the heart. A butterfly needle (size NG 23) was inserted and secured for perfusion in the left ventricle of the heart and a cut in the aorta artery was performed. Immediately after this, the animal was perfused with heparinised 1x PBS (2 μg/ml heparin) with an applied pressure of 100 mmHg induced by a sphygmomanometer. Perfusion continued until the blood was cleared. 4% paraformaldehyde in PBS was then used to perfuse and fix the tissue for 12 min. The pressure was maintained as described previously. Brains were then removed and left for 24 h in 4% paraformaldehyde. Fixed brains were then transferred in 15% sucrose solution for 24 h followed by another 24 h of preservation in 30% sucrose to prevent crystal formation from the subsequent freezing process. Brains were then embedded in OCT and were kept frozen in -80°C. For immunohistochemistry tissue was cryostat sectioned at 12 μm and mounted on poly-lysine coated microscope slides. Brain sections were then stored at -80°C and staining for each of the markers was performed at least on two animals. All tissues used for immunohistochemistry were treated as described above, except for liver tissue, used as a positive control, which was snap frozen for 1 min in isopentane which was pre incubated for 10 min in dry ice. The tissue was then embedded in OCT and kept in -80°C until sectioned.

2.7.1.1 Black Indian ink perfusion

For Indian ink perfusions the same procedures were followed as described before but instead of 4% paraformaldehyde the mice were perfused for around 2 min with 30%

Black Indian ink (Winsor and Newton) in heparinised (2 μg/ml) PBS. The tissue was then preserved in 4% paraformaldehyde.

2.7.2 Immunohistochemistry

For each group of mice (i.e. WT and MASP-2 KO) two representative animals were used for staining of each marker. Tissue sections were further fixed on the slide for 10 min in ice cold acetone and air dried for a few seconds. Slides were then washed 3 times in 1x PBS. Pap pen was then used to create a hydrophobic barrier around the tissue to keep the antibody diluents in place. Sections were incubated in blocking buffer (10% Normal goat serum (NGS) and 3% bovine serum albumin (BSA) in PBS) for 1 h at room temperature, to saturate non-specific antibody binding sites, followed by 5 min washes (x3) in PBS. Sections were then incubated with appropriate concentrations of primary antibody in blocking buffer (see table 2.1) for 1 h at room temperature. . Brain sections were washed as described before followed by 1 h incubation in dark with the appropriate fluorescently labelled secondary antibody (1:1000) in PBS (Table 2.2). The following steps were also performed in the dark. Washing and counterstaining with Hoechst 33342 (fluorescent nuclear marker) at a concentration of 2.5 μg/ml in PBS for 5 min was finally performed. Tissue was then washed 3 times with PBS and 2 times with water. Aqua-polymount (Polysciences) was used as a mounting agent. When dual staining was being performed the same procedures were followed with simultaneous incubation of the primary antibodies and simultaneous incubation of the secondary antibodies. Negative controls used for assessment of secondary antibody cross reactivity with the tissue were performed by staining the tissue with only the secondary antibody. Pictures were taken using a Zeiss AxioVision 200 fluorescence microscope

or a Zeiss LSM510 laser scanning confocal microscope. The antibodies used for screening of complement deposition and activation, inflammation and different brain cells were the following (Tables 2.1 and 2.2):

Antibody	**Raised in**	**Source (code)**	**Marker for**	**Concentration**
C3c	Rabbit	Dako (A0062)	Complement activation	1/100
C1q	Rat	mAb D6.1s	Recognition molecule for classical pathway	1/50
MBL-A				
MBL-C	Rat	Hycult biotechnology (HM1038)	Recognition molecule for lectin pathway	1/100
Ficolin A	Rabbit	T. Fujita (7mg/ml)	Recognition molecule for lectin pathway	1/250
Collectin 11	Rabbit	1.26mg/ml	Recognition molecule for lectin pathway	1/250
Neuronal nuclei (NeuN)	Mouse	Millipore (MAB377)	Neurons	1/250
Glial fibrillary acidic protein (GFAP)	Rabbit	DakoCytomation	Astrocytes	1/500
Ionised calcium binding adaptor molecule 1(Iba1)	Rabbit	Wako (019-19741)	Microglia	1/200

Table 2.1: Primary antibodies

Antibody against	**Raised in**	**Against**	**Source (Code)**	**Concentration**
Alexa Fluor 488	Goat	Mouse IgG (H+L) (A11029)	Invitrogen	1/1000
Alexa Fluor 546	Goat	Rat IgG (H+L) (A11081)	Invitrogen	1/1000
Alexa Fluor 488	Goat	Rabbit IgG (H+L) (A11034)	Invitrogen	1/1000

Table 2.2: Secondary Antibodies

2.8 mRNA quantification for gene expression

mRNA up-regulation of genes of interest was quantified using real time PCR. Total RNA was isolated from mouse tissue, reverse transcribed into cDNA and finally quantified using real time PCR relative to GAPDH (housekeeping gene) mRNA (see below). For tissue collection, mice were culled by cervical dislocation. Mouse tissues were removed and flash frozen for 1min in dry ice cold iso-pentane (Fisher Chemical). For mRNA isolation from brain tissues, the two hemispheres were snap frozen separately into ipsilateral and contralateral sites after cerebellum was carefully separated (which was not of interest as the infarctions were not expanding to this area). The tissue was then stored in -80°C for later use.

2.8.1 Extraction of total RNA

Total RNA was isolated using the NucleoSpin RNA II Kit (Macherey- Nagel) according to the manufacturer's instructions. 30mg of each tissue was homogenised on dry ice using mortar and pestle. The tissue was then lysed by vortexing vigorously in 6µl of β-mercaptoethanol and 600µl of Buffer RA1. The lysate was then spun down at 11000 rpm for one minute through NucleoSpin Filter to clear tissue lysate and reduce viscosity. The homogenised lysate was then mixed with 600µl ethanol to adjust the RNA binding conditions. The lysate was passed through NucleoSpin RNA II column and centrifuged for 30 seconds at 11000 rpm to allow RNA binding to the column. For more effective rDNase treatment the silica membrane with the bound RNA was then desalted using the membrane desalting buffer (MDB) followed by centrifugation at 11000 for another 30 seconds. DNA was digested using rDNase in rDNase buffer (10 µl and 95 µl respectively) for 15min at 37°C. Finally the silica membrane was washed

3 times using RA2 and RA3 buffers. Excess buffers were removed by centrifugation at 11000 rpm for 2 minutes and purified RNA was eluted in 60µl of RNase-free water upon centrifugation at 11 000 rpm for 1 min. RNA was then stored at -80°C until use.

2.8.2 Measurement of concentration and purity of RNA

The absorbance of purified RNA was measured at 260nm and 280nm using NanoDrop (Thermo Scientific). The purity of the RNA sample was determined by calculating the ratio between A_{260}/A_{280}. Ratios of 1.9 to 2.1 represent pure RNA.

2.8.3 cDNA generation

One µg of purified RNA was reverse transcribed into cDNA using SuperScript II Reverse Transcriptase (Invitrogen) according to the instruction manual under the following cycling conditions:

Steps		**Temperature (°C)**	**Duration (min)**
1	Denaturation step	70	10
2	Extension	45	60
3	Enzyme inactivation	70	10
4		4	∞

The following RNA mixture was added and the mixture heated to 70°C to unfold the RNA strands:

	Per reaction
1µg RNA in nuclease free water	20 µl
500 ng/µl Oligo$(dT)_{23}$ anchored primers (Sigma Aldrich)	1 µl

When the denaturation step was finished and the temperature reached 45°C the following enzyme mixture was added for each sample:

	Per reaction
Reverse Transcriptase buffer 5x (Invitrogen)	10 µl
DTT (0.1 M, Invitrogen)	10 µl
dNTPs (10 mM, Promega)	5 µl
RNaseOUT (40 U/µl, Invitrogen)	0.5 µl
SuperScript II reverse transcriptase (Invitrogen)	1 µl
Nuclease-free water	2.5 µl

After cDNA synthesis, one µl of RNase H was added to each sample and incubated at 37°C for 20 min to remove any remaining RNA.

2.8.4 Analysis of gene expression using Real time PCR

Real time PCR was chosen for quantification of the expression of different markers of inflammation including: IL6, IL10, MIP-2 and C1q. Glyceraldehyde-3-phosphate dehydrogenase (GAPDH) was chosen as the housekeeping gene, to assess the baseline levels of cDNA synthesis and to normalise the expression of genes. 1 µl of cDNA, equivalent to 20 ng, was amplified for quantification using the QuantiTect SYBR Green, (Qiagen) mastermix (7.5 µl SYBR Green, 1.5 µl of each of the 5 µM primers, 2.5 or 3.5 µl nuclease-free water). Equal amounts (5 µl) from cDNA samples were pooled together as a separate sample that was used for four serial dilutions (1/5, 1/10, 1/25, 1/125) and the generation of the standard curve in each amplification run. Dilutions of the standard curve, with the exception of the pooled sample that was always set at a concentration of 1, were prepared differently for each gene depending on

its expression levels. The quantification of each individual sample in each run was calculated using as a template the standard curve. The reactions were performed on Roche Applied Science LightCycler Real Time PCR instrument (Mannheim, Germany). The 15 µl reaction mixtures were quantified based on the fluorescence signal generated at the end of each cycle while the specificity of the products was assessed from melting curve analysis (see figures 2.4, 2.5 and 2.6). The cycling program used was the following:

Program	**Denaturation**			**Type**	**None**	**Cycles**	**1**
Segment Number	Temp. Target (^oC)	Hold Time (Sec)	Slope (^oC/Sec)	2^o Target Temp (^oC)	Step Size (^oC)	Step Delay (Cycles)	Acquisition Mode
1	95	900	20	0	0	0	None
Program	**Cycling**			**Type**	**Quantification**	**Cycles**	**45**
Segment Number	Temp. Target (^oC)	Hold Time (Sec)	Slope (^oC/Sec)	2^o Target Temp (^oC)	Step Size (^oC)	Step Delay (Cycles)	Acquisition Mode
1	95	15	20	0	0	0	None
2	58	20	20	0	0	0	None
3	72	20	15	0	0	0	Single
Program	**Melt**			**Type**	**Melting curve**	**Cycles**	**1**
Segment Number	Temp. Target (^oC)	Hold Time (Sec)	Slope (^oC /Sec)	2^o Target Temp (^oC)	Step Size (^oC)	Step Delay (Cycles)	Acquisition Mode
1	95	2	20	0	0	0	None
2	65	10	1	0	0	0	None
3	95	0	0.1	0	0	0	Continuous
Program	**Cool**			**Type**	**None**	**Cycles**	**1**
Segment Number	Temp. Target (^oC)	Hold Time (Sec)	Slope (^oC /Sec)	2^O Target Temp (^oC)	Step Size (^oC)	Step Delay (Cycles)	Acquisition Mode
1	40	30	20	0	0	0	None

Primer	**Sequence**	**Product Size**
GAPDH_F2 GAPDH_R1	5`-GTGCTGCCAAGGCTGTG-3` 5`-AGACAACCTGGTCCTCAGTGTA-3`	211bp
IL6_F IL6_R	5`-CAAAGCCAGAGTCCTTCAGA-3` 5`-CACTCCTTCTGTGACTCCA-3`	95 bp
IL10_F IL10_R	5'-CTTGCACTACCAAAGCCACA-3' 5'-TAAGAGCAGGCAGCATAGCA-3'	86 bp
C1q B-chain F1 C1q B-chain R2	5'-CTTCGAAAAGGTGATCACCA-3' 5'-CTGTGGCCTGCAGGTGA-3'	266 bp
MIP-2_F MIP-2_R	5'-ATCCAGAGCTTGAGTGTGAC-3' 5'-AAGGCAAACTTTTTGACCGCC-3'	90 bp

Table 2.3: Primer Sequences

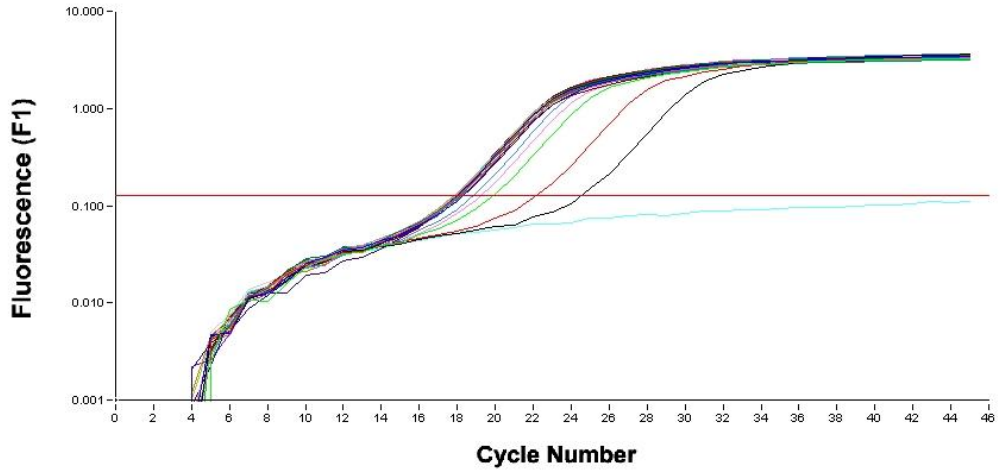

Figure 2.4: GAPDH amplification curve using real time PCR.

Each colour represents one sample. The graph represents the fluorescence intensity per cycle number of each of the amplified products in coloured lines. In fit points settings the background noise was removed by manually adjusting the threshold line at the beginning of the exponential curve phase.

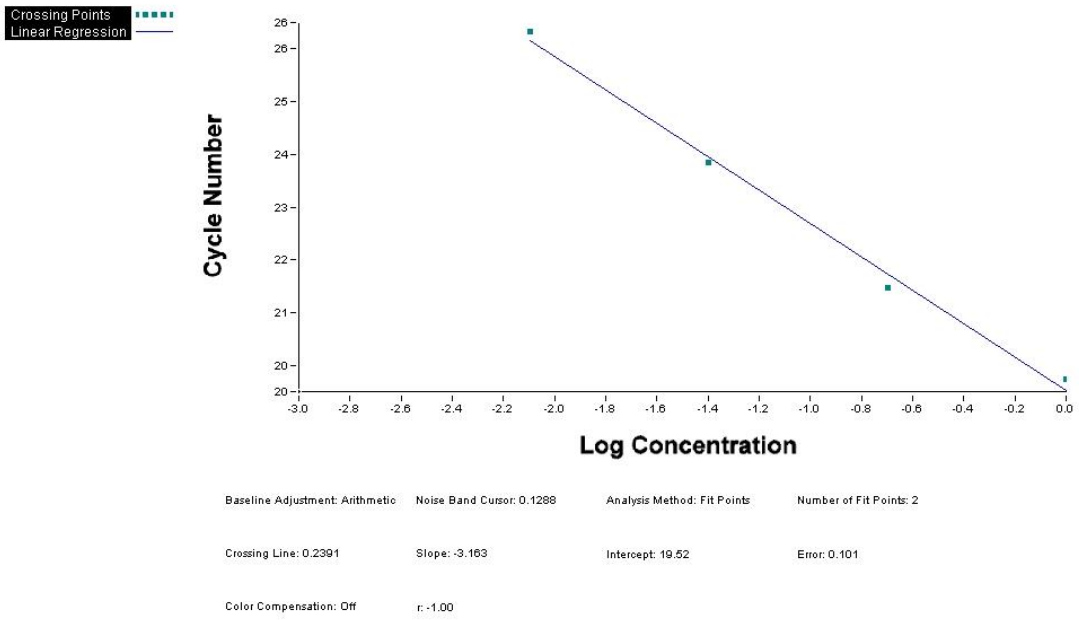

Figure 2.5: Standard curve in RT-PCR for cDNA quantification

Representative of a standard curve (cycle number vs log concentration) prepared by serial dilutions of the pooled sample used to relatively quantify the experimental cDNA copies in each individual sample.

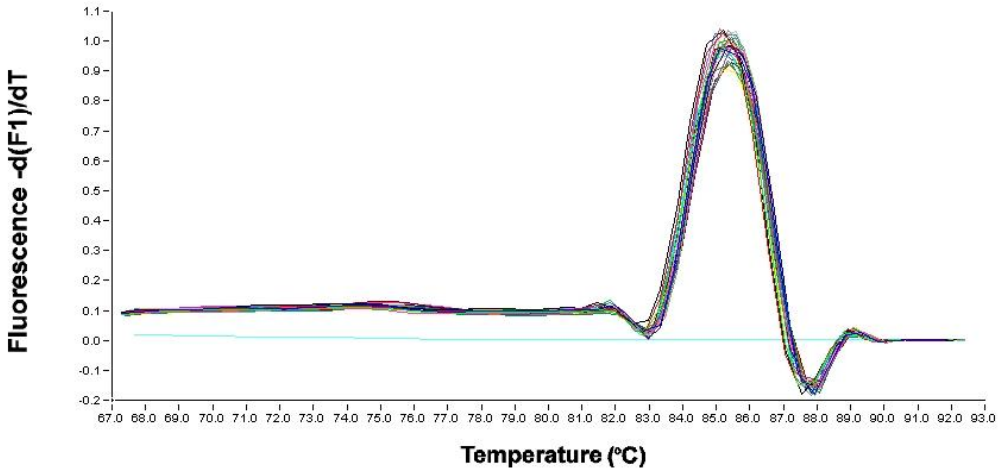

Figure 2.6: Melting curve of GAPDH prepared from fluorescence vs temperature of different samples following real time PCR.

The melting temperature equivalent to the peak of the curve is characteristic of the primer amplicon product. The single peak at the characteristic temperature in the curve signifies the specificity of the product as well as the linear line in light blue (absence of peak) in the negative control sample exempts sample contamination.

2.9 Serum preparation from blood

Any blood samples used in the study were isolated either by tail bleed or cardiac puncture. Blood was isolated and left to clot on ice for 2-6h followed by centrifugation at 12 000 rcf for 12 minutes at 4 °C. Serum was separated from the remaining blood components and stored in -80°C. Isolation and any use of serum was always performed on ice to prevent complement activation and subsequent depletion.

2.10 MASP-2 Inhibitory antibody

Omeros Corporation supplied all the MASP-2 inhibitory and isotype control antibodies used in this study. The mouse monoclonal IgG2a MASP-2 inhibitory antibody (mAb) AbD04211, as well as the isotype matched control antibody MOR 03207, were produced in transfected mammalian cells by AbD Serotec, Munich, Germany, subcontracted by OMEROS Corporation. The anti-human MASP-2 inhibitory antibody OMS646-016 (which gave a degree of cross reactivity with mouse MASP-2) was prepared by Catalent using a transduced CHO cell line and it was also used to assess its effect *in vivo*.

2.11 C3c assay using Enzyme linked immunosorbent assay (ELISA)

The assay is designed to assess lectin pathway dependent C3c deposition on mannan. Nunc Maxisorb microtiter plates were coated with 1µg/well mannan diluted in coating buffer (15 mM Na_2CO_3, 35 mM $NaHCO_3$, pH 9.6) and incubated overnight at 4°C. Residual protein binding sites were saturated by incubating the plate with 0.1% HSA-

TBS blocking buffer (0.1% (w/v) HSA in 10 mM Tris-CL, 140 mM NaCl, 1.5 mM NaN_3, pH 7.4) for 2 hrs or left overnight at 4°C. ELISA plates were washed in TBS/tw/Ca^{++} buffer (TBS with 0.05% Tween 20 and 5 mM $CaCl_2$). Serum samples that were stored in -80°C were slowly left to thaw on ice and 1% serum dilution from each sample was prepared in barbital buffered saline (BBS; 4 mM barbital, 145 mM NaCl, 2 mM $CaCl_2$, 1mM $MgCl_2$, pH 7.4) for the MASP-2 inhibitory studies. Wells receiving only BBS buffer were used as negative controls. Samples were loaded on ice and placed at 37°C for 15 min. Following incubation the plates were washed in TBS/tw/ Ca^{++} buffer (x4) and bound C3 was detected with a polyclonal anti-human-C3c Antibody (Dako, A0062) diluted in TBS/tw/ Ca^{++} buffer at 1:5000). The antibody was incubated for 1 hour at room temperature. Another washing step followed antibody incubation (x4) and administration of the secondary antibody took place using goat anti-rabbit IgG (whole molecule) conjugated to alkaline-phosphatase (Sigma A-3812) diluted 1:5000 in TBS/tw/Ca^{++}. This was incubated again for 1 h at room temperature. The extent of C3c deposition and subsequently lectin pathway activation was determined by addition of 100 µL substrate solution (Sigma Fast p-Nitrophenyl Phosphate tablets, Sigma) and incubation at room temperature. The absorption (OD) at 405 nm was then measured using the BioRad micro-titre ELISA plate reader model 608.

Chapter 3: MASP-2 Deficiency in Cerebral Ischaemia and Reperfusion Injury, Results Part A

3.1 MASP-2$^{-/-}$ mouse colony

For the generation of MASP-2 deficient mice a MASP-2 targeting construct (carrying a neomycin resistance gene as a selective marker with two cassettes containing defined regions of the murine *MASP2* gene) was used to disrupt MASP2 by homologous recombination in 129/Sv embryonic stem cells. This resulted in the replacement of exon 11, intron 11 and part of exon 12 (Figure 3.1). These exons encode the C-terminal part of the CCP-2 domain and an essential part of the serine protease domain respectively, resulting in a truncated MASP-2 protein devoid of the serine protease domain. After positive selection, clones carrying the recombinant allele were microinjected into C57BL/6J blastocysts generating chimeras. These chimeras were then backcrossed to C57BL/6J to allow transmission of the targeted allele. Subsequently, the heterozygous line containing the disrupted allele was backcrossed to a pure C57BL/6J background for 11generations (Schwaeble *et al.* 2011).

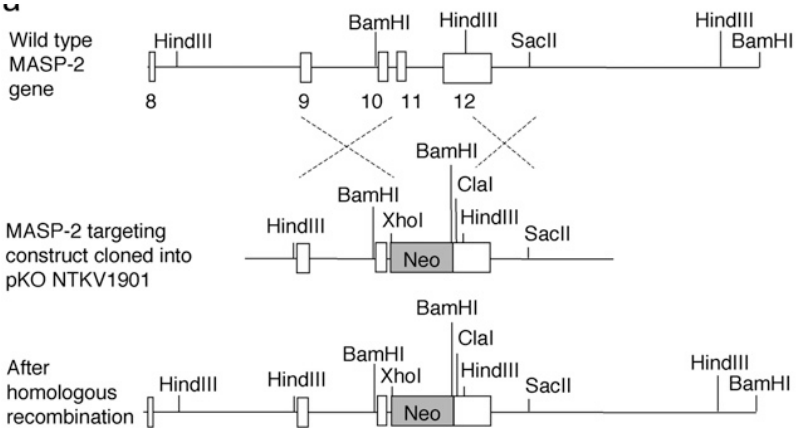

Figure 3.1: Establishment of the MASP-2 deficient mouse line

Homologous recombination of the MASP-2 targeting construct (cloned in pKO NTKV1901 vector and carrying the Neomycin cassette) with the wild type MASP-2 gene in the establishment of the MASP-2 deficient mouse line. Replacement of exon 11 and part of exon 12 leads to a truncated and dysfunctional MASP-2 protein in homozygous MASP-2 deficient mice (Schwaeble *et al.* 2011).

3.2 Genotyping

As it is necessary to constantly monitor and validate the homozygosity of the disrupted allele of all mice used in the studies, genotyping by PCR was carried out before and after each experimental procedure. Three primers were used in a heteroduplex PCR analysis. Primers 1 (M2screen_F1) and 2 (Neo5_R1) were designed to amplify a 500 bp PCR product from the truncated allele with the reverse primer hybridising to the neomycin cassette of the targeting construct present only on the MASP-2 disrupted allele. Similarly primers 1 and 3(M2wto_R1) were designed to amplify the wild type allele with the reverse primer hybridising to the wild type genomic sequence which is replaced and thus absent in the MASP-2 allele with the insertion of the neomycin cassette. The amplification product from the wild type allele is 750 bp long. DNA of homozygous MASP-2$^{-/-}$ mice gives rise to a single 500 bp PCR product only, while

homozygous DNA of MASP-$2^{+/+}$ gives rise to a single 750 bp PCR product and DNA of the heterozygous MASP-$2^{+/-}$ gives rise to both PCR products as they carry both alleles (figure 3.2).

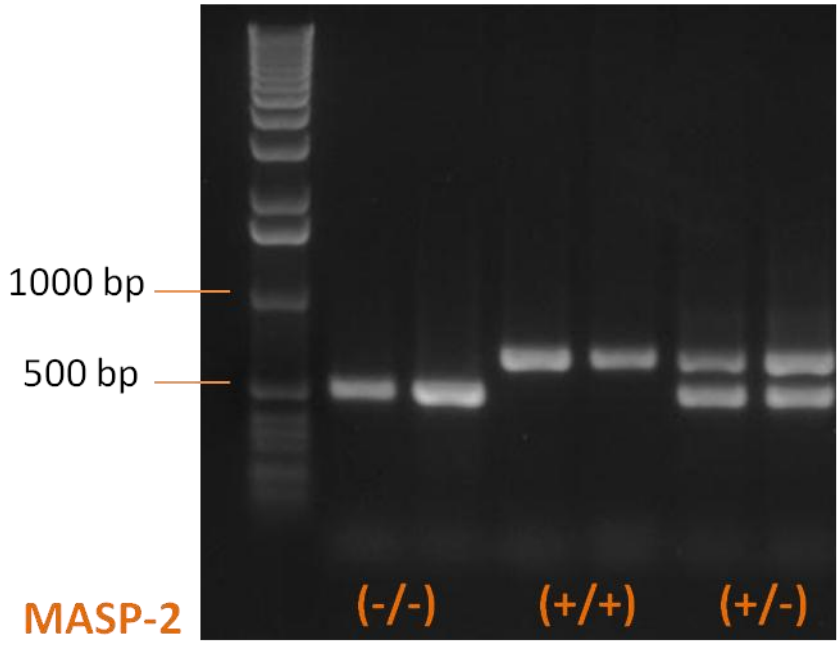

Figure 3.2: PCR products from MASP-2 genotyping.

DNA of MASP-$2^{-/-}$ mice gives rise to a single 500 bp PCR product, DNA of MASP-$2^{+/+}$ gives rise to a single 750 bp product and MASP-$2^{+/-}$ gives rise to both products.

3.3 Middle Cerebral Artery Occlusion stroke model (MCAO)

The middle cerebral artery occlusion (MCAO) model is the most frequently used experimental stroke model in mouse stroke research. MCAO was performed in these studies using female MASP-2 sufficient and MASP-2 deficient mice for the duration of 1 h of ischaemia followed by 24 h of reperfusion. This was sufficient to induce a lesion extending in the cortical and subcortical regions of the left hemisphere (see figure 3.5). The extent of the damage in the WT and MASP-$2^{-/-}$ mice was assessed with TTC

staining performed 24 h after the ischaemic insult. The cerebral blood flow (CBF) was being monitored during the operation to ensure that at least 70% decrease in the blood flow was observed upon insertion of the filament in the MCA for the initiation of the ischaemic time (see figure 3.3) and continued for at least 5 min post filament insertion. A general 47.6% (SEM +/-) cerebral blood flow reduction was observed in wild type and MASP-$2^{-/-}$ upon occlusion of the CCA during the process of the operation and prior to MCA occlusion. However, to ensure a sufficiently uniform blood flow reduction in the MCA of all operated mice, 100% blood flow was set for the recording taken after CCA occlusion and before the insertion of the filament in the MCA. The percentage of cerebral blood flow (CBF) was not statistically different following the occlusion of the MCA amongst WT and MASP-$2^{-/-}$ (14.8% +/- 3.18 SEM and 20.7% +/- 3.05 SEM respectively). Animals not reaching the required 70% decrease in the blood flow after the insertion of the filament and subsequent occlusion of the MCA were excluded. This resulted in infarct sizes which were not statistically different in the MASP-$2^{+/+}$ with a mean of 46.42mm^3 and the MASP-$2^{-/-}$ with a mean of 33.98mm^3, whilst no lesions were observed in sham operated animals (see figures 3.4 and 3.5). Although these MCAO operated mice showed a significant CBF decrease (70%) for at least 5 min post filament insertion, a wide variability in the resulting lesion sizes was observed (including mice with no lesions making the collection of samples more difficult). In order to avoid any experimental uncertainties, measurements of blood flow throughout the ischaemic time were taken as well as the level of reperfusion upon withdrawal of the obstructing filament. Interestingly, different profiles of CBF were observed throughout the ischaemic time as well as during the reperfusion period (see figure 3.6). The first profile observed in either WT or MASP-2 deficient mice was the one following the successful occlusion of the MCA during the duration of 1 h and leading to a more than

70% decrease of the CBF. This, however, was followed by insufficient reperfusion following the withdrawal of the filament. Within this CBF profile unsatisfactory infarctions were noticed, of which some mice appeared to show no defined infarcts at all, while other mice appeared with lesions in the usual cortical and subcortical areas and other mice died minutes post operation with lesions covering half of the hemisphere (see figure 3.7). During the second observed CBF profile, the CBF was first reduced to 30%, but then the CBF profile revealed an early reperfusion prior to filament withdrawal, despite the fact that the position of the filament did not changed. Another profile was recorded in which a fluctuation of CBF was observed during the ischaemic time. As before, the lesions in the latter two CBF profiles were again not informative resulting in either small or not measurable lesions (Figure 3.6 and figure 3.7).

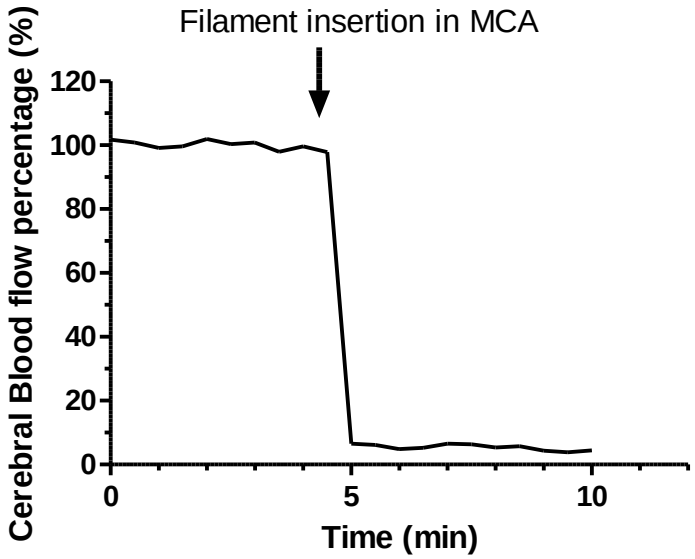

Figure 3.3: Cerebral blood flow after a successful intraluminal filament application

A representative successful MCAO cerebral blood flow recording expressed as a percentage 5min before the insertion of the intraluminal filament in the MCA and 5 min after showing more than 70% decrease in CBF.

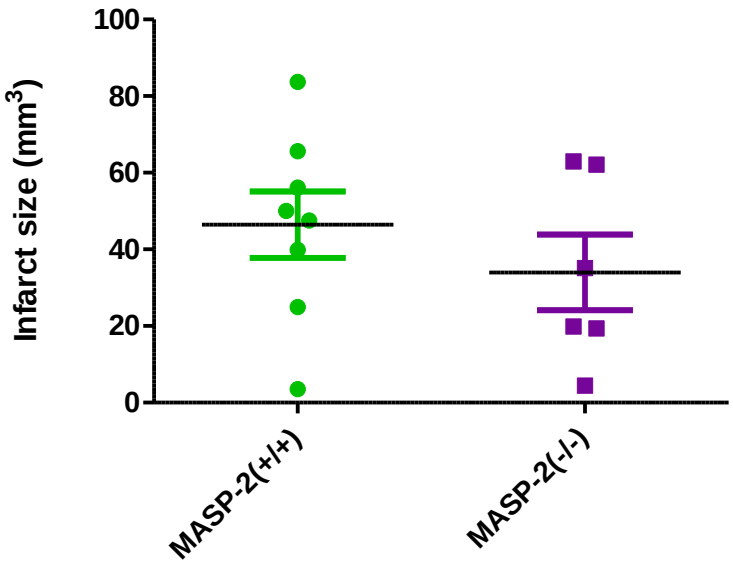

Figure 3.4: Infarct sizes (mm^3) obtained following TTC staining of coronal brain sections after 1 h of ischaemia and 24 h of reperfusion using the MCAO stroke model.

This model produced a superficially visible, but statistically not significant difference (p=0.363) in infarct sizes between MASP-$2^{+/+}$ (n=8) and MASP-$2^{-/-}$ (n=6) mice. Data are reported as scatter-dots with mean values (black bars) and standard error bars (coloured bars).

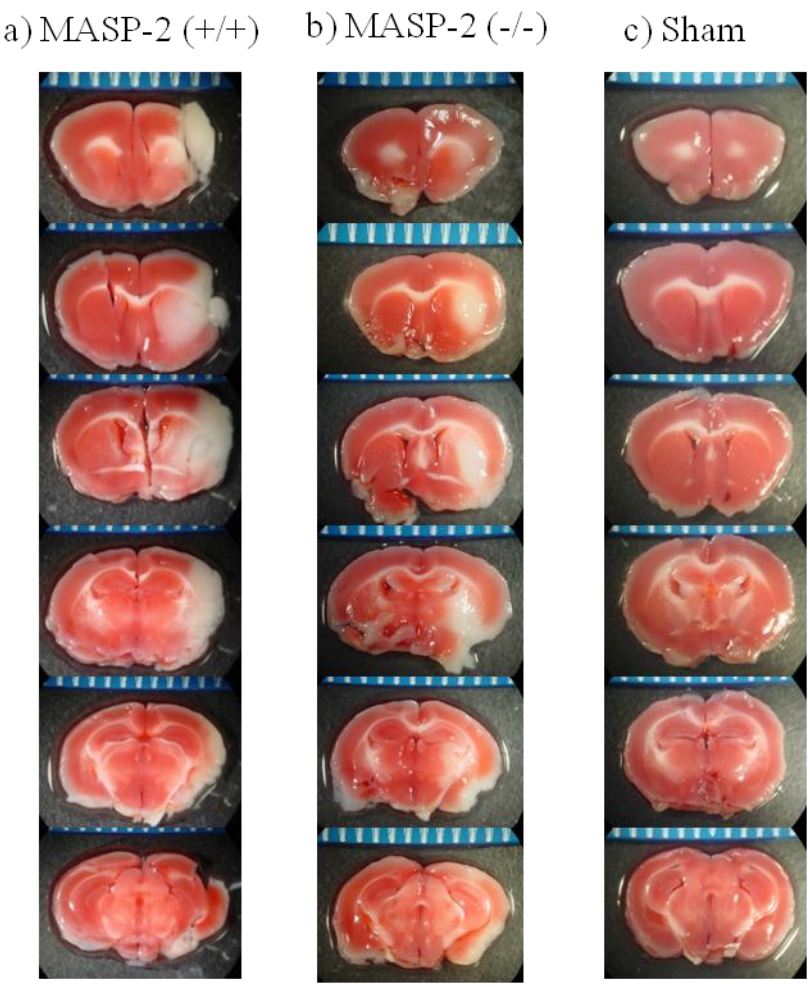

Figure 3.5: TTC staining following MCAO

TTC staining following MCAO at 1 h of ischaemia followed by 24 h of reperfusion; a) coronal brain sections from a WT, b) a MASP-2 deficient and a sham operated mouse (c) indicating in white colour the subcortical and cortical lesions that developed following operation. MASP-2 deficient mice show a trend towards reduced infarct sizes. Sham operated animals have undergone the MCAO procedure without occlusion of the MCA by the intraluminal filament.

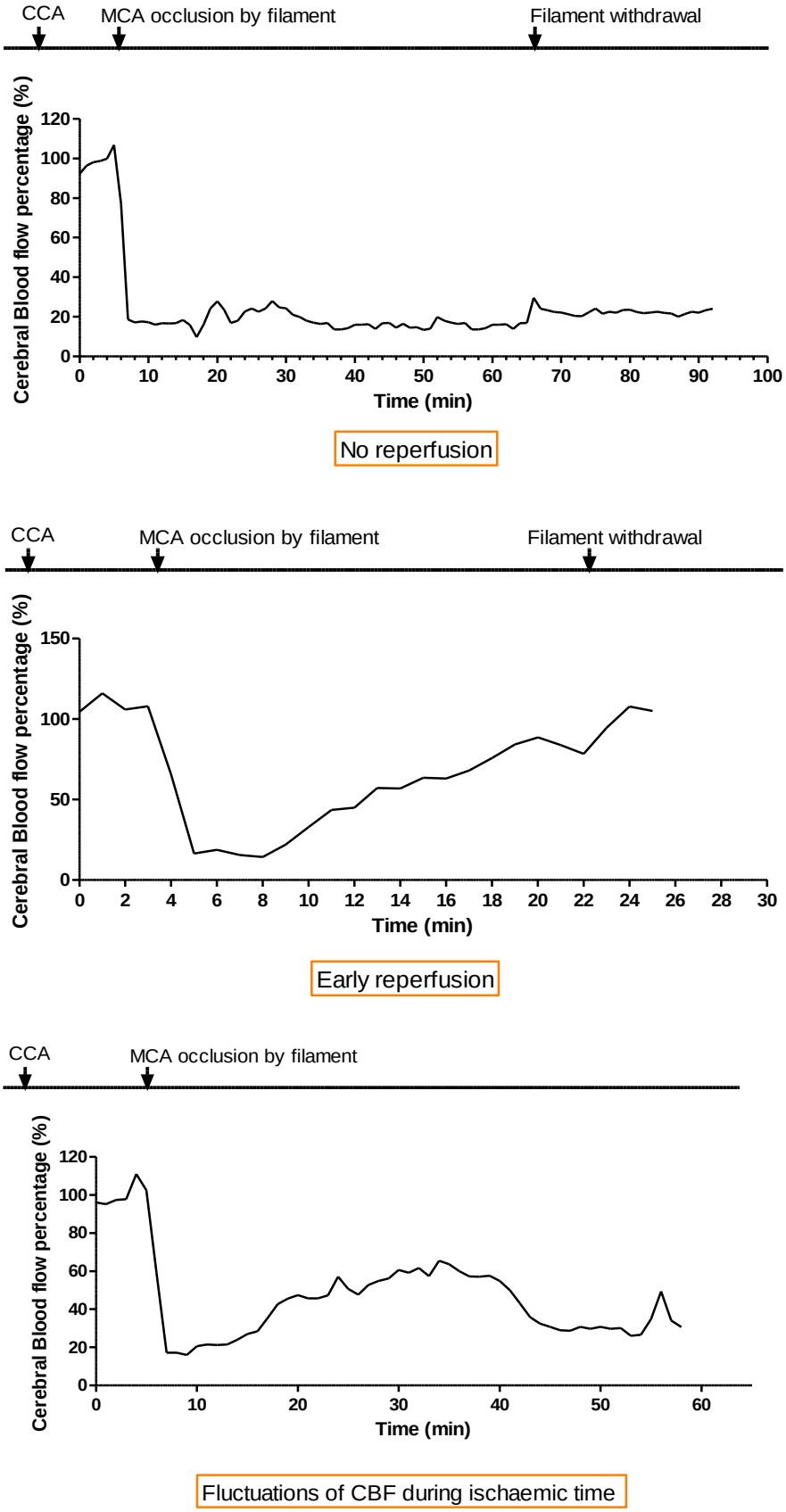

Figure 3.6: Cerebral blood flow percentage during the ischaemic time of the MCAO stroke model indicating the variable CBF patterns.

Figure 3.7: Variable infarct size profiles observed when the CBF was successfully decreased up to 30% followed by an unsuccessful reperfusion.

A) No lesion, B) lesion in the cortical and subcortical regions, C) lesion covering almost half of the hemisphere collected post mortem of an animal dying 10 minutes after the end of the MCAO procedure.

For animal wellbeing body weights were recorded giving a similar range of weight decrease following operation. Wild type mice had a 13% and MASP-2 deficient mice a 9% decrease in body weight 24 h after MCAO. The neurological scores among the two groups of mice were not significantly different and no improving functional outcome was observed in the MASP-2 deficient mice following 1 h of ischaemia and 24 h of reperfusion (see figure 3.8).

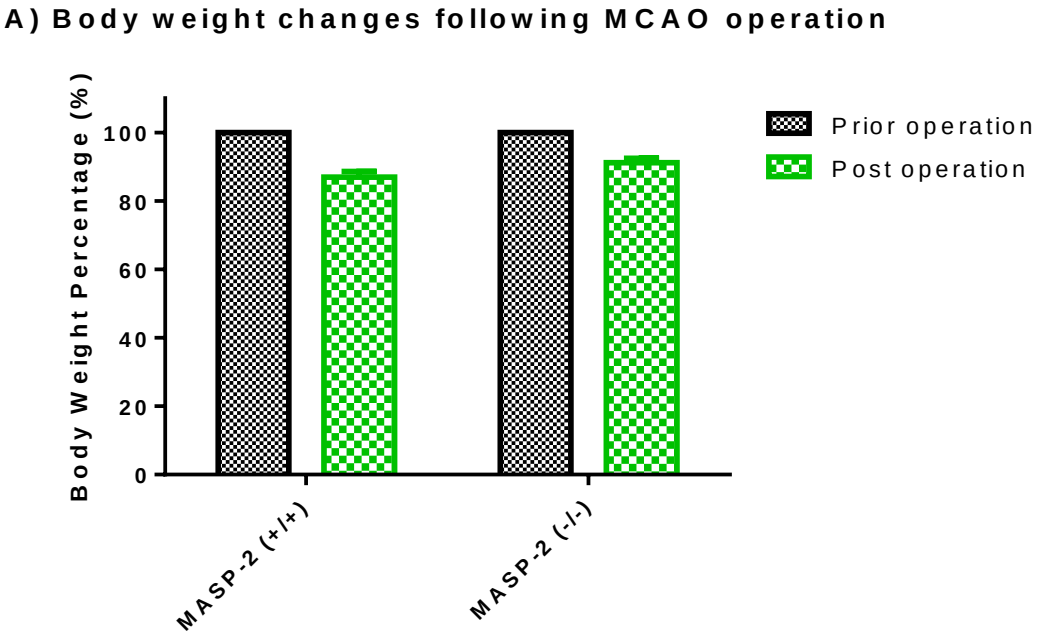

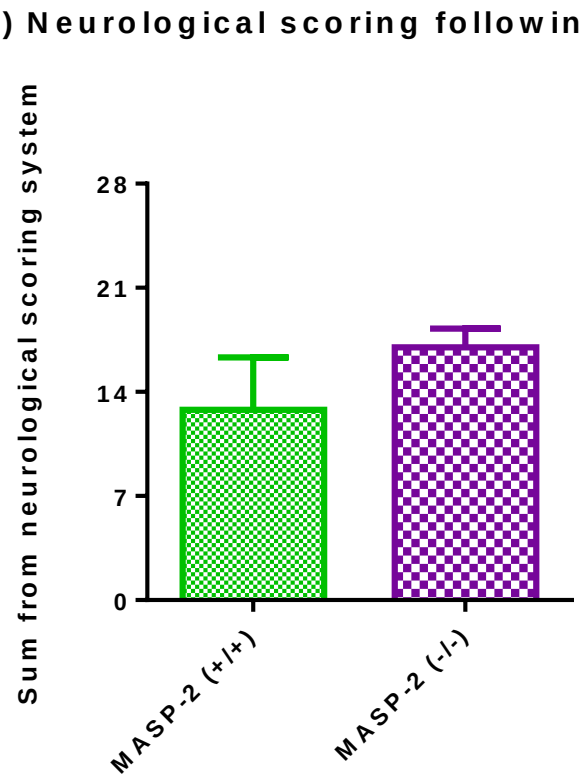

Figure 3.8: Body weight changes and neurological scoring after MCAO

A) Body weight changes after the MCAO occlusion stroke model in MASP-2 sufficient (n=5) and deficient mice (n=4) were used for animal well-being. B) Neurological scoring in MASP-$2^{+/+}$ (n=5) and MASP-$2^{-/-}$ (n=5) mice after MCAO.

3.4 3-Vessel Occlusion stroke (3-VO) model

3.4.1 Establishment of the model

In order to establish an alternative stroke model with a lower degree of variability, an initial series of experiments were performed where I assessed several variables on the basis of animal welfare. The aim was to introduce the shortest time of ischaemia necessary to cause a relatively big lesion in the brain that we could compare in the two lines of mice (MASP-$2^{-/-}$ and MASP-$2^{+/+}$ controls). 30 min of ischaemia followed by 24 h of reperfusion was sufficient to introduce a big enough lesion for our studies leading to clear infarcts that covered around 15% of the affected brain area. 24 h was the time point chosen to reperfuse the tissue giving sufficient time for the post-ischaemic events to have an effect on brain damage, including complement mediated inflammatory conditions like ischaemia and reperfusion injury (IRI). Longer periods of reperfusion time were avoided as severe damage leads to tissue dissolution in the lesion, interfering with infarct estimation. Variations introduced by sex differences also had to be excluded. Therefore, a pilot study was performed to decide the most appropriate sex. Pilot experiments revealed that female mice were more stable during the operations whilst male mice developed breathing complications more often than females resulting in a higher percentage of mortality (see figure 3.9). Mortality observed in MASP-$2^{-/-}$ was most probably the result of bleeding complications either during operation or post cauterisation of the MCA as it was observed that MASP-$2^{-/-}$ were more susceptible to bleeding. In wild type mice, males (n=5), showed an intra operative mortality of 60% while none of the females died (n=5). In the MASP-$2^{-/-}$ group, females (n=7) showed a postoperative (within 24 h post operation) mortality of 43% while no mortality was recorded intra operatively. MASP-$2^{-/-}$ males (n=8) showed a total mortality of 75% following 24 h of reperfusion with 50% intra operative mortality and a 25% mortality

within 24h post operation. Female mice were therefore chosen for the study and were grouped in cages of 4 to 5 to minimise differences coming from oestrous cycle variations as grouping suppresses the oestrous cycle (Champlin 1971).

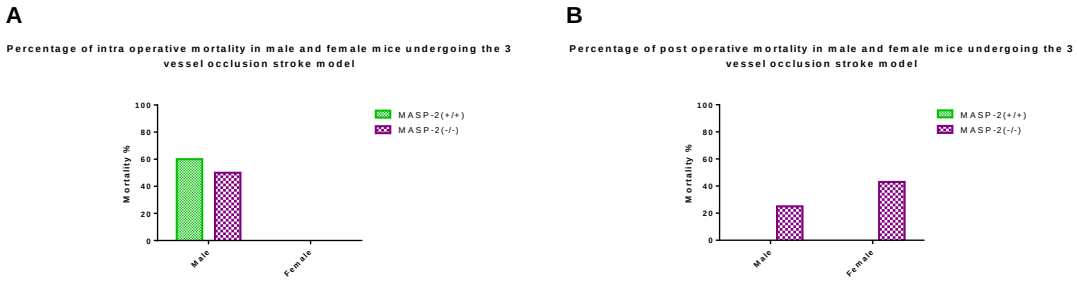

Figure 3.9: Percentage of intra and post operative mortality in male and female mice undergoing the 3 vessel occlusion procedure.

A) Male wild type mice (n=5), had a mortality of 60% which occurred during the operation, mainly resulting from breathing complications leading to death and no death in females (n=5). In the MASP-2$^{-/-}$ group, females (n=7) had 43% mortality occurring within 24 h post operation (B) but no death was recorded during the operation (A). MASP-2$^{-/-}$ male mice (n=8) had a total mortality percentage of 75% of which 50% was coming from death during surgery (A) and 25% from death within 24h post operation (B). N numbers represent the total number of mice used in the particular group.

3.4.2 Blood flow during 3-VO and reperfusion

As permanent cauterisation is performed in the proximal MCA a non-reperfused area was to be expected and the extent of reperfusion was assessed using Indian ink perfusion of the animal. Although the blood flow was disrupted and Indian ink did not reach in close proximity to the cauterised site, distal parts covering the MCA territory maintained blood supply though collateral circulation and anastomosis (see figure 3.10).

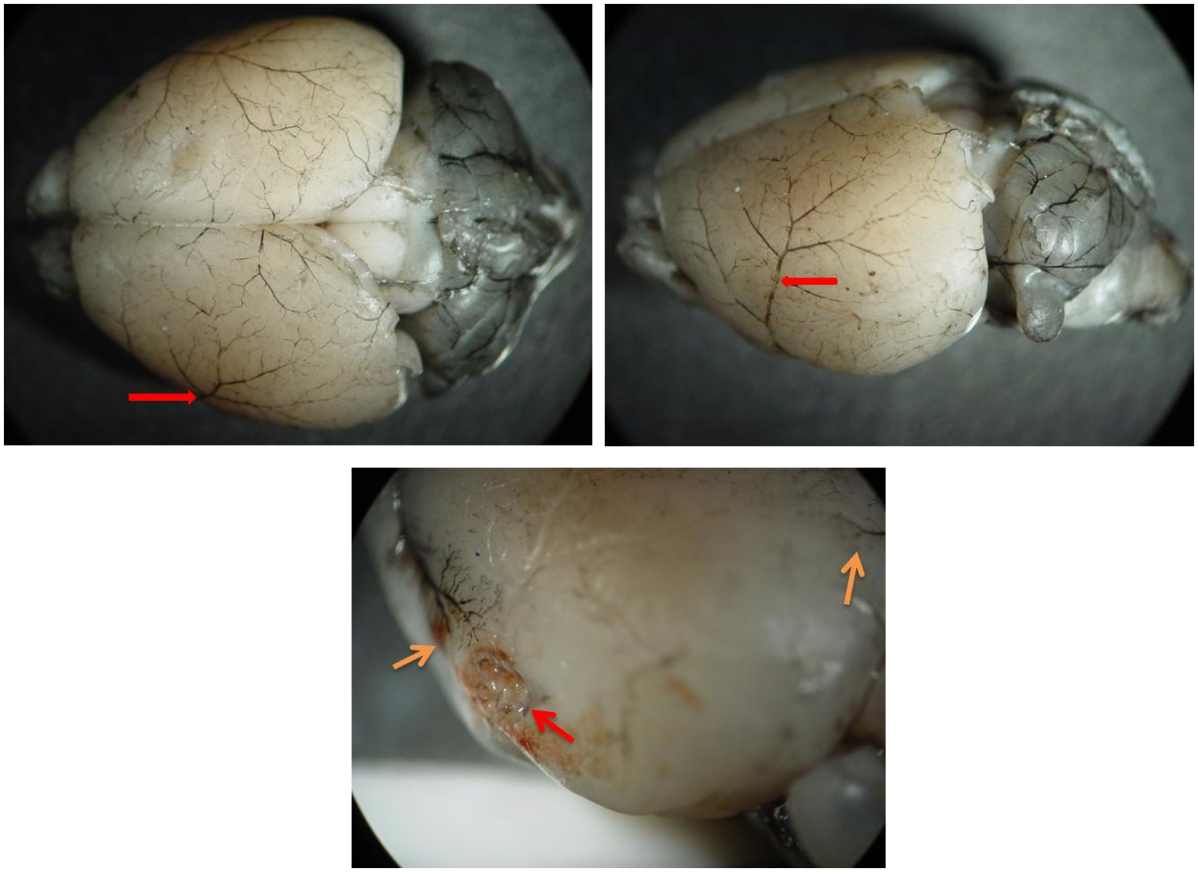

Figure 3.10: Indian ink perfusion

Top: Indian ink perfused mouse brain without 3-VO operation indicating in black the blood vessels. The red arrows indicate the cauterisation point on the middle cerebral artery. Bottom: Left lateral view from a mouse brain perfused with Indian ink 24 h post 3-VO showing in red arrow the cauterisation point on the MCA and in orange arrows vessels supplying blood to the MCA area at the distal edge of the MCA.

In addition, the ischaemia and reperfusion levels were monitored throughout surgery for regional cerebral blood flow (CBF) by Laser Doppler (see figure 3.11). Analysis was performed as previously applied for the MCAO stroke model, with the 100% CBF in the 3-VO operated mice being determined from the recording taken after the ipsilateral CCA occlusion (CCA1). The CBF recorded from three 3-VO operated animals was reduced through CCA1 occlusion by 40.2% (SEM +/- 5). As the 100% value of the CBF was set after CCA1 occlusion MCA cauterisation reduced the CBF to 43.8% (SEM +/-6.6) which was later further reduced to 9.8% (SEM +/-4) following the

contralateral CCA occlusion (CCA2). This CBF was maintained within the same levels thoughout the ischaemic time. Upon completion of the ischaemic time both of the CCAs were released taking the CBF levels up to 56.4% (SEM +/- 21). CBF recordings were also obtained from a control mouse with bilateral CCA occlusion but with no cauterised MCA. The CBF was reduced to 56% after CCA1 occlusion and immediately after to 4% upon CCA2 occlusion. Release of the carotids lead to increased CBF and 5 min after it reached to 60%. Laser Doppler recording from a control mouse with cauterised MCA with no bilateral CCA occlusion was collected indicating a reduction of CBF after CCA1 occlusion to 79%. MCA cauterisation lead to 34% CBF and 5 min after the release of the CCA1 CBF increased to 76%.

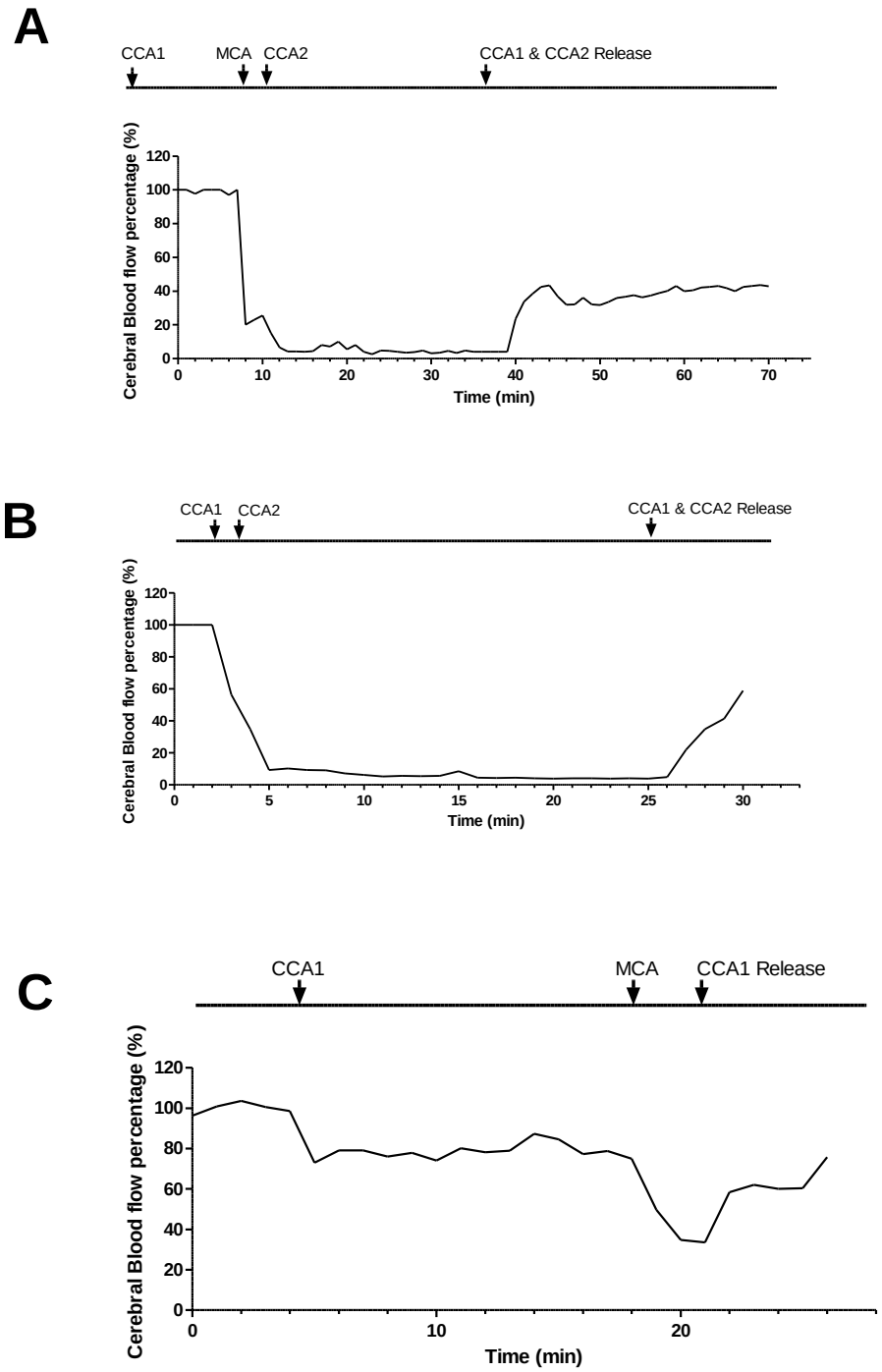

Figure 3.11: Cerebral blood flow percentage in the 3-VO stroke model.

A) A representative CBF recording in an animal undergoing 30 min of ischaemia. The laser Doppler recording is expressed as a percentage indicating the steps in operation considering the CBF after the clipping of the ipsilateral CCA (CCA1) as 100%. Cauterisation of the MCA (MCA) followed CCA1 occlusion and immediately after the cauterisation, occlusion of the contralateral CCA (CCA2) initiated the 30 min ischaemic time. Release of both the CCAs took place after 30min. B) Representative control CBF percentage recording after bilateral occlusion of the CCAs for 30min. C) Representative control CBF percentage recording after cauterisation of the MCA with absence of bilateral CCA occlusion.

3.5 Impact of MASP-2 deficiency on the size of infarction using in 3-VO stroke model

TTC staining is widely used to assess cerebral damage following stroke as red staining would stain metabolically active cells in healthy tissue and unstained white tissue the infracted area with metabolically compromised cells. The model was set up using female MASP-$2^{+/+}$ and MASP-$2^{-/-}$ undergoing the 3-VO operation for 30 min of ischaemia followed by 24 hours of reperfusion. Upon completion of the reperfusion time, the animals were sacrificed and brain was taken out and prepared for assessment of the damaged areas in the two groups. The TTC staining revealed that MASP-$2^{-/-}$ mice were significantly protected from cerebral damage compared to the wild type controls (see figure 3.12 and 3.13). With a mean infarct volume of 26.8 mm^3 the MASP-$2^{-/-}$ showed 30.7% smaller lesion areas in comparison with wild type control mice with a mean infarct volume of 38.7mm^3 ($p=0.0157$). Sham operations without CCA occlusions and no MCA cauterisation as well as 30 min CCA occlusions with the absence of MCA cauterisation produced no infarcts. Single cauterisation of the MCA varied from no infarctions to minor lesions in the cortex. On some occasions following 3-VO the striatum gave a mild pinkish colouration bilaterally or unilaterally (figure 3.14). However, only clear white lesions with definitively metabolic inactive cells were included for lesion estimation. Variability in this could probably be due to intra individual variations of cerebral vasculature within the strain or the presence or absence of the posterior communicating artery supply (figure 3.15).

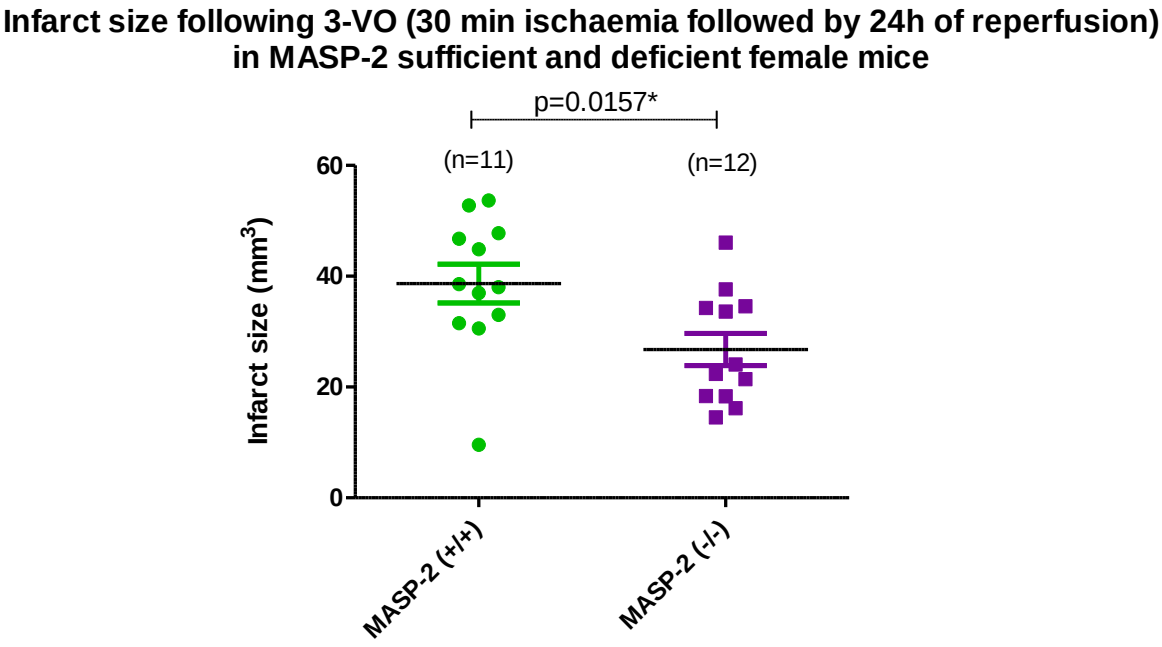

Figure 3.12: The volume of cerebral infarcts is significantly reduced in MASP-2 deficient mice compared to wild type mice.

Mice had undergone the 3-vessel occlusion stroke model for 30 minutes of ischaemia followed by 24 hrs of reperfusion. With a mean infarct volume of 26.8 mm^3 (SEM +/- 2.9) the MASP-$2^{-/-}$ (n=11) had 30.7% smaller lesions in comparison with their wild type controls (n=12) with a mean infarct volume of 38.7mm^3 (SEM +/- 3.5) (p=0.0157). Data are reported as scatter-dots with mean values (black bars) and standard error bars (coloured bars). The statistical test used for analysis was the unpaired *t* test;*p<0.05.

The neocortical lesions from coronal sections obtained from the 3-VO in the two group of mice are shown in figure 3.13. For animal wellbeing following stroke operation, body weight recordings were obtained showing a 10.6% body weight decrease in wild type animals and an 8% decrease in MASP-2 deficient mice. Along with their body weights mice were assessed 24 hrs post reperfusion for neurological deficits and motor function impairments. Both parameters revealed no significant differences amongst the two groups. The relatively low scores recorded implied no significant motor function impairments in this model of stroke (see figure 3.16).

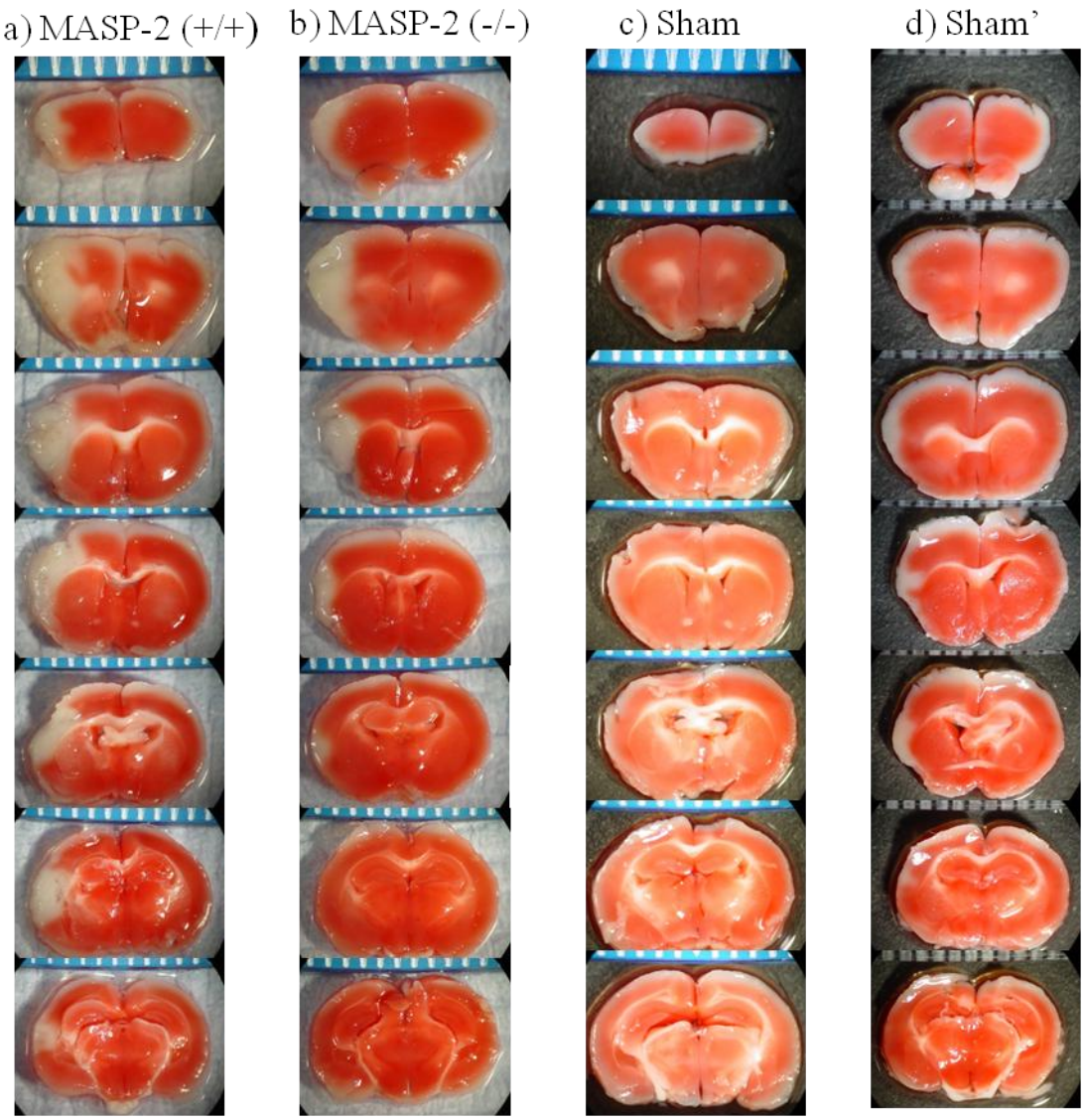

Figure 3.13: TTC staining for infarct size calculation in infarcted brains of WT and MASP-2 deficient mice.

The infarcted area is shown in white. A) Representative 1 mm thick coronal brain sections from a WT mouse following 3-VO after 30 min of ischaemia and 24 hrs of reperfusion. B) Representative coronal brain sections from a MASP-2 deficient mouse following 3-VO. MASP-2 deficient mice show a reduced infarct size compared to the WT mice. C) A sham operated mouse without occlusion of the common carotid arteries and cauterization of the MCA. The operation was the same up until until the removal of the zygomatic arch. D) Sham operated mouse. MCA cauterisation without clipping of the two common carotids for 30 min gives no or a minor infarction in the cortex. Scale in mm.

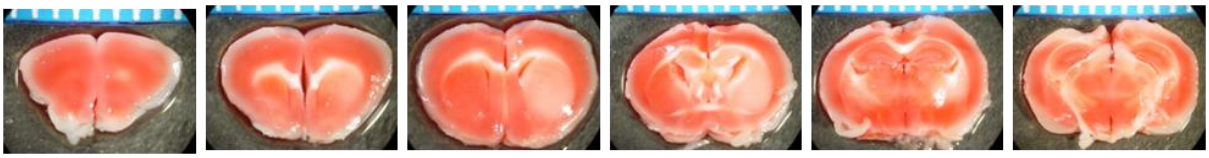

Figure 3.14: In rare occasions following 3-VO the striatum area seemed to be mildly affected based on the pinkish colouration following TTC.

TTC staining of coronal brain sections from a control animal having bilateral common carotid artery occlusions for 30 min without MCA cauterisation and without distinctive white lesions.

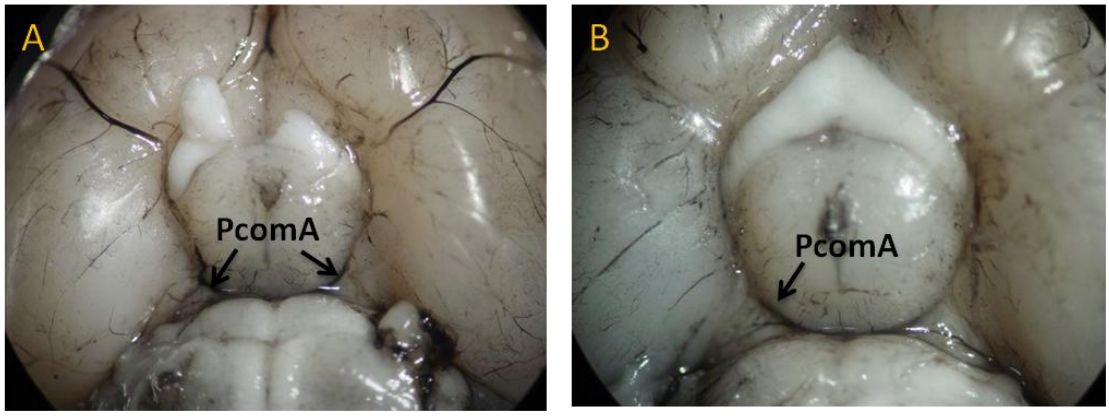

Figure 3.15: Indian ink perfusion of mice indicating variability in the presence of the posterior communicating artery (PcomA).

The PcomA on the left is present bilaterally (A) while on the right the PcomA is unilateral (B).

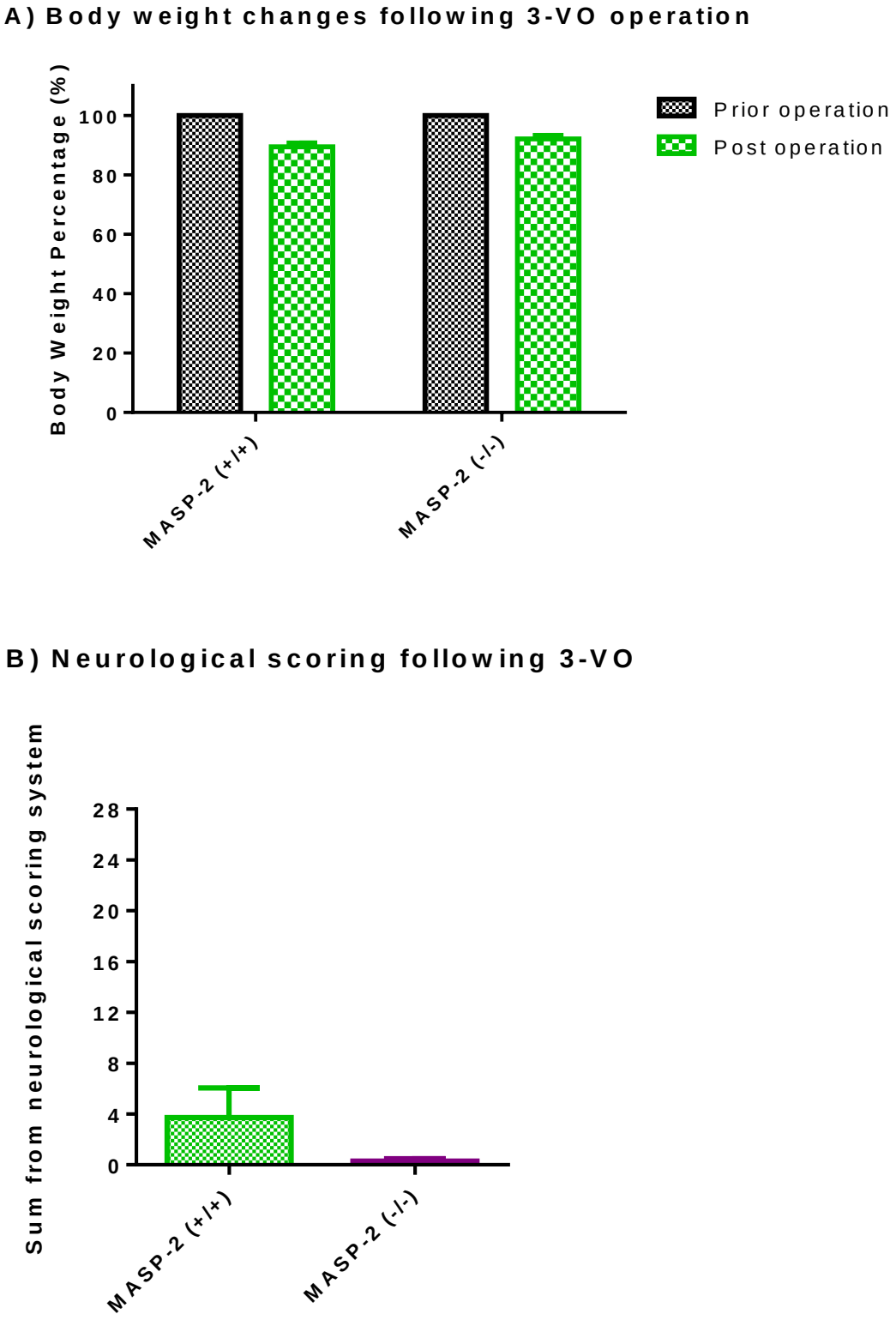

Figure 3.16: Body weight changes and neurological scores after 3-VO

A) Body weight changes after 3-vessel occlusion stroke model in MASP-2 sufficient (n=6) and deficient mice (n=7) were recorded for animal well-being. B) Neurological scoring in MASP-$2^{+/+}$ (n=7) and MASP-$2^{-/-}$ (n=7) mice after 3-VO. No significant differences were observed for either measure.

3.6 Immunohistochemical analysis

In order to assess the extent of damage in more detail, including cellular and immunological changes that occur as a consequence of the ischaemic insult, various markers have been chosen for the immunohistochemical analysis of the brain tissue harvested from 3-VO operated animals after reperfusion.

3.6.1 Differential staining of brain cells:

3.6.1.1 Neurons

NeuN is a protein which is specifically present in most neuronal nuclei (Mullen *et al.* 1992). It was chosen in this study to identify neurons and their phenotypic state following ischaemia and reperfusion. Most neurons carry this protein in their nucleus, although low levels were also found to be present in the cytoplasm. The exception are pyramidal neurons present in the cerebral cortex where NeuN is not present in the nucleus (Mullen *et al.* 1992). MASP-$2^{+/+}$ and MASP-$2^{-/-}$, which had undergone 30 min of ischaemia followed by 24h of reperfusion, as well as sham operated animals, were stained with NeuN. Staining had clearly revealed the ischaemia affected area in the ipsilateral hemisphere in both MASP-$2^{+/+}$ and MASP-$2^{-/-}$ mice. This was identified by the various degrees of loss of NeuN staining resulting from the loss of neuronal cells and neuronal cell death (figure 3.17 and 3.18). This pattern of NeuN loss in the cortical area in both groups of mice matched well with the TTC unstained area (i.e. white) in the cortex. Similarly, nuclear staining by Hoechst was characterised by fragmented condensed nuclei giving bright blue fluorescence in the same area where NeuN was lacking, thus also marking the lesion areas. Hoechst stained healthy looking nuclei with

a lighter blue colour and they covered the remaining unaffected cerebral areas. In contrast to the staining pattern seen in 3-VO operated mice, sham operated mice (having no CCA occlusion and MCA cauterisation) showed positive NeuN staining throughout the brain without any signs of cerebral lesion in the cortical area. Staining in the contralateral hemisphere in all assessed groups was also left intact.

3.6.1.2 Astrocytes

Glial fibrillary acidic protein (GFAP) was used as a marker to identify astrocytes and their response to cerebral ischaemia. GFAP is a cytoskeletal protein and belongs to the major intermediate filaments of mature astrocytes (Eng *et al.* 2000). As a cytoskeletal protein, it accounts for the motility and shape of astrocytes. Astrogliosis is the response of astrocyte activation which is accompanied by subsequent GFAP synthesis. Astrogliosis can be observed in many pathological conditions including stroke (Kimelberg 2005, Zhao & Rempe 2010). Activated astrocytes, identified by high levels of GFAP expression, were localised in the boundary of the damaged ischaemic area in both MASP-$2^{+/+}$ and MASP-$2^{-/-}$ mice following 30 min of ischaemia and 24 h of reperfusion (figure 3.19 and 3.20) apparently forming a glial scar around the lesioned area. Glial scar formation in general is a result of secondary damage that is also highly triggered by the BBB destruction, the infiltration of macrophages and the subsequent upregulation of cytokines and interleukins that takes place several hours following the ischaemic event and continues up to days depending on the severity of the insult (Silver & Miller 2004). Resting astrocytes were found throughout the brain at lower density (i.e. Corpus callosum, cortical and subcortical areas) expressing relatively low levels of GFAP. Sham operated mice lacked the astrocytic scar pattern (Figure 3.20).

Interestingly, astrocytes localised around the lesion area in the MASP-$2^{+/+}$ mice had a much more aggregated/ activated appearance compared to the phenotype in MASP-$2^{-/-}$ mice. Astrocytes in MASP-$2^{+/+}$ mice showed longer projections and showed an apparently more abundant GFAP expression. In addition, astrocytes in MASP-$2^{+/+}$ mice appeared to be associated in closer proximity to each other (see figure 3.20).

3.6.1.3 Microglia

Another key type of cell that was examined in post ischaemic brain tissue was the resident macrophages of the brain, the microglia. These were identified by staining of the microglial marker, the ionised calcium adaptor molecule 1 (Iba1), which is an EF hand calcium binding protein specifically expressed in macrophages and microglia (Ohsawa *et al.* 2000). Iba1 staining was performed in tissue sections of brains harvested after 3-VO operation with 30 min of ischaemia followed by 6 h, 12 h and 24 h of reperfusion using MASP-$2^{+/+}$ mice. Iba1 staining was used to monitor microglial changes during the development of IRI mediated lesions (see figure 3.21, 3.22 and 3.23). Resting microglia in sham operated mice expressed Iba1at low abundance throughout the brain. In brains subjected to 3-VO mediated ischaemia followed by 6 h of reperfusion, the Iba1 staining of microglial cells was more pronounced than in the brains of sham operated control mice in the ipsilateral as well as in the contralateral site indicating a global response to the ischaemic insult. At this early time point a small lesion area could already be identified by the condensed nuclei shown by Hoechst staining. Ramified (i.e. activated) microglia were observed and equally scattered throughout the entire ipsilateral site, in the border regions as well as within the lesioned areas. The highest intensity of Iba1 staining and the longest microglial projections

(typical for activated microglia) were observed following 12 h of reperfusion. At this time point, microglial cells were scattered in the ipsilateral site in a gradient like manner with the cells expressing Iba1 at low abundance and the lowest degree of ramification being distant from the lesion and the most ramified and abundantly Iba1 expressing cells located at the border of the lesioned area. Likewise, the highest concentration of microglia was found at the border of the lesioned area. In contrast to the 6 h reperfusion time point, Iba1 staining was totally absent within the lesion area in brains following 12 h of reperfusion. A similar staining pattern as those observed at the 12 h time point was seen in brains harvested after 24 h of reperfusion. However, the density of microglia at the border of the lesion area was not as high as that seen in brains exposed to shorter reperfusion times (figure 3.21). The staining pattern for Iba1 in brains of MASP-$2^{+/+}$ and MASP-$2^{-/-}$ following 30 min of ischaemia and 24 h of reperfusion was very similar with no distinct differences between the two mouse lines (see figure 3.24).

3.6.2 Complement activation markers

3.6.2.1 C3 deposition

The degree of complement activation following stroke in the WT and MASP-$2^{-/-}$ mice was assessed using C3/C3c deposition. Upon complement activation, C3 is cleaved into C3a and C3b. C3b then binds to the activating surfaces which may lead to further complement activation. C3c is one of the cleavage products of C3b and is generated through factor I mediated inactivation of C3b (a cofactor dependent process) (Palarasah *et al.* 2010). To ensure that the C3c antibody used in my experiments was specific for C3/C3c, a *Candida albicans* infected kidney was used as a positive control (slides kindly prepared from Dr Hany Kenawy) as C3 is abundantly deposited on hyphae due

to complement activation. A strong C3 deposition was indeed observed in these slides on the surface of the fungal hyphae (see figure 3.28). C3c deposition was clearly detected in my brain sections, but only within the lesion areas in both WT and MASP-2$^{-/-}$ that had undergone the 3-VO procedure followed by reperfusion. In brain sections of brains harvested 12 h post ischaemia, C3c was deposited on lesioned cells with the majority of them being necrotic or apoptotic as judged by their nucleic phenotype (Hoechst staining). The contralateral side showed no C3c deposition. No C3 deposition was observed in sections of sham operated animals. When comparing C3 staining in brains of mice that had undergone the 3-VO mediated ischaemic insult followed by 24hs of reperfusion it appears that C3 deposition was less pronounced in the MASP-2 deficient animals (see figures 3.25 to 3.27).

3.6.2.2 Lectin pathway recognition molecules

The recognition molecules of the lectin pathway were also assessed to examine the involvement of lectin pathway activation in cerebral ischaemia and reperfusion injury, as these are required to activate the complement cascade. MBL-C was detected in brain sections of WT and MASP-2$^{-/-}$ mice that had undergone 3-VO operation and reperfusion. The deposition of MBL-C was observed in similar patterns in the two groups within severely damaged areas of the lesion as well as in the proximal blood vessels. Negative controls with incubation of only the secondary antibody were clear of any non specific staining. Deposition was not present in the contralateral site of the lesion nor in sham operated mice. MBL-C and MBL-A are primarily synthesised in liver as well as in the spleen in lower levels; therefore those tissues were used as positive controls to validate MBL-C staining (Wagner *et al.* 2003) (see figure 3.29 to

3.31). MBL-A, however, was not detected even in the positive controls i.e. liver or spleen nor in brain and further optimisations of staining and perhaps a different MBL-A specific antibody is required in the near future, as this was not achievable within the given timeframe of my project (figure not shown). Ficolin A is also synthesised in liver and was successfully detected following immunohistochemistry. In contrast to MBL-C, ficolin A was not detectable within the lesion or any site of the brain in MASP-$2^{+/+}$, MASP-$2^{-/-}$ nor the sham operated mice at 30 min of ischaemia and 24 h of reperfusion (figure 3.32). Collectin 11 (CL-11) was successfully detected in liver, but was not detectable in brain at 30 min of ischaemia and 12 h of reperfusion (figure 3.33).

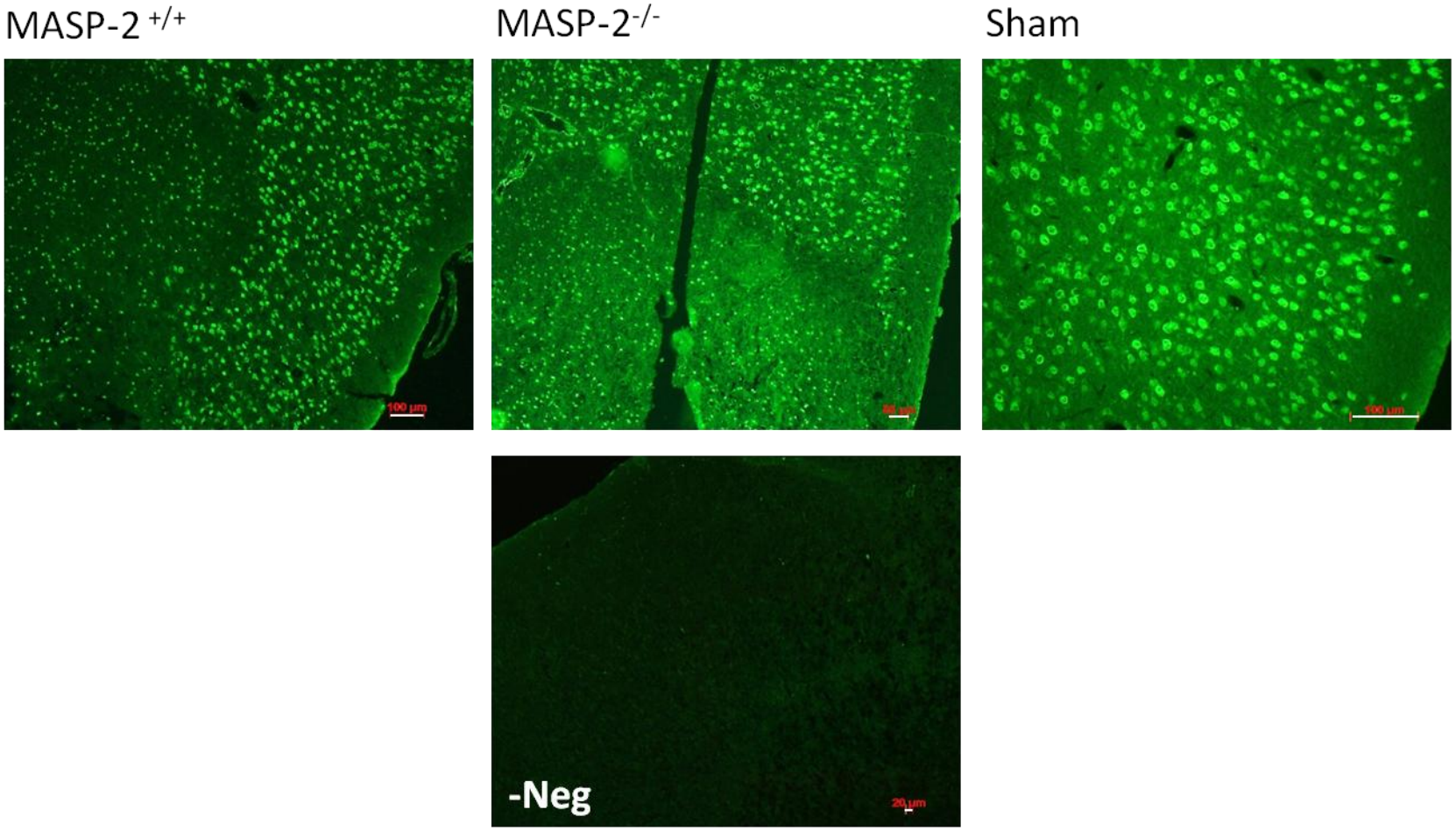

Figure 3.17: NeuN staining for neuron detection at the boundary of the damaged area following 3-VO at 30 minutes of ischaemia and 24 hours of reperfusion.

NeuN staining is weakened or lost in damaged areas. MASP-$2^{+/+}$ and MASP-$2^{-/-}$ under x10 magnification and sham section under x20. Bottom image; Secondary antibody only was applied as negative control. Scale bars 20 µm 50 µm and 100 µm.

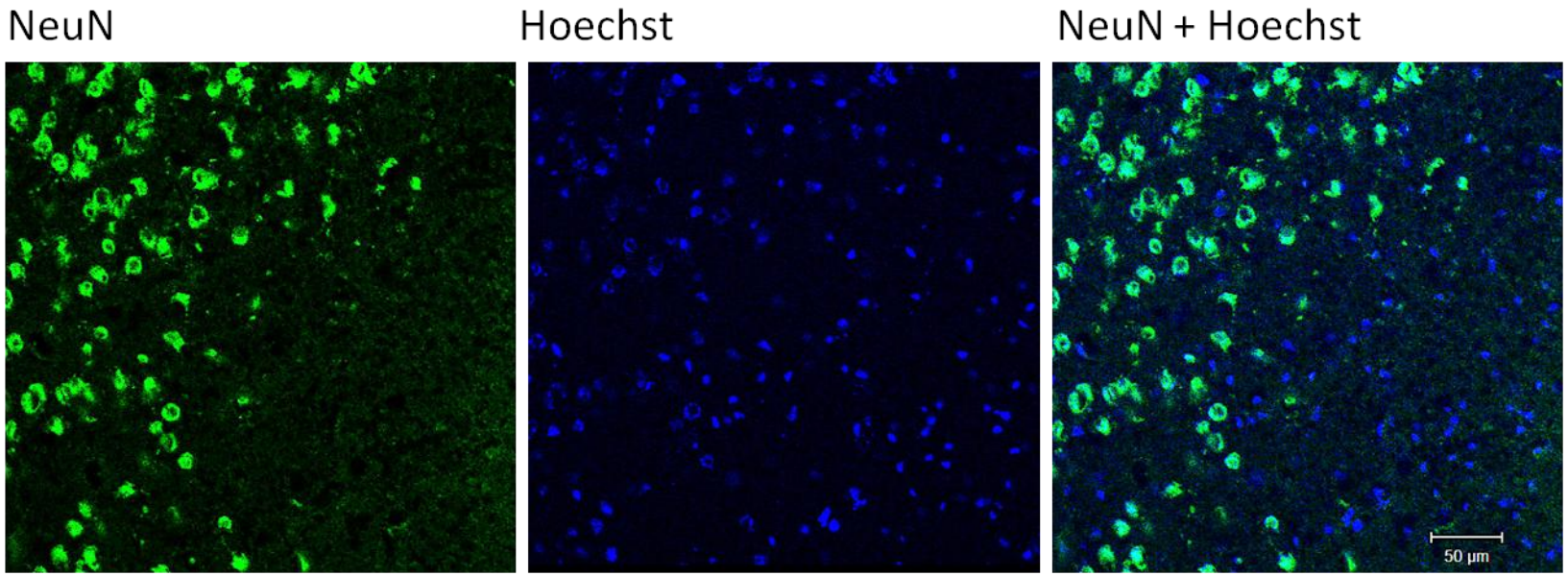

Figure 3.18: NeuN staining

Confocal image (x63) at the boundary of lesion; NeuN in green; Hoechst in blue. Note the loss of NeuN staining and pyknotic nuclei in the lesion area in the right hand side of the picture. Scale bars 50 µm.

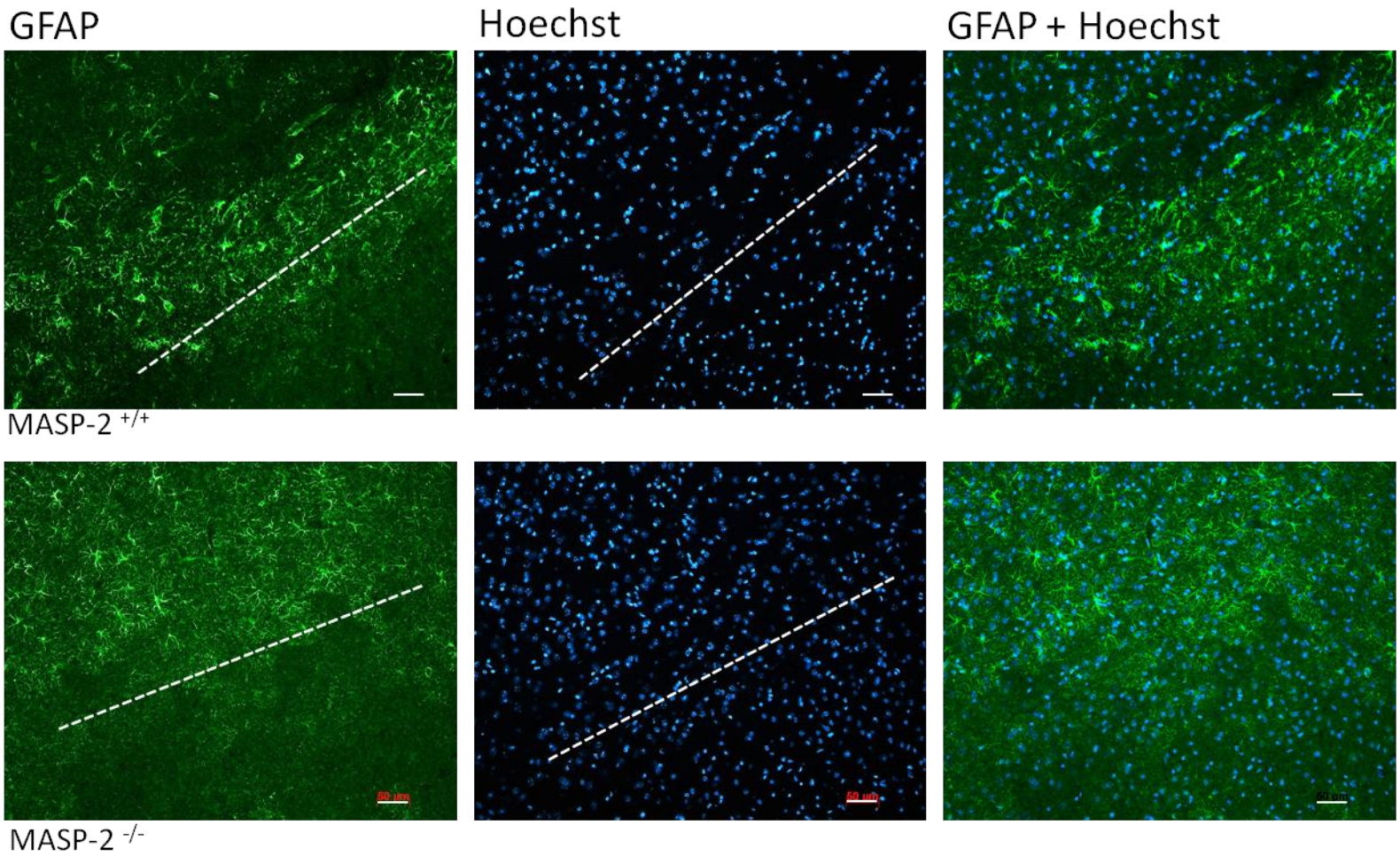

Figure 3.19: GFAP staining for astrocytes in MASP-2 $^{+/+}$ and MASP-2 $^{-/-}$ at the boundary of the lesion.

Lower right corner of all images is the lesion territory characterised by condensed and fragmented nuclei (Dotted line to indicate the boundary of the lesion). Green for GFAP and blue is for nuclear staining with Hoechst (x20 magnification). Scale bar 50 µm.

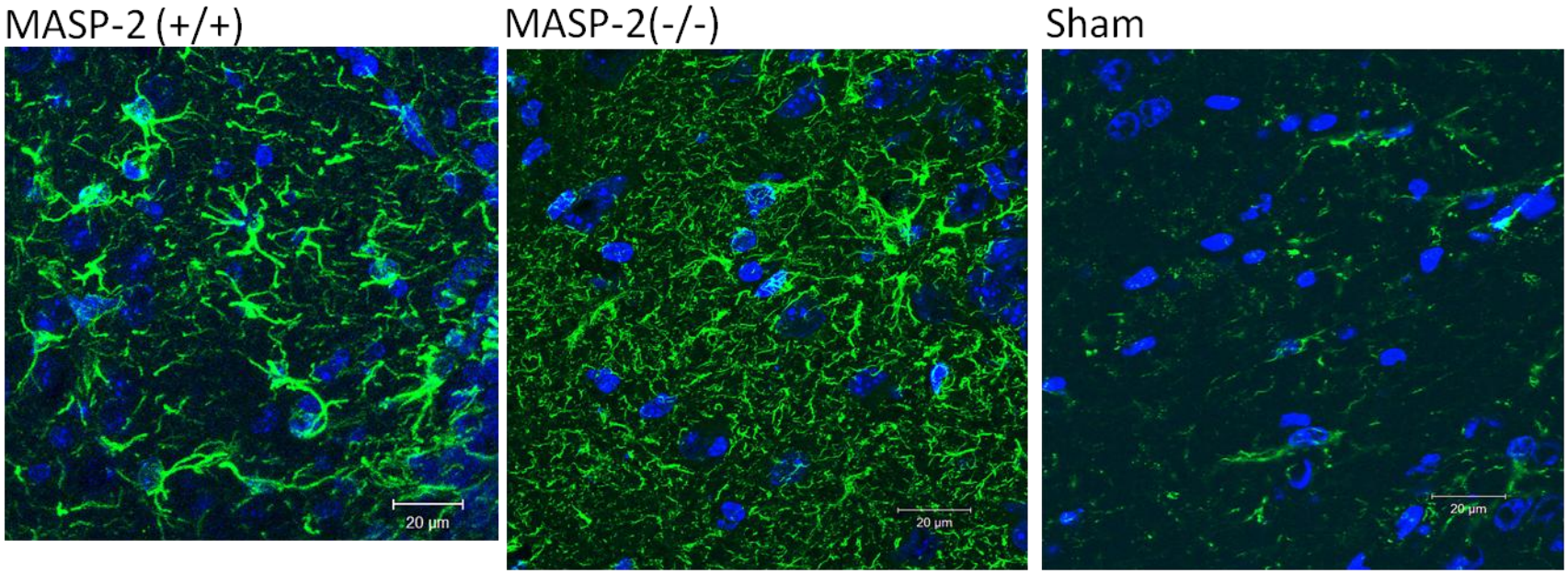

Figure 3.20: GFAP staining

Confocal images from GFAP staining in astrocytes at the ipsilateral site in close proximity to the lesion area. Green for GFAP and blue for nuclear staining with Hoechst (x63 magnification, maximum intensity projection from z-stack images). Scale bars 20 µm.

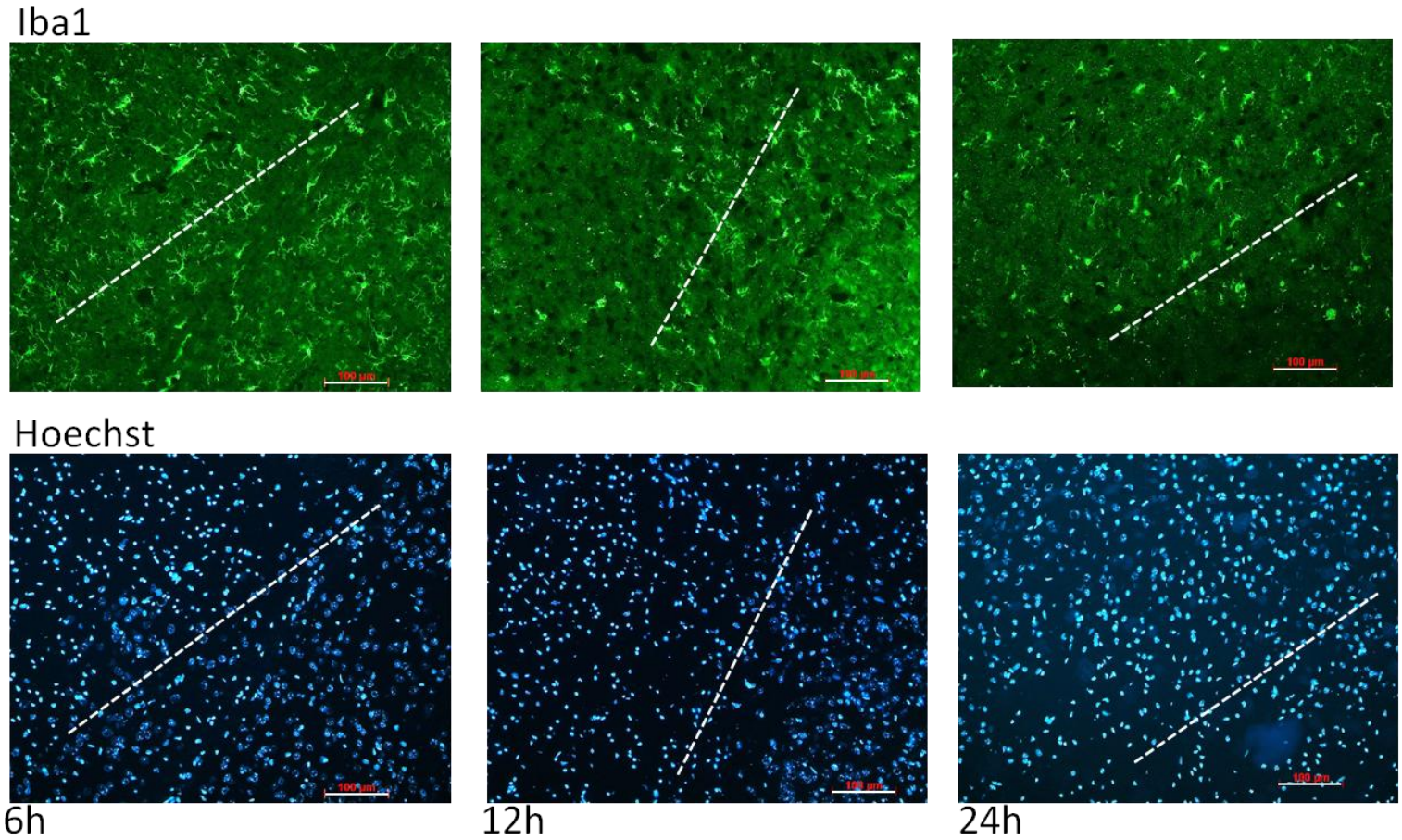

Figure 3.21: Iba1 staining for microglia at 30min of ischaemia and 6, 12 and 24h of reperfusion at the border of the lesion.

Iba1 in green and Hoechst in blue (x20 magnification). At 6h of reperfusion microglia are present in the border as well as within the lesion as observed by the appearance of pyknotic nuclei with Hoechst staining. Highest intensity of Iba1 is observed at 12h in which microglia are found only in the border of the lesion and not within. Similar staining pattern to 12 h is observed at 24 h but the intensity is reduced. Dotted lines indicate the border of the lesion. Scale bars 100 μm.

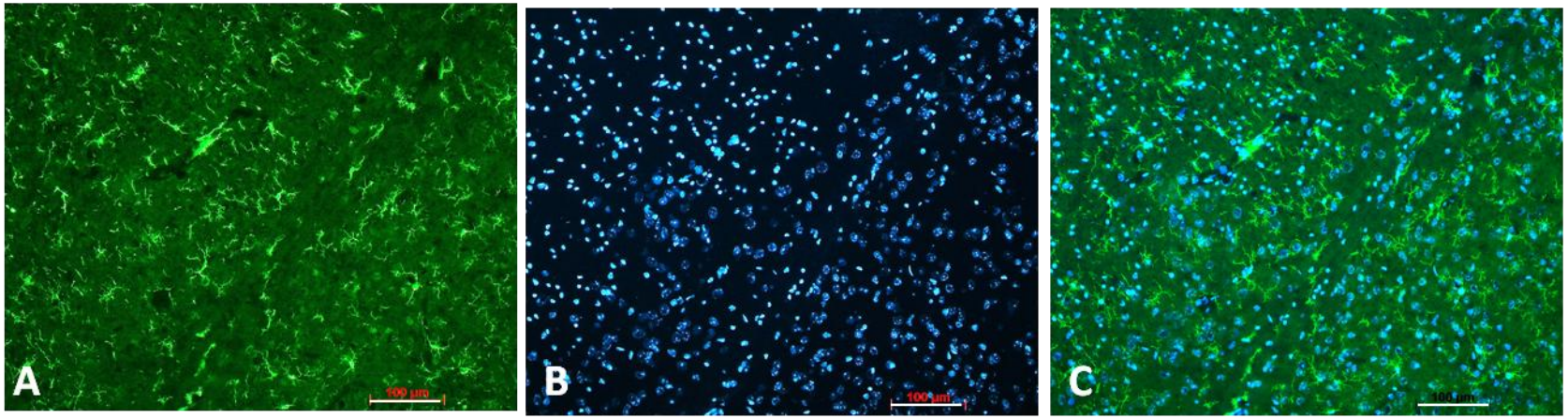

Figure 3.22: Iba1 staining

A) Iba1 staining at the boundary of the damaged area at 30 min of ischaemia and 6 h reperfusion showing microglia migrating and interacting within and surrounding the damaged area. B) Dead cells' nuclei in the ischaemia affected area stained with Hoechst can be distinguished in the top left corner by bright blue and condensed morphology. Healthy cells at the bottom right corner have a light blue colouration and wider diameter than dead ones. Scale bars 100 µm.

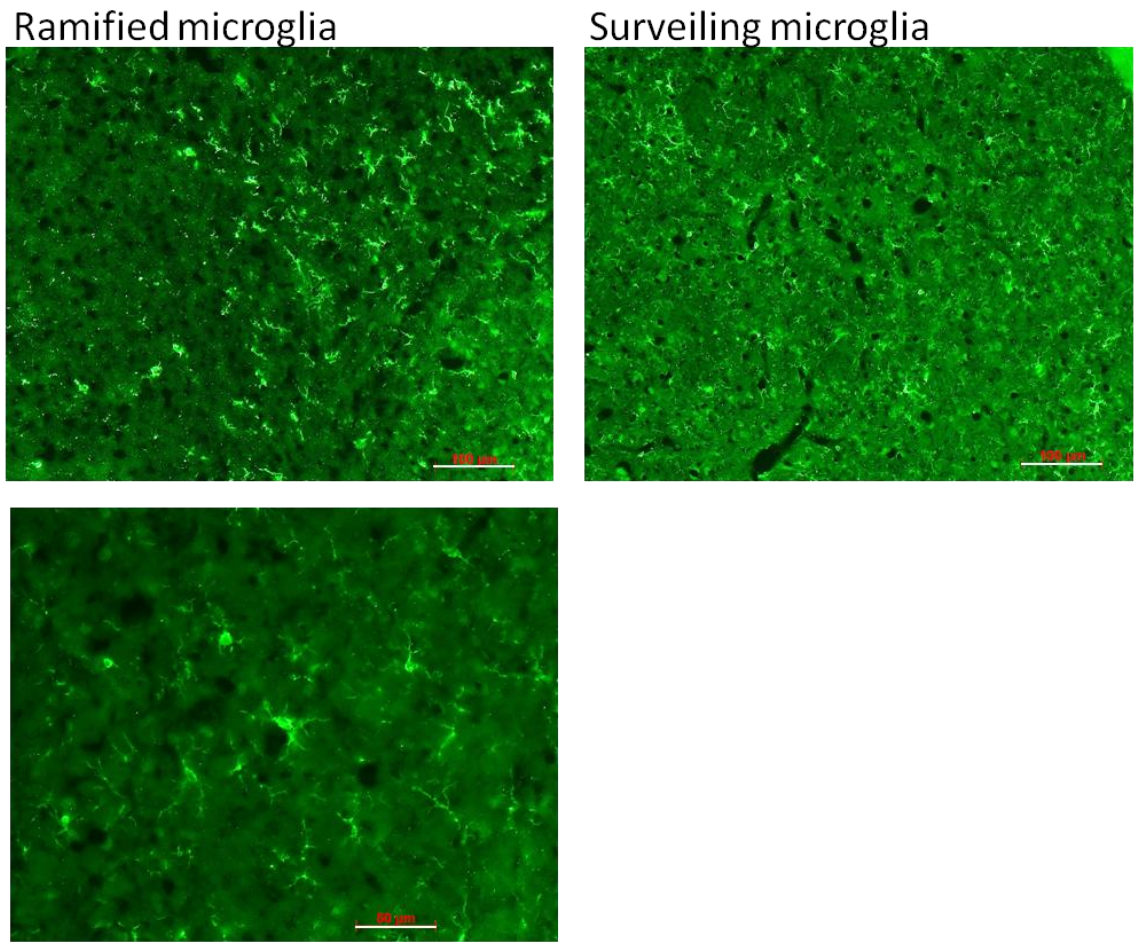

Figure 3.23: Iba1 staining for detection of microglia in WT brain at 30 min of ischaemia followed by 12 h of reperfusion using the 3-VO stroke model.

Top) Activated microglia at the boundary of the damaged area (left) and surveiling microglia at the contralateral site. Scale bars 100 µm. Bottom) Microglia at x40 magnification at the penumbra. Scale bar 50 µm.

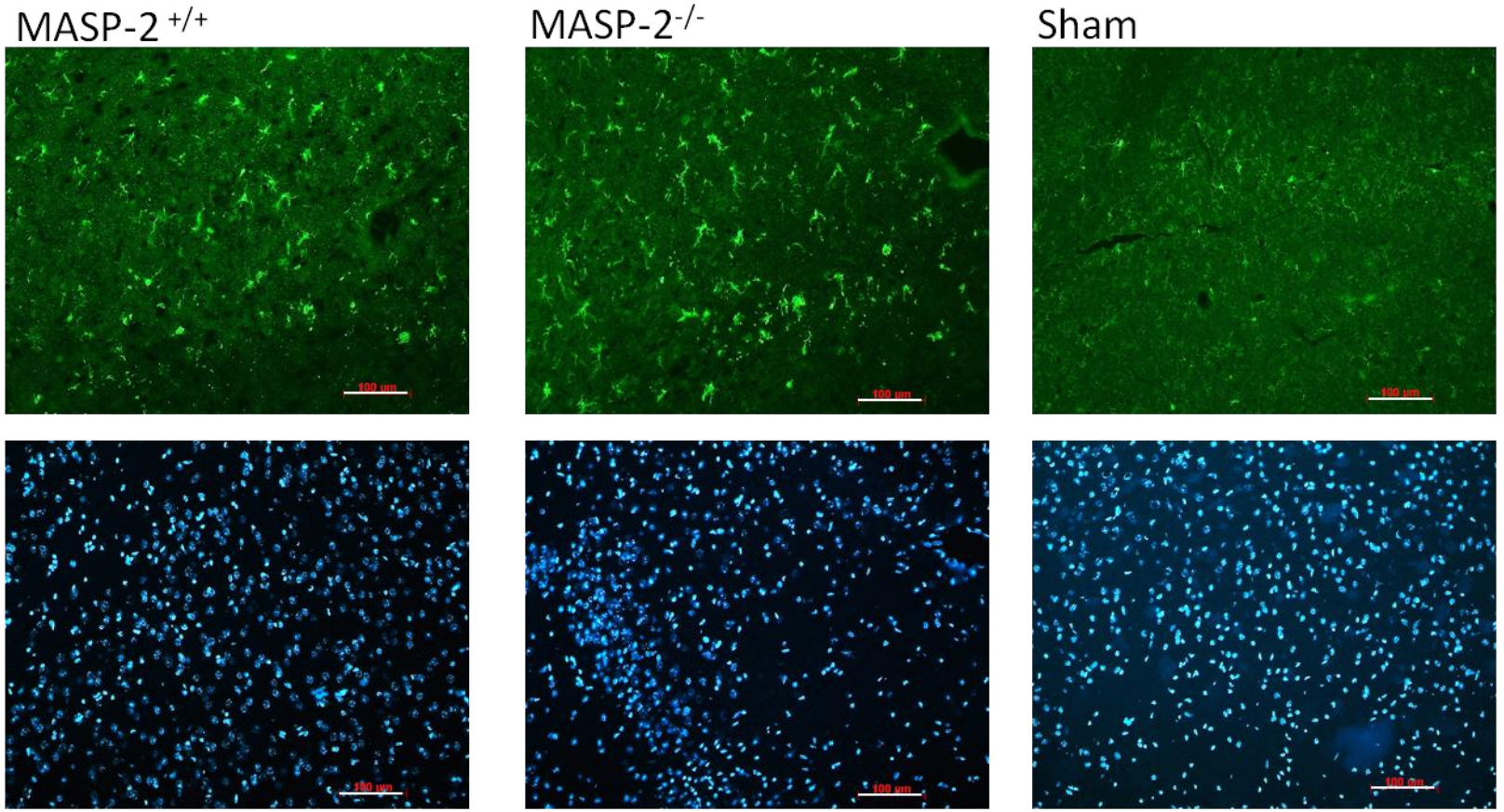

Figure 3.24: Iba1 staining for microglia in MASP-2$^{+/+}$, MASP-2$^{-/-}$ and sham operated animals at the boundary of the ischaemia insulted area.

Iba1 in green and Hoechst in blue. Scale bars 100 µm.

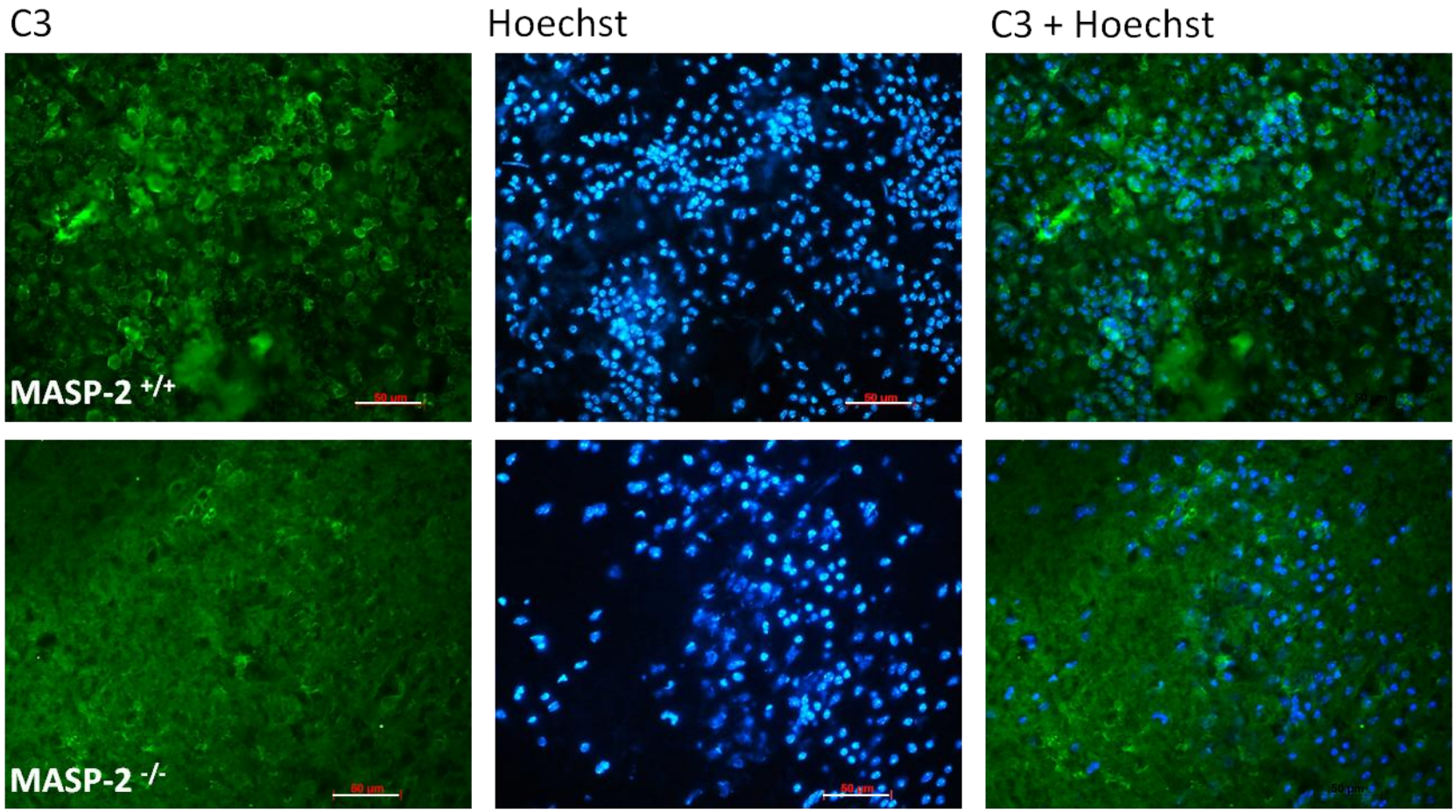

Figure 3.25: C3 deposition (a)

C3 deposition in MASP-$2^{+/+}$ and MASP-$2^{-/-}$ mouse brains following 3-VO (30 min of ischaemia and 24 h of reperfusion showing higher deposition in MASP-$2^{+/+}$ mice (x40 magnification). Scale bars 50 µm.

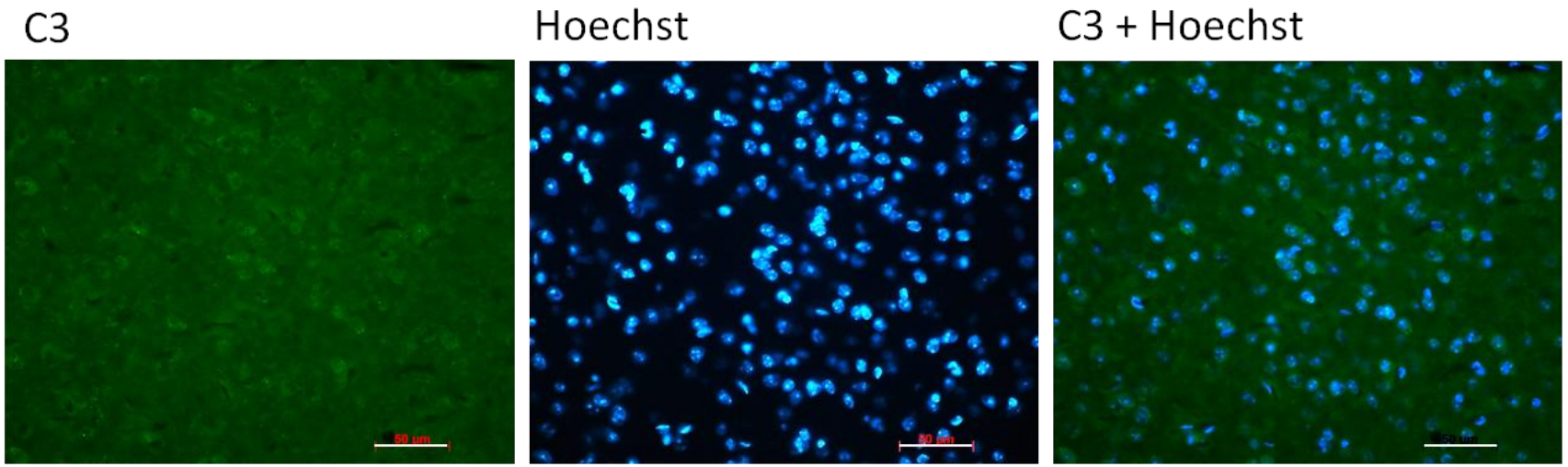

Figure 3.26: C3 deposition (b)

C3 deposition following 3-VO sham operation showing no C3 deposition in the equivalent location of the ischaemia affected area. Scale bar 50 µm.

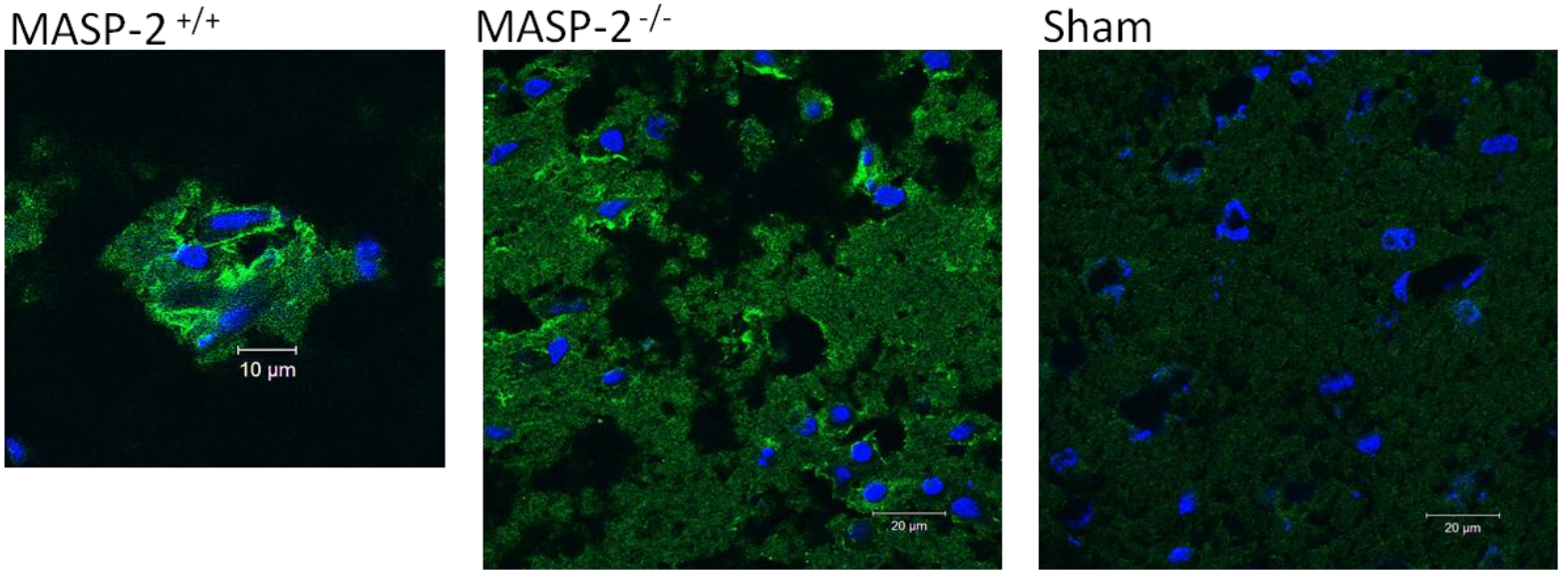

Figure 3.27: C3 deposition (c)

C3 deposition on cells in MASP-$2^{+/+}$ mouse (focused to show details), MASP-$2^{-/-}$ and sham (x63 magnified confocal image). C3 in green and Hoechst in blue. Scale bars 10 and 20 µm.

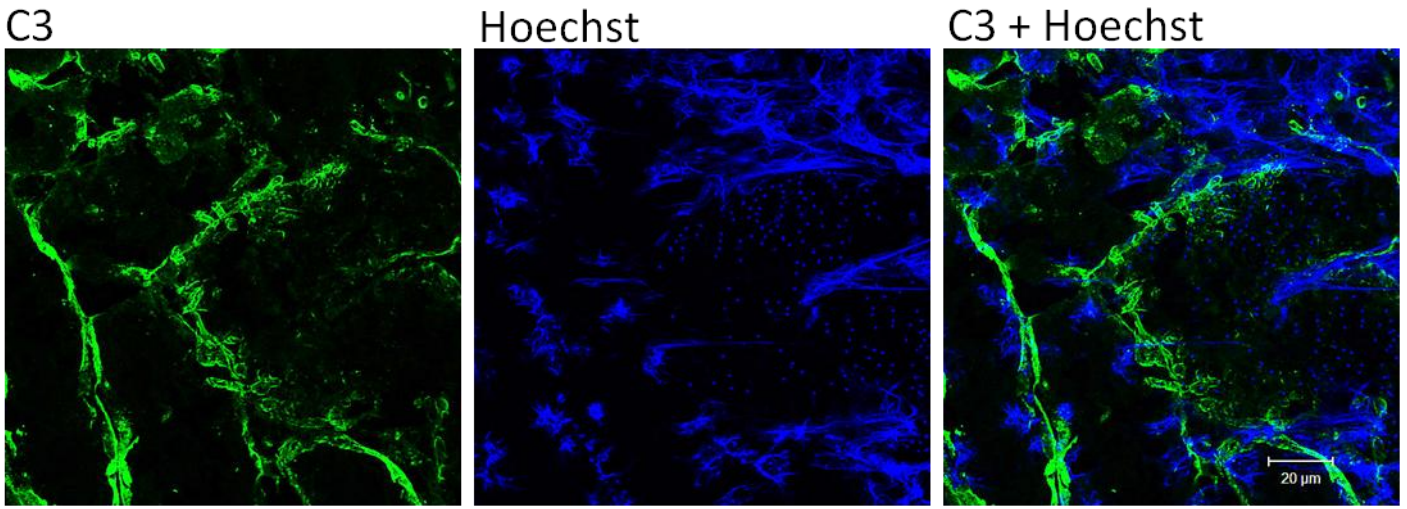

Figure 3.28: C3 deposition (d)

C3 deposition on *Candida albicans* MASP-2$^{-/-}$ infected kidney tissue was used as a positive control for C3 (Confocal imaging); x63 magnification. Scale bars 20 µm.

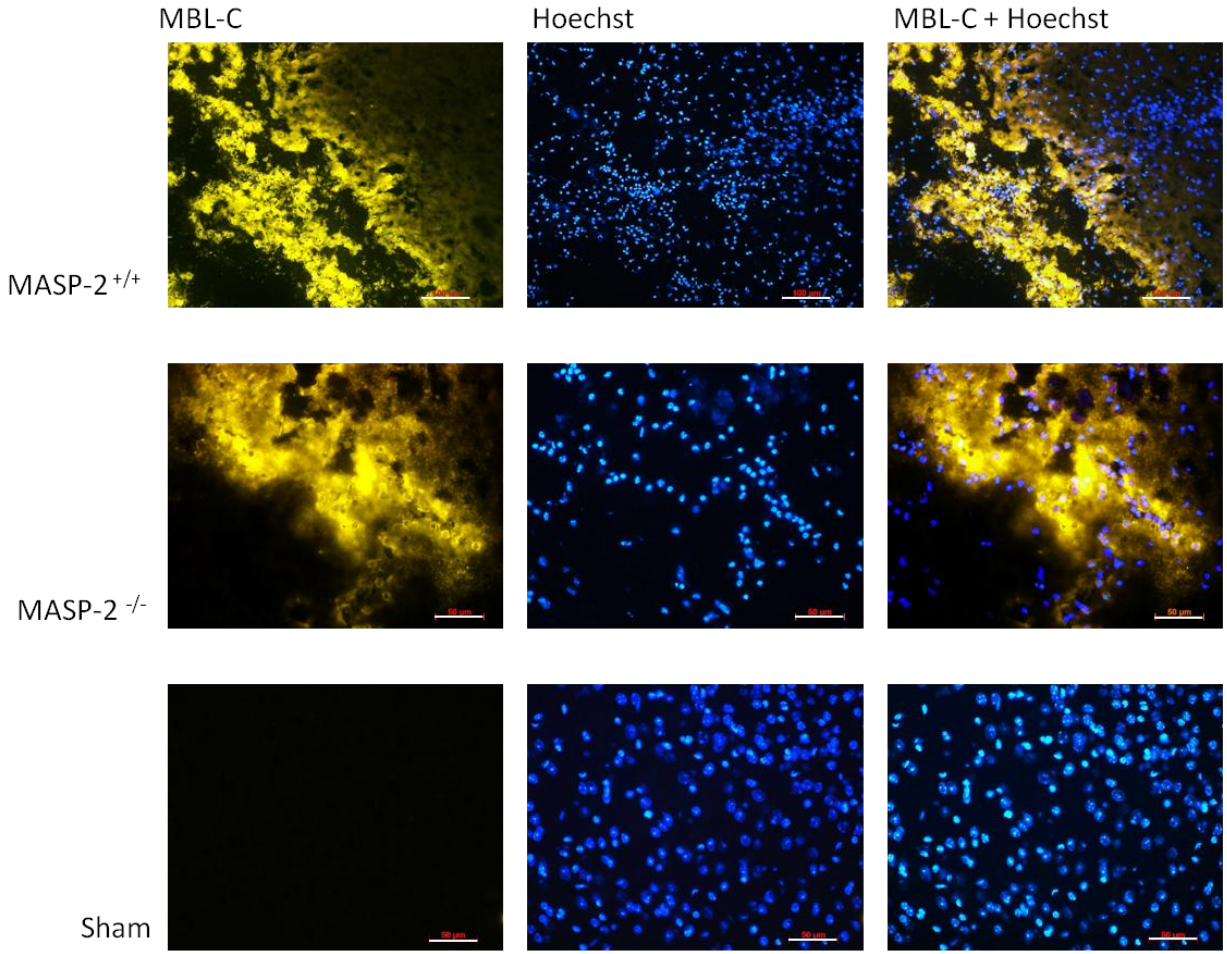

Figure 3.29: MBL-C staining (a)

MBL-C staining (in yellow) within the lesion (30 min ischaemia and 24h of rep.) following 3-VO in MASP-$2^{+/+}$ (x20 magnification), MASP-$2^{-/-}$ (x40 magn.) and sham operated mouse (x40 magn.). Scale bars 100 and 50 µm.

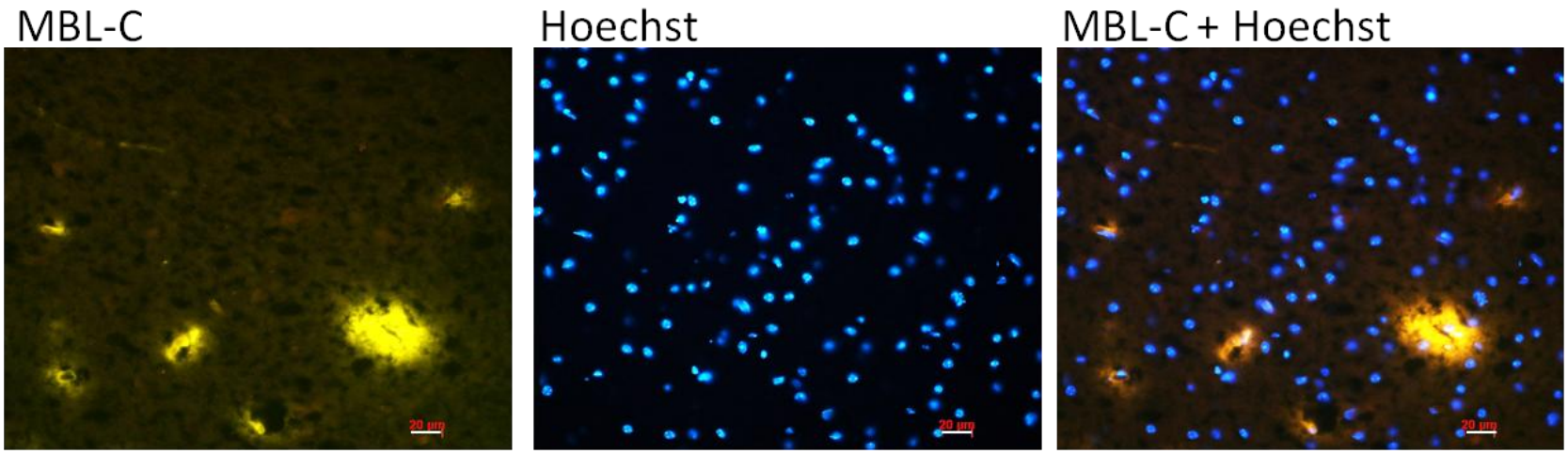

Figure 3.30: MBL-C staining (b)

MBL-C staining deposited around vessels in the damaged area following 30min of ischaemia and 12h of reperfusion (3-VO). Scale bars 20 µm.

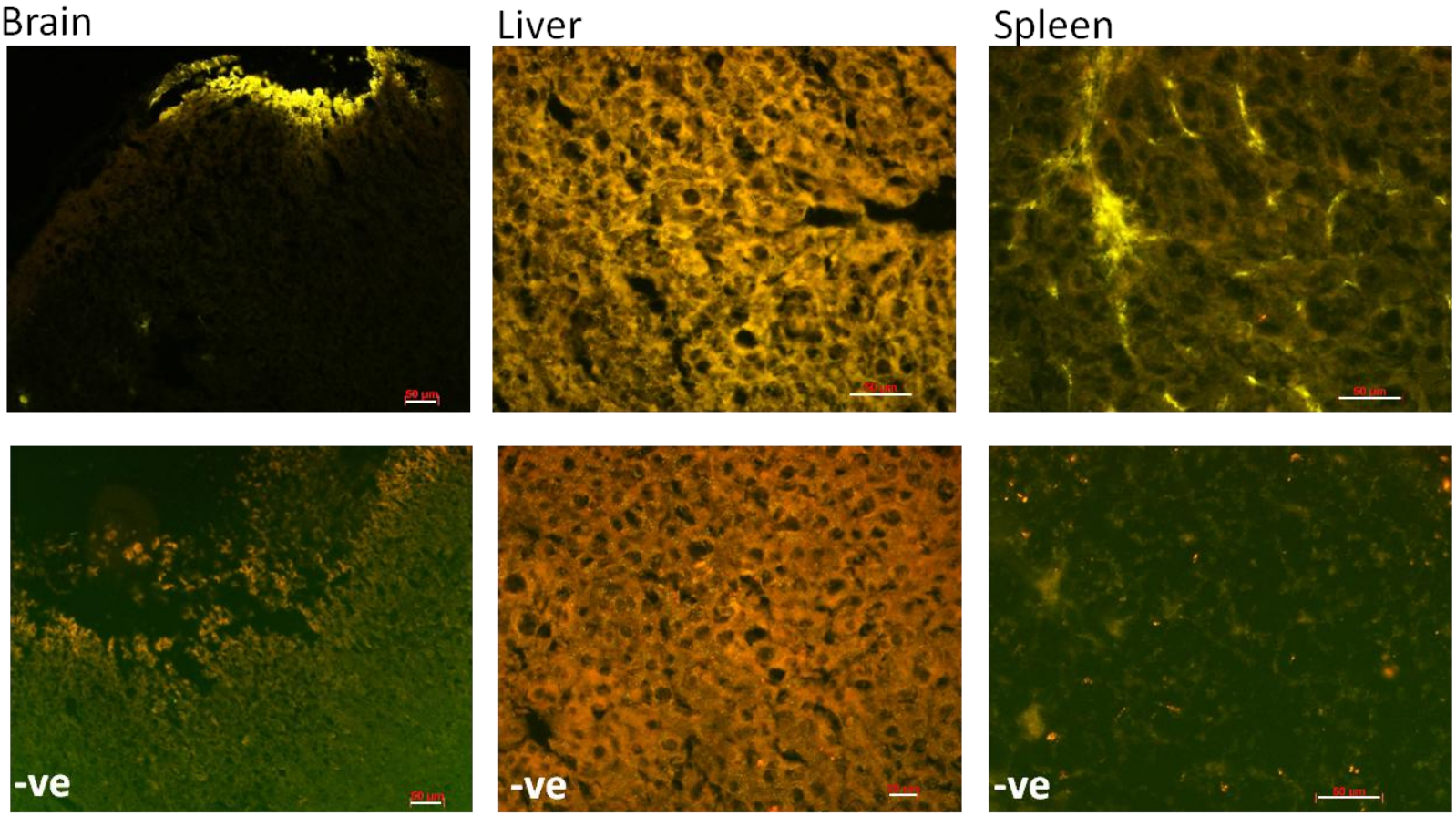

Figure 3.31: MBL-C staining (c)

MBL-C staining at cauterisation site in brain (30 min isch. 12 h of rep.) following 3-VO and its reciprocal negative control (secondary antibody only) at the cauterisation site. MBL-C staining in liver and spleen (used as positive control tissue) and their reciprocal negative controls. Scale bars 20µm and 50 µm.

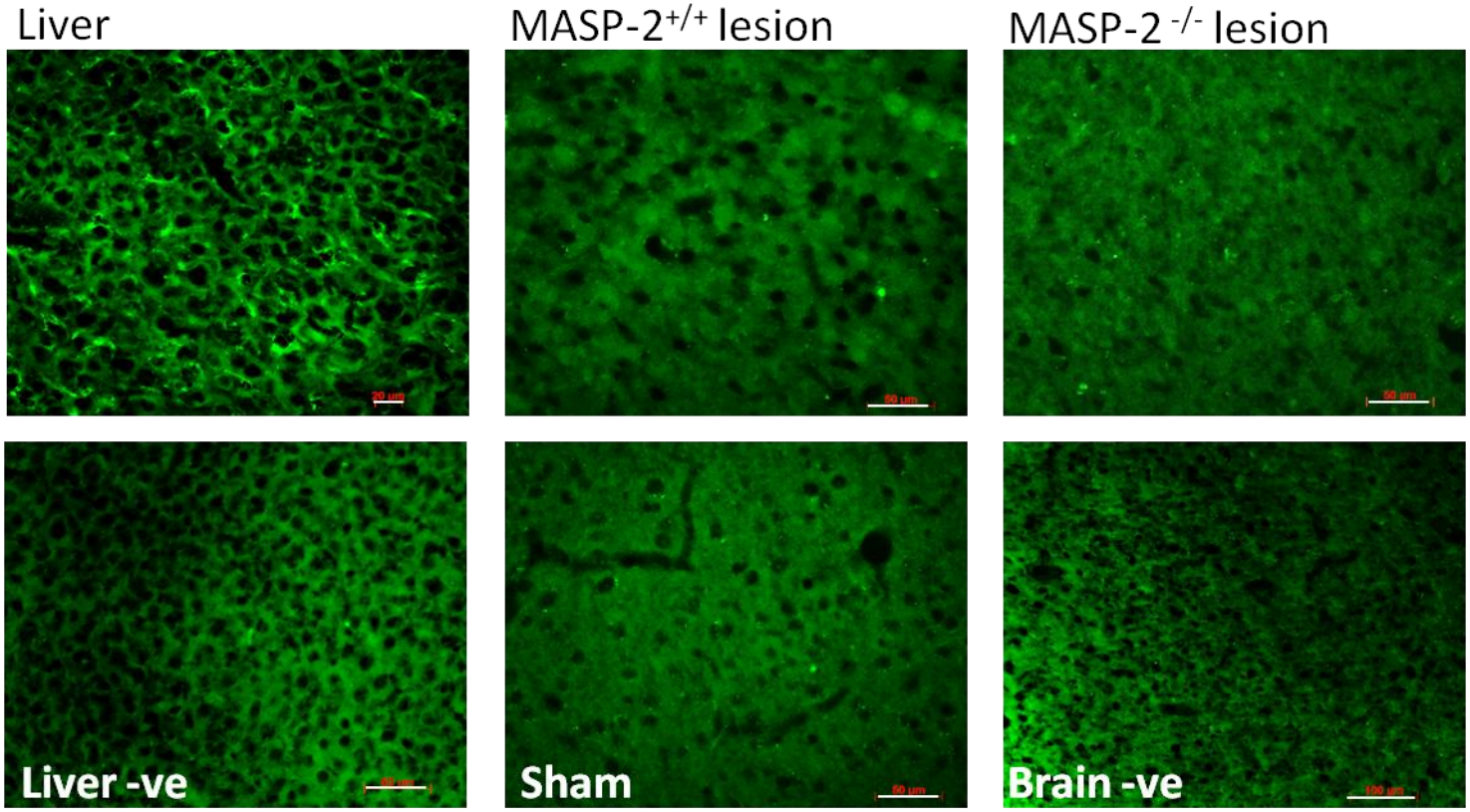

Figure 3.32: Ficolin A staining (d)

Ficolin A staining in liver and brain in MASP-$2^{+/+}$, MASP-$2^{-/-}$, and sham operated mouse at lesion area (30 min ischaemia and 24 h reperfusion; 3-VO). Their reciprocal negative controls in each tissue are also shown (administration of only secondary antibody, anti rabbit Alexa fluor 488). Liver tissue was used as a positive control with positive ficolin A staining. No deposition of ficolin A in brain at this time point. Scale bars 20µm and 50 µm.

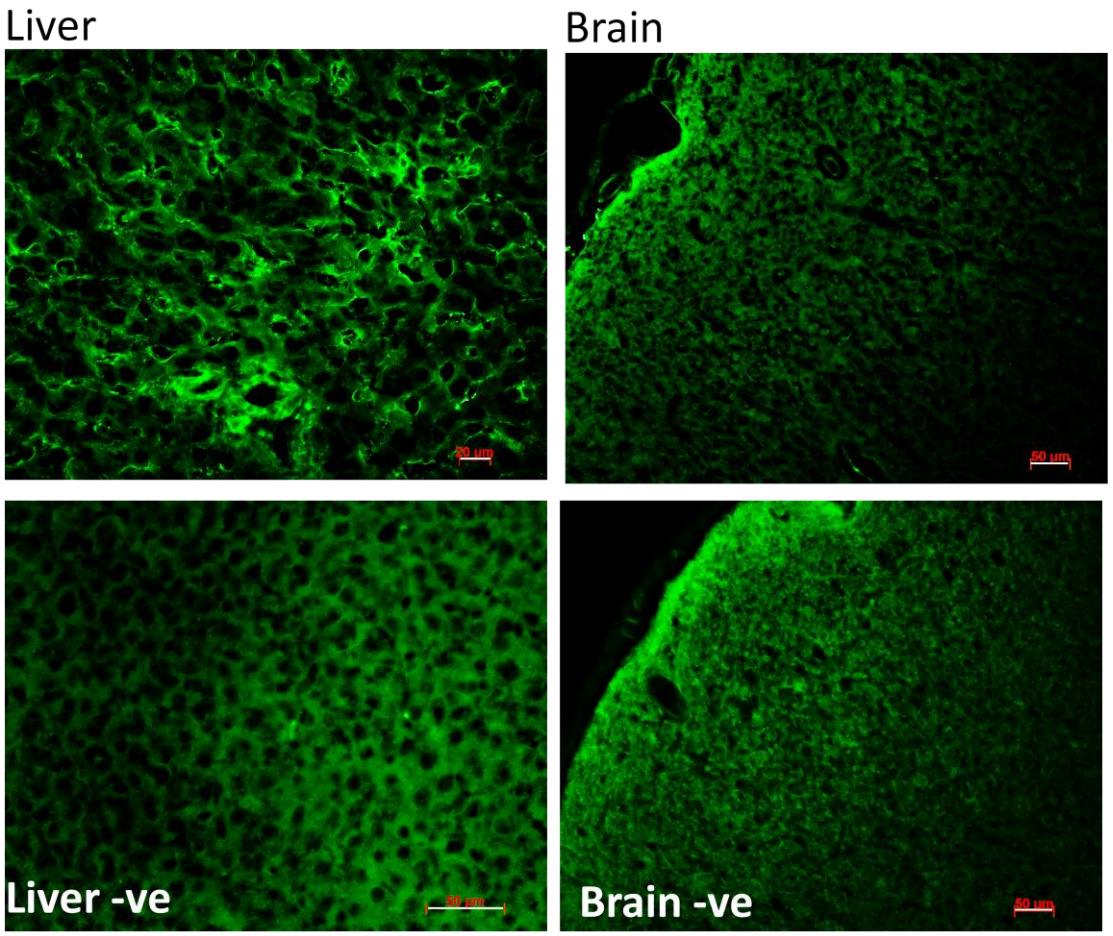

Figure 3.33: Collectin 11 (CL-11) in liver and brain.

Liver was used as a positive control for collectin 11 with deposited CL-11. No deposition of CL-11 was detected in brain lesion at 30 min of ischaemia and 12 h of reperfusion following 3-VO (x20 magnification). Scale bars 20µm and 50µm.

3.7 Expression of markers of inflammation in ischaemia and reperfusion

To assess any differences in the cytokine expression profiles or other markers of inflammation which could be reflective of the inflammatory manifestations among MASP-2 deficient and sufficient mice, real time PCR was performed. This would be useful in elucidating or explaining the protective effect of MASP-2 deficiency in infarct sizes following cerebral IRI. The mRNA expression profile for macrophage inflammatory protein 2 (MIP-2), IL-6 and IL-10 were established as well as that of C1q. MIP-2 was chosen as an example of a pro inflammatory marker as it could also be used to assess macrophage infiltration or microglial activation following stroke. IL-6 was the second marker chosen also as an example of a pro inflammatory marker as it is also reported to be involved in tissue injury in ischaemic stroke (Wang *et al.* 2000, McColl *et al.* 2007, Cojocaru *et al.* 2009). IL-10 was chosen as a marker as it is one of the major anti-inflammatory cytokines which is also found to be protective following stroke (Spera *et al.* 1998). The ipsilateral and contralateral hemispheres from brain tissue of mice that had undergone 3-VO-mediated ischaemia for 30 min followed by 2 h and 24 h of reperfusion were collected immediately after the mice were sacrificed (figure 3.34 and 3.35). mRNA abundance was measured and normalised to that of GAPDH mRNA which was used as a housekeeping gene. At the early reperfusion time point of 2 h MIP-2 mRNA was highly up-regulated (30 fold higher mRNA abundance compared to sham operated mice) in the ipsilateral site in wild type mice, which was significantly higher (with statistical significance, p= 0.0118) than the MIP-2 mRNA abundance in MASP-2 deficient mice that had undergone the same ischaemia times and reperfusion times (Figure 3.34). The MIP-2 mRNA abundance in the contralateral site was also significantly higher (p=0.0019) in the wild type mice when compared to the MASP-2

deficient mice. Compared to sham operated mice IL-6 mRNA abundance was increased by 4 fold in both the WT and MASP-2 deficient mice in the ipsilateral site and around 2 fold in the contralateral site. IL-6 mRNA expression was not statistically different amongst MASP-2 deficient mice and their WT controls. The anti-inflammatory cytokine IL-10 was up-regulated in the 3-VO operated MASP-2 deficient mice by a factor of 2.6 at the 2 h reperfusion time point in the ipsilateral site compared to the sham operated mice while no up-regulation was observed in 3-VO operated and reperfused brains of wild type mice or in the contralateral site in brains of both the WT and MASP-2 deficient mice. C1q mRNA expression did not change in 3-VO operated brains at 2 h of reperfusion when compared to sham operated mice. In 3-VO operated brains harvested after 24 h of reperfusion, C1q B-chain mRNA was up by 2-3 fold in both the ipsilateral and contralateral site when compared to shams. This 2-3 fold up-regulation was identical in WT as well as in MASP-2 deficient mice. MIP-2 and IL-6 mRNA expression profiles looked very similar in 3-VO operated animals after 24 h of reperfusion. The mRNA levels of both cytokines were up-regulated in the ipsilateral site by up to10 fold compared to the sham operated mouse brains in both the MASP-2 sufficient and MASP-2 deficient mice. IL-10 on the other hand at 24 h of reperfusion was up-regulated even more compared to 2 h in the ipsilateral site in both the WT and MASP-2 deficient mice but it was up-regulated 3 times higher in the knock outs (9 fold) than the WT mice (3 fold) (figure 3.35).

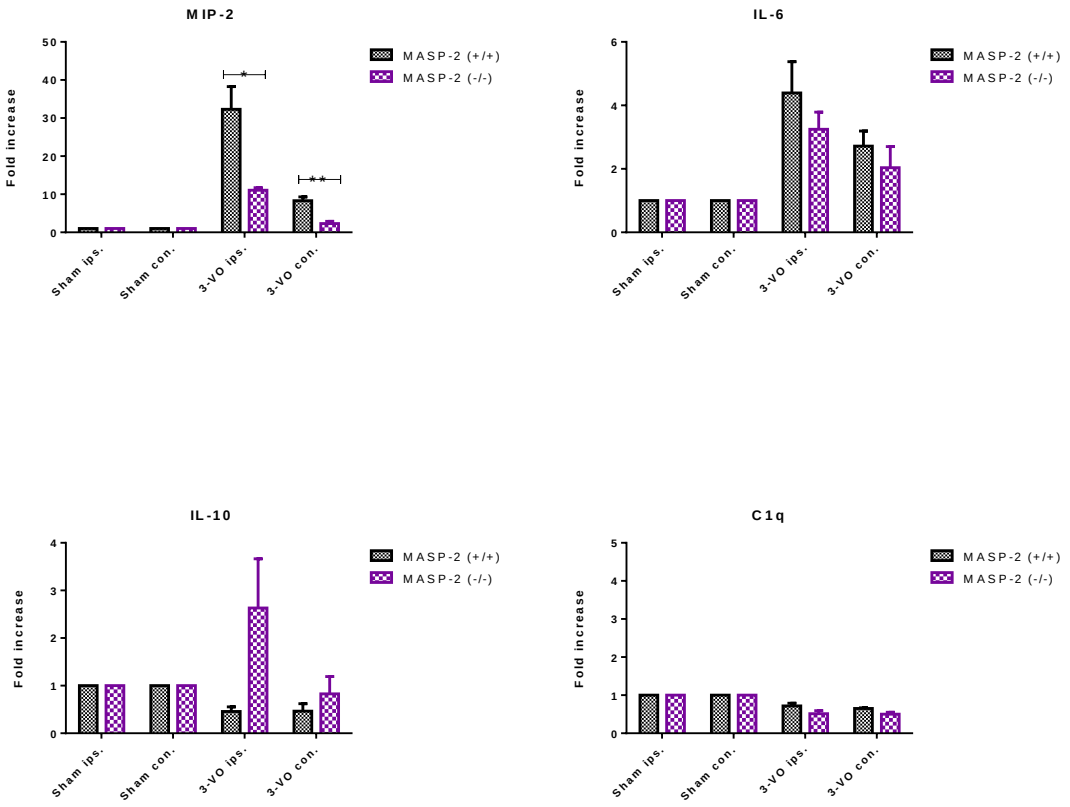

Figure 3.34: Relative changes of mRNA abundance for MIP-2, IL-6, IL-10 and C1q in brains subjected to 30 min of ischaemia and 2 h of reperfusion.

Each cDNA preparation used for this analysis was normalised relative to GAPDH levels of each individual sample. The fold increase of expression was compared to the expression of sham operated mice according to the genetic background (MASP-$2^{+/+}$ or MASP-$2^{-/-}$) and part of brain (ipsilateral or contralateral). Sham operated mice (wt; n=3, MASP-$2^{-/-}$; n=5) and 3-VO operated mice (wt; n=4, MASP-2 KO; n=4) were used. Only MIP-2 expression shows a significant difference between MASP-$2^{+/+}$ and MASP-$2^{-/-}$ mice (p=0.0118 among the ipsilateral site, p=0.0019 among the contralateral site) Error bars show SEM; *p<0.05, **p<0.01, unpaired *t* test.

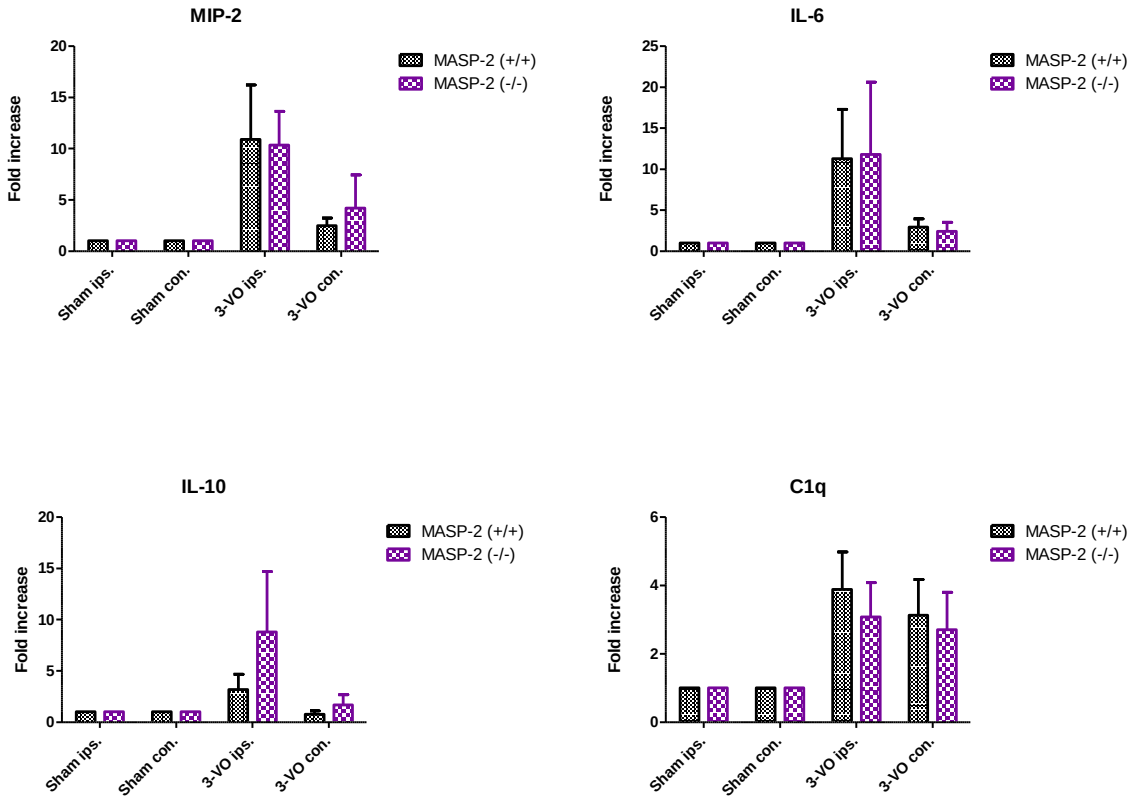

Figure 3.35: Relative changes of mRNA abundance for MIP-2, IL-6, IL-10 and C1q in brains subjected to 30 min of ischaemia and 24 h of reperfusion.

Quantification of the markers was normalised relative to GAPDH levels of each individual sample. The fold increase of expression was compared to the expression of sham operated mice according to the genetic background (MASP-$2^{+/+}$ or MASP-$2^{-/-}$) and part of brain (ipsilateral or contralateral). Sham operated mice (wt; n=3, MASP-$2^{-/-}$; n=5) and 3-VO operated mice (wt; n=6, MASP-2 KO; n=4) were used. No statistical differences were found when comparing wild type to MASP-2 deficient mice at 24h of reperfusion. Error bars show SEM.

Chapter 4: Discussion Part A

As part of the innate immune response the complement system becomes activated when invading pathogens fall under its surveillance. Pathological conditions, however, can also be related to uncontrolled complement activation. This is observed in deficiencies or defects of complement regulators, for example as seen in paroxysmal nocturnal haemoglobinuria were absence of CD59 on erythrocytes leads to unregulated cell lysis through the membrane attack complex (MAC) (Parker 2009). In case of ischaemia and reperfusion injury altered self ligands and changes in the glycocalyx of oxygen deprived cells drive complement activation, leading to pathology (Platts *et al.* 2003). Components of the lectin pathway have been shown to be involved in ischaemia-reperfusion injury (IRI) and complement-mediated IRI has recently been shown to be dependent on the lectin pathway key enzyme MASP-2 in models of myocardial infarction, gastrointestinal ischaemia and renal ischaemia (Schwaeble *et al.* 2011). However, this is the first report that demonstrates that also cerebral IRI is also significantly reduced in the absence of MASP-2.

4.1 Experimental stroke models tested

The MCAO and the 3-VO stroke models of transient cerebral ischaemia were used to assess the phenotype of MASP-2 deficiency in cerebral IRI. Premenopausal females are considered to be more robust compared to males of the same age (due to sex steroidal hormones i.e. progesterone) and have a significantly lower risk of a stroke incidence (Barrett-Connor & Bush 1991, Gibson & Murphy 2004). Due to the poor survival of

male mice during and post surgery in the 3-VO pilot study and in order to reduce sex dependant variation, only female mice were used in this project. However, a degree of variability (due to differences in the progesterone levels within the oestrus cycle) was expected, therefore female mice were caged in groups of 4 to 5 as grouping suppresses the oestrus cycle (Champlin 1971). Technically, the 3-VO model was easier to perform with higher success rates and therefore lower numbers of mice were needed, compared to the MCAO model. The latter involved a more invasive surgical procedure involving an intravascular filament induction in the MCA that was prone to more intrinsic variability. A particular challenge in this model, however, is the degree of anatomical variability between individual mice which did not always allow proper placement of the filament which in turn prevented sufficient occlusion of the MCA (as determined by <70% reduction in cerebral blood flow). In comparison, however, the 3-VO stroke model proved to be a more reliable model and was therefore used throughout my study as it produced less variability in infarct sizes and cerebral blood flow changes during the operation, avoiding the high degree of variability in lesion volumes and blood flow seen in the MCAO model. The high degree of variability in lesion volumes derived following MCAO stroke model has also been noted in other studies, including uncorrelated lesion sizes to the induced ischaemic time (Yanamoto *et al.* 2003). In my experience, the most limiting parameters in the MCAO stroke model were the unpredictable cerebral blood flow profiles after insertion of the filament in the MCA. This model failed to generate the standardized and reproducible ischaemia insult that was required to assess the role of the lectin pathway in cerebral IRI. The unpredictable cerebral blood flow profiles that were obtained when using the MCAO model made the comparison between the phenotypes of MASP-2 sufficient and MASP-2 deficient mice significantly less reliable. These profiles included i) early reperfusion (before the end of

the ischaemic time and the withdrawal of the occluding filament), ii) no reperfusion upon withdrawal of the filament and iii) fluctuations of the cerebral blood flow during the ischaemic time. Similar complications were also reported in other studies using the MCAO stroke model (Yanamoto *et al.* 2003, Livnat *et al.* 2010). Therefore the MCAO model was not used further.

In terms of animal welfare the 3-VO stroke model induces a milder injury and in terms of neurological deficits the 3-VO model was barely affecting motor functions. In contrast, the MCAO model affects both the cortical and subcortical regions in the brain and can lead to severe motor disabilities. For this reason a more delicate somatosensory behavioural testing system had to be used as the 28-point neurological scale scoring system (Clark *et al.* 1998) was not able to detect any major neurological changes induced following 3-VO operation. The main limitation of the 3-VO model is that part of the MCA is cauterised. Similar to the Indian ink perfusion staining in this study (used to assess reperfusion), another study using the same 3-VO model (Yanamoto *et al.* 2003), reported that the 3-VO procedure disrupted the blood flow to the proximal area around the cauterised site of the MCA, but the distal parts covering the MCA territory maintained blood flow through collateral circulation and anastomosis. This was as observed in this study.

4.2 MASP-2 deficiency is protective in cerebral IRI

As seen in chapter 3, MASP-2 deficiency was shown to be beneficial for mice undergoing 30 minutes of ischaemia followed by 24 hours of reperfusion using the 3-VO stroke model. This was shown by TTC staining, revealing smaller infarct volumes,

when compared to wild type controls undergoing the same procedure. Neurological deficits were assessed following 3-VO using the 28 point neurological scale (see figure 2.3, chapter 2). The neurological scoring in this stroke model which compared the magnitude of motor deficits, revealed minor motor disabilities in both the assessed groups (i.e. with a mean score of 4 out of 28 in wild type mice) and gave no statistical significant differences among wild type and MASP-2 deficient mice. There are no clinical data available that correlate MASP-2 deficiency with the outcome in ischaemic strokes in humans as MASP-2 deficiency is too rare. However, this study's findings, showing that MASP-2 deficient mice are protected from cerebral IRI, do correlate very well with previous reports showing that people deficient in the lectin pathway recognition component MBL or people with very low MBL levels have a significantly better prognosis following stroke compared with patients with normal or high MBL levels (Cervera *et al.* 2010, Osthoff *et al.* 2011). Similarly, MBL deficiency in mice is also reported to be protective after experimental stroke (Cervera *et al.* 2010).

Cortical lesions have been generated in 3-VO operated animals in comparison to sham operated animals, as revealed by TTC staining as well as by the assessment of neuronal loss as seen by immunohistochemistry. MASP-2 deficient mice showed reduced depositions of C3c in the ischaemic lesions when compared to MASP-2 sufficient mice, reflecting a reduced degree of complement activation in absence of the lectin pathway. This suggests that MASP-2 driven lectin pathway activation is contributing to tissue injury and that its inhibition has a beneficial effect as it reduces complement activation during reperfusion. MBL-C was seen to be deposited within the lesion in both MASP-2 deficient and sufficient mice as expected, as depletion of MASP-2 would not affect the binding of the lectin pathway recognition molecules to the ischaemic cells.

Nevertheless, this is in accordance with other studies indicating that MBL is involved in ischaemia and reperfusion pathology. MBL-A staining was not achieved within the timeframe of this project so no conclusion as to whether it binds in the ischaemic lesions can be made in this study. However, in an experimental model of stroke in mice MBL-A binding and deposition was recorded within vessels of the lesion areas (Orsini *et al.* 2012).

Collectin-11 and ficolin-A have not been detected in the ischaemic brains at least at timepoints of 12 h and 24 h of reperfusion respectively. Ficolin-A is the murine orthologue of human L-ficolin and there is no evidence in the current literature that it is involved in stroke pathology. However, a recent study reported that patients with acute ischaemic strokes were recorded with significantly lower levels of ficolin 3 (or ficolin H; one of the three human ficolins) in serum (in the admission and the follow up samples) compared to healthy individuals and that lower levels of ficolin 3 in serum were correlated with a more severe outcome (Fust *et al.* 2011). The role of collectin-11 in stroke is still not reported in current literature. MBL is the most extensively studied lectin pathway recognition molecule and has been shown to contribute to tissue injury following stroke (Cervera *et al.* 2010, Orsini *et al.* 2012), but the report by Fust *et al.* study indicates that ficolins may also play a role in the post-ischaemic pathophysiology of ischaemic stroke and should be taken into further consideration for future investigations (Fust *et al.* 2011).

Histologically, MASP-2 deficiency presented with marked changes in the degree of astrocytic activation. The GFAP expressing astrocytes were localised in the boundary of the necrotic areas after 24 h of reperfusion with MASP-2 sufficient mice showing a

higher degree of GFAP expression in astrocytes compared to MASP-2 deficient mice. Reactive gliosis of astrocytes and glial scar formation involves structural and functional alterations in astrocytes and is observed amongst other conditions in ischaemic stroke. The role of astrocytes during ischaemia is pivotal. On one side, neuron survival post ischaemia is supported by functions of astrocytes such as glutamate uptake (essential for homeostasis and the release of neutrophins) (Zhao & Rempe 2010). On the other hand astrocytic swelling and changes in the physiological functions of astrocytes following ischaemia could be detrimental for neurons (Kimelberg 2005, Zhao & Rempe 2010). As a consequence of cerebral ischaemia or inflammation, glutamate transporter expression is down-regulated in astrocytes, which in turn can lead to loss of glutamate homeostasis and subsequent loss of neuronal cells (Dallas *et al.* 2007). It has also been reported that TNF-α down-regulates the expression of EATT2, a glutamate transporter (Boycott *et al.* 2008). Thus there is most likely a link between inflammation, ischaemia and the function of astrocytes. The reduction of inflammatory responses including TNF-α production (especially produced by infiltrating leukocytes) achieved by the inhibition of lectin pathway activation via MASP-2 depletion could also be beneficial by minimising post ischaemic reactive gliosis. The boundary of the ischaemic lesion area was also characterised by ramified (activated) microglia. However, the microglial/ macrophage recruitment between MASP-2 sufficient and deficient mice, at least at the time point of 24 h post ischaemia, appeared not to differ. The effect of MASP-2 deficiency on microglial/ macrophage activation and recruitment following stroke needs to further be characterised at different time points for a clearer overview.

4.3 Expression of inflammatory markers in MASP-2 deficiency

Pro-inflammatory mediators like IL-6 and MIP-2 were up-regulated in 3-VO operated brain tissues in the ipsilateral site of the lesion, indicating a local immunological response following the ischaemic insult. Such pro-inflammatory cytokines are involved in ischaemia induced injury in the brain (Wang *et al.* 2000, McColl *et al.* 2007). The MIP-2 mRNA expression profile indeed showed a markedly reduced or delayed immunological response in MASP-2 deficient mice when compared to MIP-2 mRNA abundance in WT mice. The reduced MIP-2 mRNA levels could account for the reduced lesion sizes in MASP-2 deficient mice through reduced recruitment of neutrophils which are found to be recruited at site of injury by MIP-2 (Ohtsuka *et al.* 2001, McColl *et al.* 2007). The exact source of MIP-2 in pathological conditions in the brain is not clearly defined. However, microglia/infiltrating macrophages, astrocytes and endothelial cells have been described in the literature and found to be capable of MIP-2 production (Otto *et al.* 2000, Wang *et al.* 2000, Ohtsuka *et al.* 2001, Tomita *et al.* 2005). The phenotypically milder astrocytic response seen immunohistochemically could be one of the reasons for reduced MIP-2 mRNA levels in 3-VO operated MASP-2 deficient mice compared to WT mice, even though microglial/macrophage recruitment patterns were similar in MASP-2 deficient mice and WT mice undergoing 3-VO.

The increased anti-inflammatory cytokine IL-10 mRNA abundance in MASP-2 deficient mice in comparison to WT control mice undergoing ischaemia and reperfusion is also supportive of reduced inflammatory reactions in MASP-2 deficient mice. These results are supported also by another study in which IL-10 post ischaemic gene transfer was found to be protective against global cerebral ischaemia (Ooboshi *et al.* 2005). In summary, MASP-2 deficiency and subsequent lectin pathway deficiency is neuroprotective following cerebral ischaemia and reperfusion injury, at least in part by

modulation of the inflammatory response reflecting on increasing anti-inflammatory mediators (i.e. IL-10) and diminishing pro-inflammatory mediators (MIP-2). The classical pathway recognition molecule C1q mRNA was also assessed and was up-regulated in both hemispheres in MASP-2 deficient and sufficient mice as a response to the ischaemic insult at 24h of reperfusion. This is in agreement with another study recording highly up regulated C1q expression following global cerebral ischaemia (Schafer *et al.* 2000). C1q was shown in a different study to increase microglial phagocytosis and could therefore mediate clearing of apoptotic cells and cellular debris (Fan & Tenner 2004).

4.4 Conclusion

In conclusion, my assessment of the phenotype of the MASP-2 deficiency in the 3-VO model of stroke shows a significant neuroprotective phenotype following ischaemia and reperfusion injury compared to MASP-2 sufficient age, strain and sex matched control animals. This identifies therapeutic MASP-2 inhibition as a very promising target for stroke treatment.

Chapter 5: The Effect of Anti-MASP-2 Antibody Treatment in Cerebral Ischaemia and Reperfusion Injury, Results Part B

As shown in the previous chapter MASP-2 deficient mice showed a significant degree of protection from cerebral ischaemia and reperfusion injury, presenting with significantly smaller infarct sizes compared to wild type control mice in the 3-VO model of stroke. Based on this very clear phenotype of MASP-2 deficiency and the protective effect of the application of a MASP-2 inhibitory mAb in models of myocardial and gastrointestinal I/R injuries (Schwaeble *et al.* 2011), the inhibitory anti-MASP-2 antibody, AbD04211, a murine specific MASP-2 inhibitor, was assessed for the therapeutic MASP-2 inhibition in the 3-VO cerebral I/R injury model of stroke.

5.1 Inhibitory antibody and infarct size

Initially, the inhibitory effects of the AbD04211 and OMS646-016 antibodies were validated and the inhibitory activity of the antibodies in blocking lectin pathway functional activity *in vitro* was shown. 1% of wild type mouse serum was incubated together with serial dilutions of the inhibitory antibodies, control antibody and saline control taken from the different aliquots of stocks used *in vivo*. As indicated in figure 5.1 the anti-mouse specific mAb as well as the anti-human MASP-2 inhibitory antibodies were successfully blocking lectin pathway specific C3 activation on mannan in contrast to the control groups which were not.

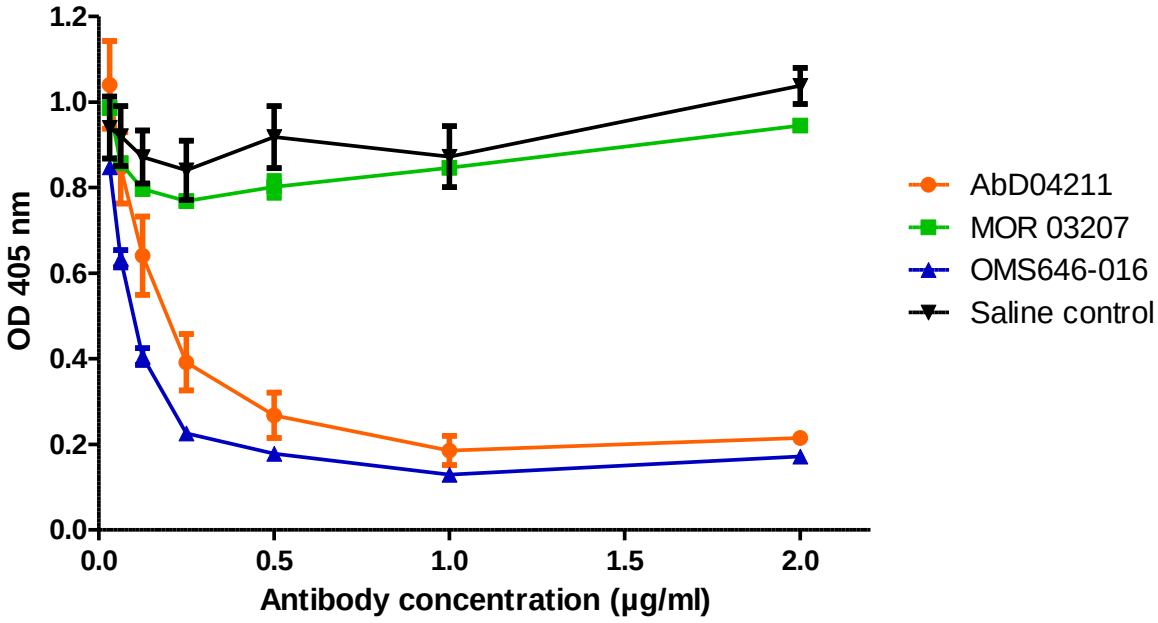

Figure 5.1: ELISA for lectin pathway C3 activation assay showing the inhibitory effect of the inhibitory anti-mouse MASP-2 Ab, its isotype control, the inhibitory anti- human MASP-2 Ab and the saline control using 1% of wild type mouse serum.

The graph is a representative experiment from a series of identical experiments (taken from different stock aliquots of the same antibodies used *in vivo* following 3-VO) giving the same pattern of results. For each individual experiment duplicate readings were taken for each concentration of Ab or control groups. The measurements are represented as means +/- SEM.

The following studies were performed using two different doses of inhibitory antibodies. In the first series, an antibody concentration of AbD04211 and MOR03207 of 1 mg of antibody per kg of body weight and 10 mg of the OMS646-016 antibody per kg of body weight was used. In the second study the dose of AbD04211 was increased to 5 mg of antibody per kg of body weight. While the lower dose of MASP-2 inhibitors (AbD04211 and MOR03207) revealed no statistically significant effect on the brain infarct sizes of MASP-2 inhibitor treated WT controls, the second series of experiments

revealed that the use of MASP-2 inhibitor (AbD04211) at a dose of 5 mg/kg body weight achieved a significant protective effect with infarct sizes in AbD 04211 being reduced by up to 30% compared to the isotype control treated or saline treated controls.

5.1.1 Low dose antibody treated group

The MASP-2 inhibitory antibodies, as well as the isotype control antibody and saline controls, were administered in wild type mice through intraperitoneal injection 18 h prior to 3-VO operation. Following 30 min of ischaemia and 24 h of reperfusion, mice were sacrificed and blood samples were collected by cardiac puncture (figure 5.2). TTC staining for determination of infarct sizes in coronal brain sections was immediately performed indicating that the infarct sizes in the inhibitory MASP-2 treated groups (A and C) of mice were not statistically different from the control treated groups (B and D) (figure 5.3).

Group ID	Test Article	Target MASP-2	Type	Dose	Dosing volume
A	AbD04211	Mouse	Inhibitory	1mg/kg	10ml/kg
B	MOR 03207	Mouse	Control	1mg/kg	10ml/kg
C	OMS646-016	Human	Inhibitory	10mg/kg	10ml/kg
D	Saline	-	Control	-	10ml/kg

Figure 5.2: Timeline of events from left to right and table of the MASP-2 inhibitory antibodies and their controls.

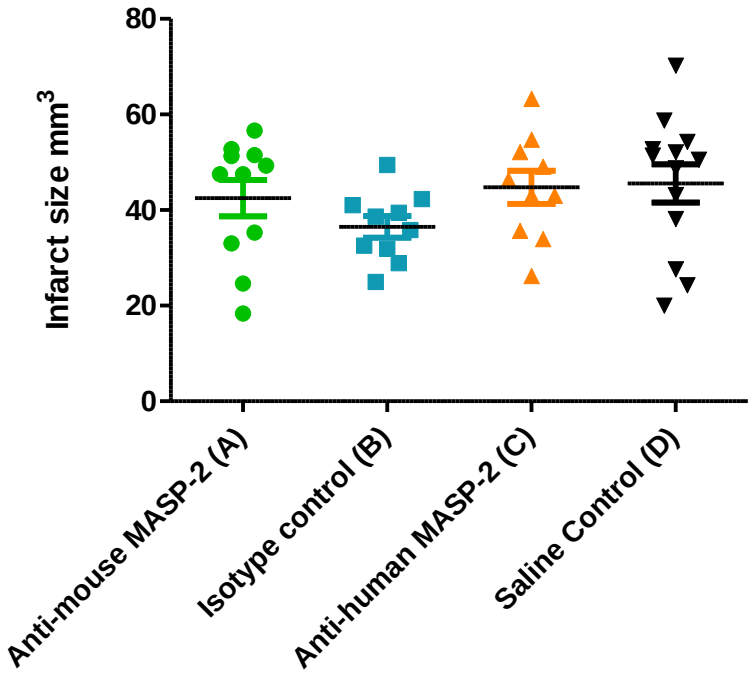

Figure 5.3: Infarct sizes following 3-VO for 30 min of ischaemia and 24h of reperfusion when inhibitory MASP-2 antibodies and their controls were administered 18h before the ischaemic event.

Group A (antibody AbD04211 used at 1mg/kg; n=11), group B ((isotype control antibody AbD 0411 used at 1mg/kg; n=11), group C (OMS721 used at 10mg/kg; n=10) and group D (n=13). Two tailed t-test statistical analysis for each group with its reciprocal control group was performed indicating no statistically different infarct sizes among the different treated groups. Data represented as means+/- SEM.

In order to assess whether the dosing of the therapeutic MASP-2 antibody was sufficient to mimic the CNS MASP-2 deficient protective phenotype seen in the mouse line (see chapter 3) the extent of residual lectin pathway specific C3 activation was determined in sera of MASP-2 inhibitor treated mice. The inhibitory effect of the antibodies *in vivo* was assessed by the lectin pathway specific C3 activation of serum by samples collected by each individual animal prior to the administration of the antibodies and comparing it to the C3 activation 24 h after 3-VO operation and 42 h after the administration of the inhibitory antibodies (*in vivo* administration dose 1 mg per kg of body weight). Mannan

was the activating surface component of choice and complement activation was measured in 1% serum. Although both of the inhibitory antibodies were shown to have blocking activity *in vitro*, in serum extracted from the 3-VO operated animals it was clear that the majority of the animals receiving the MASP-2 inhibitory antibodies (at a dose of 1 mg/kg of body weight) had more than 50% residual lectin pathway functional activity. Only 1 out of 11 mice showed more than 50% inhibition of lectin pathway functional activity after the inhibitory anti mouse MASP-2 antibody treatment at a final concentration of 1mg/kg of body weight. Furthermore, only 3 out of 9 mice showed more than 50% inhibition of lectin pathway functional activity after treatment with the established antibody against human MASP-2 (see figure 5.4).

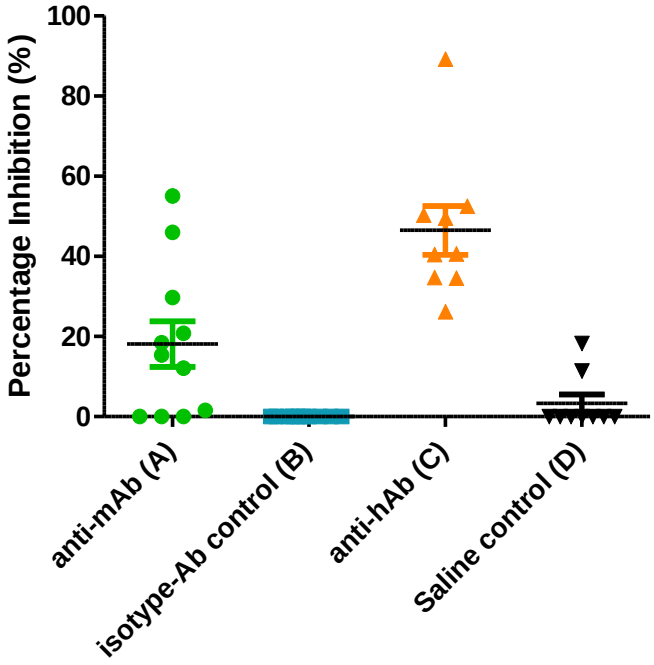

Figure 5.4: Percentage inhibition of lectin pathway specific C3 activation in mouse sera collected 24h post 3-VO operation and 42h post inhibitory MASP-2 antibody or control group administration.

Group A (n=11), group B (n=10), group C (n=9) and group D (n=9). The measurements are represented as means+/-SEM.

The results showing the percentages of inhibition of the lectin pathway functional activity after the administration of the MASP-2 inhibitory antibodies at a low dose concentration raised further questions about the optimum dosage for the particular antibodies for sufficiently blocking the pathway. In order to investigate this in more detail a further experiment was performed where mice were injected with different dosages of the anti-mouse MASP-2 inhibitory antibody AbD04211. When looking at the inhibitory effects of the given dosages in serum collected 16 h later after i.p. injection of the MASP-2 inhibitors, as expected, a dose-dependent response was observed with the highest inhibitory effect observed when the antibody was dosed at 6mg/kg (Figure 5.5).

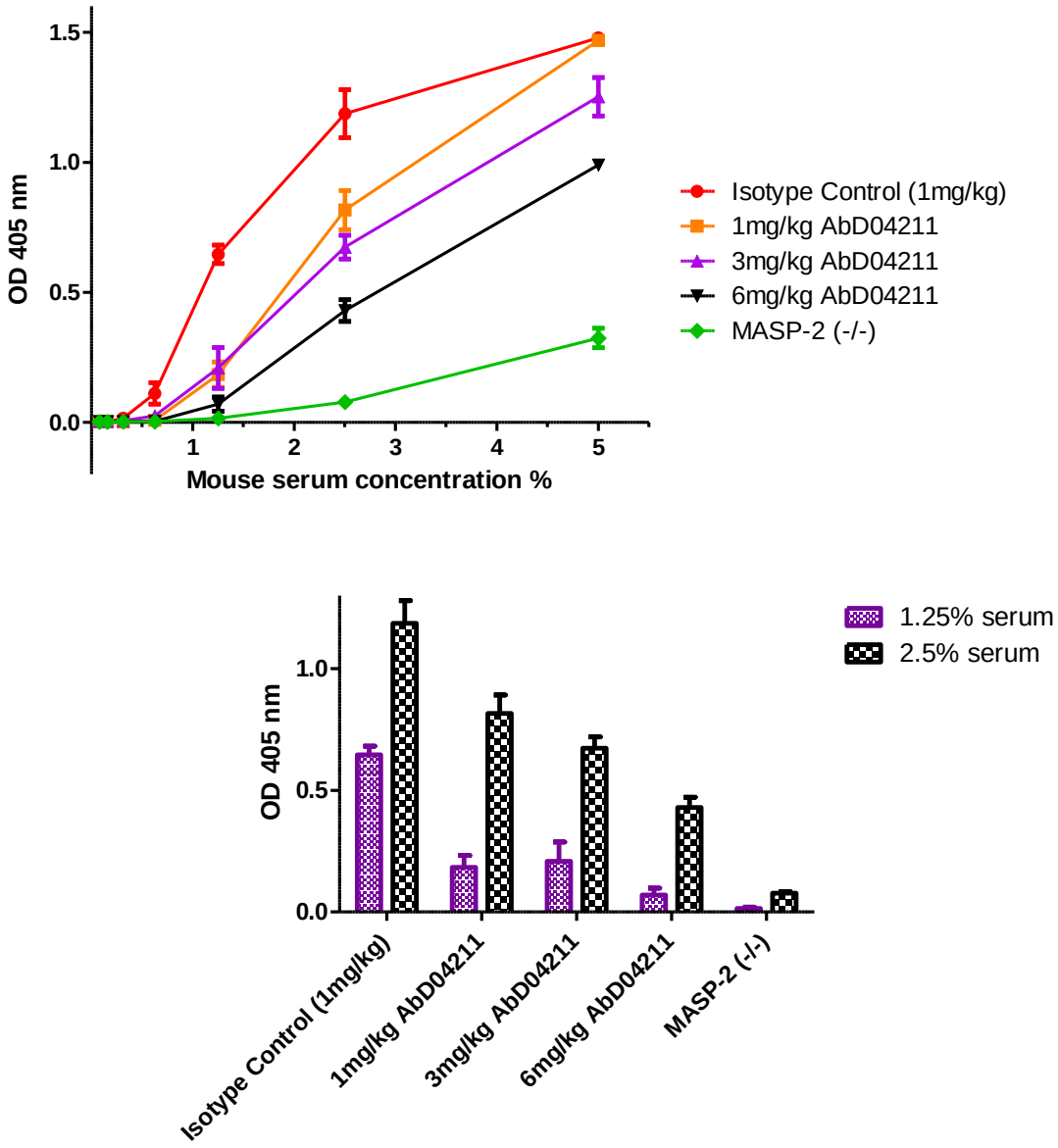

Figure 5.5: Lectin pathway C3 activation assay, assessing lectin pathway inhibition in mice dosed with different concentrations of anti-mouse MASP-2 inhibitory antibody and its isotype control 16 h after their administration.

Data represented as means +/- SEM from two dosed animals from each treated group.

5.1.2 High dose antibody treated group:

The 6mg/kg dose of inhibitory antibody was blocking the lectin pathway 2.6 times more effectively than the 1 mg/kg dosage. These results indicated that a higher dose of the

inhibitory antibody was necessary to block the lectin pathway and therefore a second set of experiments was carried out using 5 mg/kg of the anti-mouse MASP-2 antibody administered i.p. around 32 h prior to 3-VO operation. Likewise, a dose of 5 mg/kg was also used for the isotype control antibody mAb205P. Blood samples were collected prior to, at 18 h and 66 h post antibody administration to monitor the levels of lectin pathway inhibition at the different stages of the experiment (Figure 5.6).

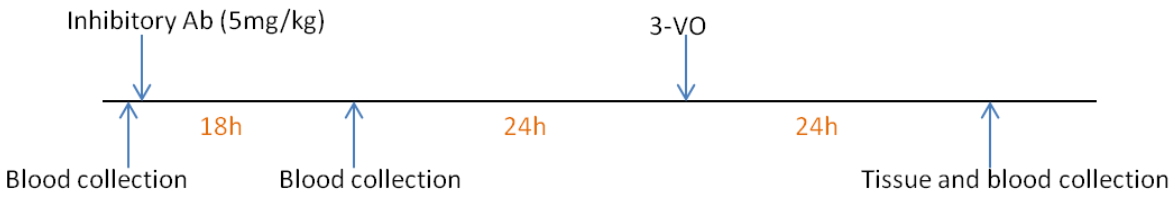

Figure 5.6: Timeline illustrating the events occurring during the 5 mg/kg inhibitory antibody administration.

With a mean value of 34.11mm^3, the inhibitory MASP-2 antibody treated mice had statistically significant smaller lesion sizes compared to the isotype control treated mice (48.5mm^3, p= 0.0272) and to the saline control treated mice (47.1mm^3, p=0.0418). These results showed that therapeutic MASP-2 inhibition is infarct protective, leading up to 30% smaller lesion volumes of the MASP-2 inhibitor treated animals compared to the isotype antibody treated group (see figure 5.7). This effect was not seen when animals were treated with 1 mg/kg of the same antibody. As mentioned in chapter 4 the 3-VO stroke model was giving minor to insignificant motor deficits (using the 28 point neurological scale) making the neurological assessment and comparison among the different treatment groups less apparent. However, statistical analysis indicated significantly improved neurological scoring in MASP-2 antibody treated mice compared to the isotype control treated mice (see figure 5.8).

As before the levels of lectin pathway inhibition were assessed at two time points using a lectin pathway driven C3 activation assay and mice not showing at least 50% inhibition of lectin pathway functional activity at both time points (18 h and 66 h post antibody injection) were excluded from the measurement of infarct sizes. A dosage of 5 mg/kg offered an average of 77% inhibition of C3 driven lectin pathway activation at 18 h post administration of the antibody which dropped at 66 h time point to 61% of average inhibition. The 3-VO procedure and reperfusion was performed at 42 h (Figure 5.9). Indeed, MASP-2 inhibition led to statistically significant decrease of the lesion volume which underlines the therapeutic utility of MASP-2 inhibition to reduce the size of cerebral infarction.

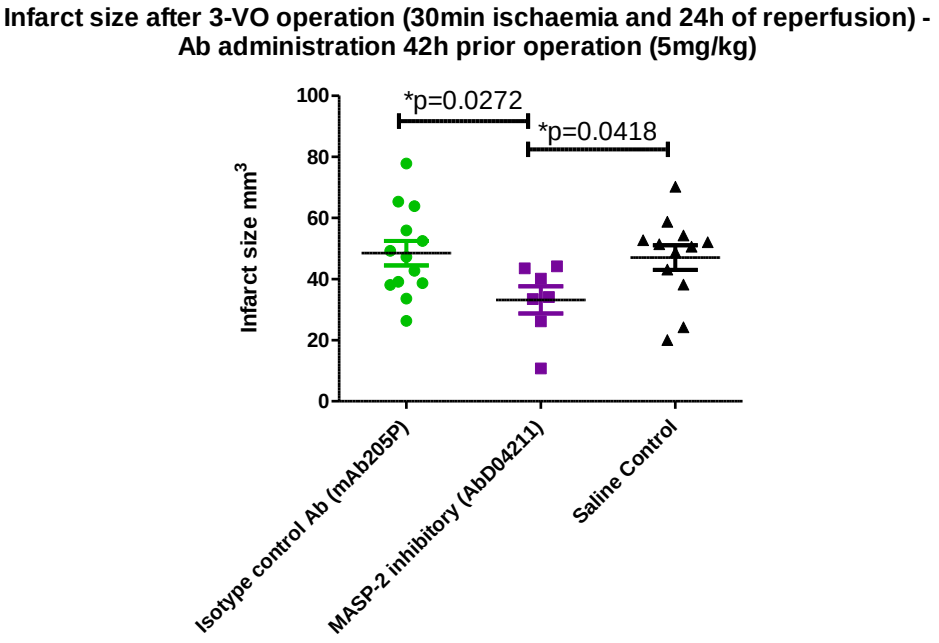

Figure 5.7: Infarct size of mice administered with inhibitory MASP-2 antibody AbD04211 (5mg/kg) 42h prior to 3-VO stroke surgery.

Data are reported as scatter-dots with mean values (black bars) and standard error bars (coloured bars). The statistical test used for analysis was the unpaired *t* test;*p<0.05.

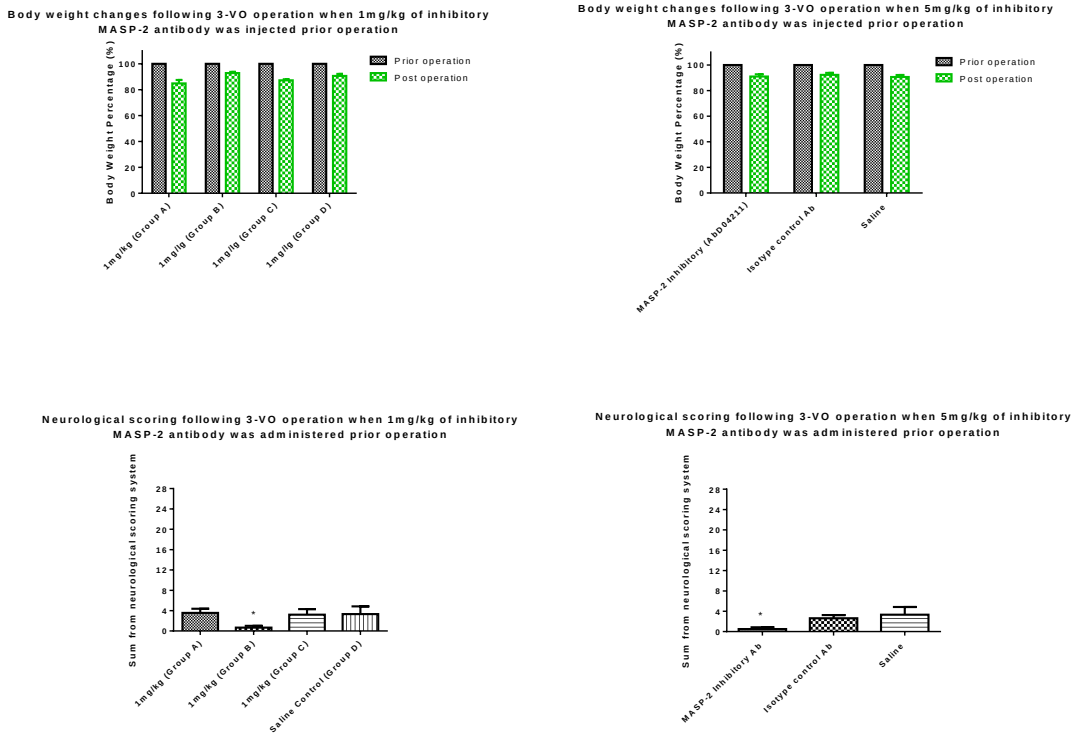

Figure 5.8: Body weight changes and neurological scores from mice receiving 1mg/kg or 5mg/kg of the anti-MASP-2 inhibitory antibodies.

The 1 mg/kg dose of the isotype control treated group (Group B) showed a significantly improved neurological score compared to the AbD04211 antibody treated group (Group A) when using the same concentration of inhibitory antibody. No significant difference in scoring was observed between the human anti-MASP-2 treated group (Group C) and saline control (Group D). The 5 mg/kg dose of the AbD04211 treated group showed a significantly improved neurological score compared to the isotype control treated group when using the same concentration of isotype control;*$p<0.05$, unpaired *t* test.

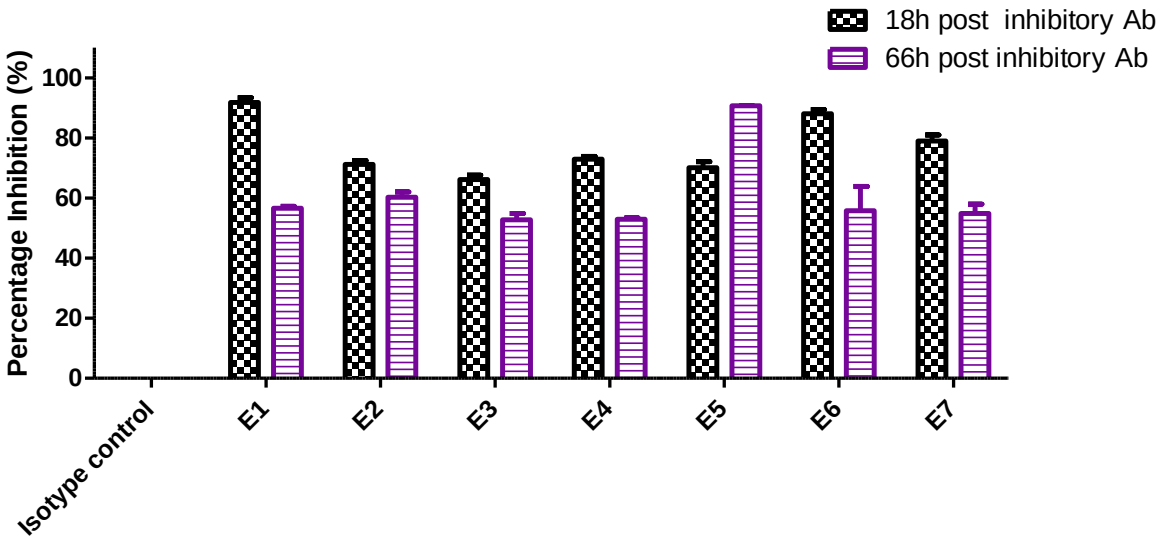

Figure 5.9: Percentage inhibition of lectin pathway specific C3 activation

Percentage inhibition of the lectin pathway specific C3 activation in different mice (E1 to E7) showing more than 50% inhibition of lectin pathway functional activity assessed in 1% serum at 18 h and 66 h post inhibitory MASP-2 antibody AbD04211 (5 mg/kg) administration. Data represented as the mean from duplicates in the experiment +/- SEM.

Chapter 6: Discussion Part B

6.1 Ischaemia and reperfusion studies

The temporary loss of blood supply followed by reperfusion of the oxygen deprived tissue drives a severe inflammatory response, leading to tissue injury and damage. Ischaemia reperfusion injury (IRI) is observed in stroke, myocardial or gastrointestinal infarction as well as during organ transplantation. One of the major contributors to IRI-injury mediated tissue loss is the complement system. Three different activation pathways of complement known as the classical, the lectin and the alternative pathway have been studied in order to understand the contribution of each individual pathway in ischaemia and reperfusion tissue injury. Some older studies suggested that the classical activation pathway is key to IRI mediated tissue loss, as it could be initiated by either natural antibodies or autoantibodies against antigens exposed as a consequence of ischaemic insults. A classic paper supporting this view point is reported in a study on C4 or RAG1 deficient mice (RAG1 deficient mice are IgM and IgG deficient), using a gastrointestinal IRI model. C4 as well as RAG1 mice both presented with reduced C3 deposition in tissue (Williams *et al.* 1999). Likewise, C4 and RAG2 deficiency (i.e. resulting in a total antibody deficiency) were shown to be beneficial in skeletal IRI models (Weiser *et al.* 1996). However, the assumption that complement activation was driven by the classical pathway (as it was thought in the previous studies) was challenged by the more recent finding that showed that classical pathway deficient mice (lacking the critical component C1q) were not protected from gastrointestinal or myocardial infarction IRI in contrast to C2/fB deficient mice (Hart *et al.* 2005, Walsh *et*

al. 2005). When the C2/fB deficient mice were reconstituted with human recombinant C2 IRI injury was restored. This suggests a C2 dependent activation mechanism (mediated either by the lectin or the classical pathway) that critically contributes to tissue injury and possibly was also amplified by alternative pathway activation (Hart *et al.* 2005, Gorsuch *et al.* 2012). Considering that C1q deficiency was not protective in IRI, this study suggests that the lectin pathway is most likely involved in inducing tissue injury rather than the classical pathway.

It is important to bear in mind that immunoglobulin and natural antibody driven complement activation (Zhang *et al.* 2004), is not exclusively mediated by the classical pathway and later work of the same group that published the early studies (Zhang *et al.* 2004) shifted their paradigm from the classical pathway to lectin pathway mediated activation events (Zhang *et al.* 2006). In addition, when C4, C3, RAG1 deficient mice and C1-inhibitor or soluble complement receptor 1 (sCR1) treated mice were tested in models of IRI, they had significantly reduced tissue damage and it is clear that these mice are compromised in both the lectin pathway and the classical pathway (Williams *et al.* 1999, Fleming *et al.* 2002, Hart *et al.* 2005, Storini *et al.* 2005). Moreover, it was shown that immunoglobulins can also bind to lectin pathway recognition molecules like MBL. Examples of MBL- immunoglobulin interactions have recently been published where the lectin pathway drove antibody directed haemolysis and enhanced phagocytosis of particles opsonised by IgG or IgM (Suankratay *et al.* 1999, Arora *et al.* 2001). Furthermore, in a model of intestinal IRI MBL was found to be co-localised with IgM and MBL deficient mice were protected from injury in contrast to C1q deficient mice. This suggests that the lectin pathway can be activated by the binding of

MBL to natural antibodies as *in vitro* binding of MBL to mouse IgM was also clearly shown (Zhang *et al.* 2006).

A clear and strong support for the central role of the lectin pathway in the mediation of IRI was recently published (Schwaeble *et al.* 2011). The current work has now assessed these models of MASP-2 dependent lectin pathway deficiency in models of cerebral ischaemia.

6.2 Stroke

Stroke is the second leading cause of death worldwide after ischaemic heart disease, and the leading cause of permanent disability and morbidity leaving surviving patients with severe cognitive of physical impairments (Leys *et al.* 2005). The current stroke therapy is the application of recombinant tissue plasminogen activator (rTPA) which acts as a thrombolytic agent resolving the blood clot and thereby minimising the ischaemic insult to achieve better recovery.

6.3 Study Strategy

The previous chapter has clearly demonstrated that MASP-2 deficiency reveals a protective phenotype following cerebral IRI. In order to assess the therapeutic utility of MASP-2 inhibition, MASP-2 depleting antibodies were used to treat wild type mice to block lectin pathway activation with assessment of the outcome of this treatment by comparing cerebral infarct sizes between MASP-2 depleted and isotype control treated MASP-2 sufficient controls. MASP-2 has also recently been shown to be involved in

clotting events (Gulla *et al.* 2010), irrespective of complement activation. However, the present view point is that lectin pathway inhibition reduces the detrimental inflammatory secondary damage in the tissue to allow a better recovery of cells affected by ischaemia. This therapeutic strategy could complement thrombolytic therapies to give extra protection from secondary cerebral IRI during reperfusion of the ischaemic tissue.

6.4 Inhibitory MASP-2 antibodies and outcome

Initial experiments were performed using MASP-2 inhibitory antibodies (anti-mouse MASP-2 and anti-human MASP-2) administered i.p. to C57/BL6J female mice at a relatively low concentration of 1mg/kg. Although *in vitro* this antibody concentration was sufficient to inhibit lectin pathway functional activity on mannan coated ELISA plates, the results of this pilot study of low dose MASP-2 antibody treated mice, in comparison to isotype control antibody treated mice or the saline control group, failed to reveal statistically significant differences in the size of cerebral infarcts. Analysis of the residual lectin pathway functional activity in sera of low dose anti MASP-2 antibody treated mice revealed that this dosing failed to ablate lectin pathway activity efficiently and therefore a second experimental series was started using a higher dose (5mg/kg) of the inhibitory anti-murine MASP-2 antibody and its respective control in the 3-VO model of stroke. Inhibition of MASP-2 functional activity with the higher dosing of the AbD04211 therapeutic antibody was shown to successfully block lectin pathway activation *in vivo*. In more detail, the results showed that the administration of the murine anti-MASP-2 antibody (5mg/kg), was blocking lectin pathway functional activity as assessed by C3 deposition on mannan with a sustained significant reduction

(up to 66 h) in lectin pathway activity. The reduction of inhibitory activity may either be due to clearance of the antibody from the body and/ or by the replacement of MASP-2 through ongoing biosynthesis. As shown before in the MASP-2 deficient mouse line, the MASP-2 depleted mice presented with significantly smaller infarct sizes compared to the MASP-2 sufficient mice treated with either the isotype antibody or saline alone. Therapeutic MASP-2 inhibition yielded a reduction of lesion volume by about 30%. Such a reduction in CNS tissue loss would certainly improve patient recovery following stroke.

6.5 The complement system in stroke therapeutics

The results of this study are in good agreement with previous studies using MBL null mice. These studies revealed a reduction of infarct sizes when compared to WT controls in the cortical and subcortical regions using the MCAO model of stroke. Along with reduced infarct sizes a reduced neutrophil infiltration and C3 deposition was also observed indicative of a reduced inflammatory response in MBL null mice (Cervera *et al.* 2010). In another study, a synthesised mannosylated molecule called polyman2, that binds MBL and therefore acts as a competitive inhibitor of MBL, was also found to be protective in mice when polyman2 was administered up to 24 h after ischaemia (Orsini *et al.* 2012). The same study demonstrated that an anti-MBL-A antibody had a long lasting protective effect reflected by smaller infarct volume and improved neurological deficits when given up to 18 h after cerebral ischaemia. These data support a wide therapeutic window for intervention and much greater than the 4 hour window for the current tPA therapy (Orsini *et al.* 2012).

In a study using C1-inhibitor it was shown that C1-inhibitor wild type treated mice, as well as C1-inhibitor C1q -/- treated mice, were appearing with significantly reduced lesion volumes when compared to wild type controls, while untreated C1q -/- mice revealed a non significant reduction of infarct sizes compared to wild type control mice in an MCAO model of stroke. (De Simoni *et al.* 2004). This indicated a C1q independent mechanism of cerebral IRI induction. Furthermore, unpublished data (W. Schwaeble, unpublished data) using C1q -/- mice in an MCAO model of stroke actually revealed that C1q-/- mice had significantly increased infarct volumes when compared to wild type controls, indicating that C1q is neuroprotective in cerebral IRI and loss leads to a worse outcome. These studies show that most probably the classical pathway does not play a direct role in cerebral IRI. Studies on the involvement of the alternative pathway (AP) in IRI have identified that the AP has an amplifying, rather the initiating role, in the pathophysiology of complement-mediated tissue damage. This aggravating contribution was recently shown using factor B deficient mice and mice treated with the alternative pathway inhibitor CR2-fH in an MCAO model of stroke resulting in reduced infarct volumes, better neurological outcome and reduced neutrophil infiltration in both factor B -/- and CR2-fH treated mice compared to control animals (Elvington *et al.* 2012).

It has become clear that targeting the MASP-2 driven effector lectin pathway is the only efficient approach to target complement-dependent IRI. Targeting MASP-1 and MASP-3 is unlikely to be efficient in preventing IRI since MASP-1/3 deficient mice are not protected (Farrar *et al.* 2012). Targeting MASP-2 is advantageous in order to achieve an efficient, rapid and systemic depletion of lectin pathway functional activity and make it superior to the other so far reported therapeutic approaches in preventing

lectin pathway driven IRI (Gorsuch *et al.* 2012). MASP-2 is present at a very low plasma concentration of approximately 0.4 μg/ml in comparison to MASP-1 (11 μg/ml), MASP-3 (5 μg/ml), MBL (1.1 μg/ml), H-ficolin (19.5 μg/ml), M-ficolin (1.4 μg/ml), L-ficolin (3.4 μg/ml) and CL-11 (2.1 μg/ml) (Thiel *et al.* 2012). The MASP-2 gene is not an acute phase gene that rapidly increases biosynthesis in response to inflammatory stimuli and there is no extra hepatic biosynthesis as its promoter region contains regulatory elements that allow expression in highly specialised hepatic cells only (Stover *et al.* 1999b, Endo *et al.* 2002). MBL-C and MBL-A have also been recorded to be up-regulated in liver as a result of cerebral ischaemia and reperfusion injury (Morrison *et al.* 2011).

6.6 MASP-2 and coagulation

The interaction of MASP-2 with the coagulation system was recently suggested in a study in which it was shown that MASP-2 was capable of prothrombin cleavage with the resulting formation of thrombin promoting the fibrinogen turnover important in cross linked fibrin formation (Krarup *et al.* 2007). MASP-2 was also found in another study to promote fibrin clot formation (Gulla *et al.* 2010).This is an area of ongoing research and there are clear present indications that MASP-2 functional activity not only drives complement activation but additionally promotes thrombosis (Schwaeble et al, unpublished data). Further work is required to fully understand to what extent MASP-2 driven formation of microthrombi contributes to the IRI phenotype. Therefore, it would be very interesting to investigate in any IRI as to whether depletion of MASP-2 could interfere with the coagulation cascade and aid blood clot clearance while in the meantime limiting the inflammatory reactions leading to tissue injury. The same stands

for cerebral IRI as reduction of inflammation combined with thrombolysis by targeting the same agent would be beneficial for ischaemic strokes. However especial care would need to be taken in the case of haemorrhagic strokes.

6.7 Conclusion

In conclusion this study underlines that MASP-2 inhibition is a very promising therapeutic approach to limit IRI-mediated tissue and function loss. Future studies will address the therapeutic window for intervention in order to reduce morbidity and mortality in ischaemic human disease. These studies would involve administration of the inhibitory MASP-2 antibody at different time points after ischaemia and reperfusion and assessment of the cerebral damage.

Chapter 7: Summary

This thesis has assessed the impact of MASP-2 deficiency and MASP-2 depletion in experimental models of cerebral ischaemia and reperfusion injury. The experimental findings described in this thesis revealed the following:

- The temporary 3 vessel occlusion (3-VO) model of stroke for 30 min of ischaemia followed by 24 h of reperfusion proved to be the most appropriate model for these studies, with a significantly lower degree of variability compared to the middle cerebral artery occlusion (MCAO) (for 1 h of ischaemia followed by 24 h of reperfusion). The 3-VO model generated reproducible infarct sizes and sustainable cerebral blood flow (CBF) throughout the ischaemic and reperfusion time. The 3-VO model did not show the high degree of variability in the CBF profiles that were observed when using the MCAO stroke model. The variable infarct sizes that the MCAO model generated also precluded the use of the MCAO model to study the role of the lectin pathway in cerebral ischaemia and reperfusion injury.

- MASP-2 deficient mice undergoing the temporary 3-VO procedure presented with statistically significant smaller infarct sizes (i.e. 30%) compared to the infarct sizes seen in matched wild type control mice. C3c deposition was reduced in MASP-2 deficient mice compared to MASP-2 sufficient mice while the abundance of GFAP in astrocytes was significantly higher in the MASP-2 sufficient wild type mice.

- In brains of MASP-2 deficient mice significantly lower mRNA expression profiles for mRNA encoding the pro-inflammatory cytokine MIP-2 were observed, while the same mice showed higher mRNA expression for the anti-inflammatory cytokine IL-10 compared to wild type mice. Cerebral C1q expression was induced in all 3-VO operated mice while no C1q biosynthesis was observed in sham operated mice. IL-6 mRNA abundance was also up-regulated and showed similar expression profiles in MASP-2 deficient mice as well as in MASP-2 sufficient WT mice.

- A series of experiments using an inhibitory recombinant antibody against murine MASP-2 (AbD04211) at concentrations of 1mg/kg and 5mg/kg were performed with wild type mice being given either the inhibitory antibody, or saline or an isotype control antibody by i.p. injection prior 3-VO surgery. The low dose (1mg/kg) antibody concentration proved to be insufficient to inhibit lectin pathway functional activity *in vivo,* resulting in statistically non significant differences in infarct sizes between inhibitory antibody treated mice and the control antibody treated mice or mice injected with saline control. However, at a dose of 5mg/kg, AbD04211 inhibited lectin pathway functional activity both *in vitro* as well as *in vivo,* revealing a statistically significant reduction in infarct sizes (i.e. by approximately 30% reduction in infarct size) in animals treated with the MASP-2 inhibitory antibody compared to the control antibody treated animals. This demonstrated that similar levels of protection from cerebral ischaemia and reperfusion injury can be achieved by using a therapeutic inhibitory anti-MASP-2 antibody as the degree of protection seen in MASP-2 deficient mice.

- Finally, this study revealed that MASP-2 inhibition may present a novel therapeutic strategy to limit loss of CNS tissue and CNS function by limiting cerebral ischaemia and reperfusion injury following stroke. Future studies will direct towards examining the broadness of the therapeutic window of intervention that MASP-2 can be targeted.

Chapter 8: References

Arora, M., Munoz, E. and Tenner, A.J., 2001. Identification of a site on mannan-binding lectin critical for enhancement of phagocytosis. *J.Biol.Chem.,* **276,** 43087-43094.

Barrett-Connor, E. & Bush, T.L., 1991. Estrogen and coronary heart disease in women. *JAMA,* **265,** 1861-1867.

Barrington, R.A., Pozdnyakova, O., Zafari, M.R., Benjamin, C.D. and Carroll, M.C., 2002. B lymphocyte memory: role of stromal cell complement and FcgammaRIIB receptors. *J.Exp.Med.,* **196,** 1189-1199.

Bederson, J.B., Pitts, L.H., Germano, S.M., Nishimura, M.C., Davis, R.L. and Bartkowski, H.M., 1986. Evaluation of 2,3,5-triphenyltetrazolium chloride as a stain for detection and quantification of experimental cerebral infarction in rats. *Stroke,* **17,** 1304-1308.

Blom, A.M., Villoutreix, B.O. and Dahlback, B., 2004. Complement inhibitor C4b-binding protein-friend or foe in the innate immune system? *Mol.Immunol.,* **40,** 1333-1346.

Bokisch, V.A. & Muller-Eberhard, H.J., 1970. Anaphylatoxin inactivator of human plasma: its isolation and characterization as a carboxypeptidase. *J.Clin.Invest.,* **49,** 2427-2436.

Boycott, H.E., Wilkinson, J.A., Boyle, J.P., Pearson, H.A. and Peers, C., 2008. Differential involvement of TNF alpha in hypoxic suppression of astrocyte glutamate transporters. *Glia,* **56,** 998-1004.

Brouns, R. & De Deyn, P.P., 2009. The complexity of neurobiological processes in acute ischemic stroke. *Clin.Neurol.Neurosurg.,* **111,** 483-495.

Cervera, A., Planas, A.M., Justicia, C., Urra, X., Jensenius, J.C., Torres, F., Lozano, F. and Chamorro, A., 2010. Genetically-defined deficiency of mannose-binding lectin is associated with protection after experimental stroke in mice and outcome in human stroke. *PLoS One,* **5,** e8433.

Champlin, A.K., 1971. Suppression of oestrus in grouped mice: the effects of various densities and the possible nature of the stimulus. *J.Reprod.Fertil.,* **27,** 233-241.

Chan, P.H., 2001. Reactive oxygen radicals in signaling and damage in the ischemic brain. *J.Cereb.Blood Flow Metab.,* **21,** 2-14.

Chen, C., Hu, Q., Yan, J., Yang, X., Shi, X., Lei, J., Chen, L., Huang, H., Han, J., Zhang, J.H. and Zhou, C., 2009. Early inhibition of HIF-1alpha with small interfering RNA reduces ischemic-reperfused brain injury in rats. *Neurobiol.Dis.,* **33,** 509-517.

Chen, C.B. & Wallis, R., 2004. Two mechanisms for mannose-binding protein modulation of the activity of its associated serine proteases. *J.Biol.Chem.,* **279,** 26058-26065.

Chen, C.H., Lam, C.F. and Boackle, R.J., 1998. C1 inhibitor removes the entire C1qr2s2 complex from anti-C1Q monoclonal antibodies with low binding affinities. *Immunology,* **95,** 648-654.

Chen, M., Lu, T.J., Chen, X.J., Zhou, Y., Chen, Q., Feng, X.Y., Xu, L., Duan, W.H. and Xiong, Z.Q., 2008. Differential roles of NMDA receptor subtypes in ischemic neuronal cell death and ischemic tolerance. *Stroke,* **39,** 3042-3048.

Choi, D.W. & Rothman, S.M., 1990. The role of glutamate neurotoxicity in hypoxic-ischemic neuronal death. *Annu.Rev.Neurosci.,* **13,** 171-182.

Chong, Z.Z., Xu, Q.P. and Sun, J.N., 2001. Effects and mechanisms of triacetylshikimic acid on platelet adhesion to neutrophils induced by thrombin and reperfusion after focal cerebral ischemia in rats. *Acta Pharmacol.Sin.,* **22,** 679-684.

Cicardi, M., Zingale, L., Zanichelli, A., Pappalardo, E. and Cicardi, B., 2005. C1 inhibitor: molecular and clinical aspects. *Springer Semin.Immunopathol.,* **27,** 286-298.

Clark, W., Gunion-Rinker, L., Lessov, N. and Hazel, K., 1998. Citicoline treatment for experimental intracerebral hemorrhage in mice. *Stroke,* **29,** 2136-2140.

Cojocaru, I.M., Cojocaru, M., Tanasescu, R., Iliescu, I., Dumitrescu, L. and Silosi, I., 2009. Expression of IL-6 activity in patients with acute ischemic stroke. *Rom.J.Intern.Med.,* **47,** 393-396.

Connolly, E.S.,Jr, Winfree, C.J., Springer, T.A., Naka, Y., Liao, H., Yan, S.D., Stern, D.M., Solomon, R.A., Gutierrez-Ramos, J.C. and Pinsky, D.J., 1996. Cerebral protection in homozygous null ICAM-1 mice after middle cerebral artery occlusion. Role of neutrophil adhesion in the pathogenesis of stroke. *J.Clin.Invest.,* **97,** 209-216.

Crane, J.W., Baiquni, G.P., Sullivan, R.K., Lee, J.D., Sah, P., Taylor, S.M., Noakes, P.G. and Woodruff, T.M., 2009. The C5a anaphylatoxin receptor CD88 is expressed in presynaptic terminals of hippocampal mossy fibres. *J.Neuroinflammation,* **6,** 34-2094-6-34.

Dahl, M.R., Thiel, S., Matsushita, M., Fujita, T., Willis, A.C., Christensen, T., Vorup-Jensen, T. and Jensenius, J.C., 2001. MASP-3 and its association with distinct complexes of the mannan-binding lectin complement activation pathway. *Immunity,* **15,** 127-135.

Dallas, M., Boycott, H.E., Atkinson, L., Miller, A., Boyle, J.P., Pearson, H.A. and Peers, C., 2007. Hypoxia suppresses glutamate transport in astrocytes. *J.Neurosci.,* **27,** 3946-3955.

D'Ambrosio, A.L., Pinsky, D.J. and Connolly, E.S., 2001. The role of the complement cascade in ischemia/reperfusion injury: implications for neuroprotection. *Mol.Med.,* **7,** 367-382.

De Simoni, M.G., Rossi, E., Storini, C., Pizzimenti, S., Echart, C. and Bergamaschini, L., 2004. The powerful neuroprotective action of C1-inhibitor on brain ischemia-reperfusion injury does not require C1q. *Am.J.Pathol.,* **164,** 1857-1863.

de Vries, B., Walter, S.J., Peutz-Kootstra, C.J., Wolfs, T.G., van Heurn, L.W. and Buurman, W.A., 2004. The mannose-binding lectin-pathway is involved in complement activation in the course of renal ischemia-reperfusion injury. *Am.J.Pathol.,* **165,** 1677-1688.

Di Napoli, M., 2001. Systemic complement activation in ischemic stroke. *Stroke,* **32,** 1443-1448.

Diepenhorst, G.M., van Gulik, T.M. and Hack, C.E., 2009. Complement-mediated ischemia-reperfusion injury: lessons learned from animal and clinical studies. *Ann.Surg.,* **249,** 889-899.

Dirnagl, U., Iadecola, C. and Moskowitz, M.A., 1999. Pathobiology of ischaemic stroke: an integrated view. *Trends Neurosci.,* **22,** 391-397.

Dodds, A.W., 2002. Which came first, the lectin/classical pathway or the alternative pathway of complement? *Immunobiology,* **205,** 340-354.

Donnan, G.A., Fisher, M., Macleod, M. and Davis, S.M., 2008. Stroke. *Lancet,* **371,** 1612-1623.

Drickamer, K. & Taylor, M.E., 1993. Biology of animal lectins. *Annu.Rev.Cell Biol.,* **9,** 237-264.

Dunkelberger, J.R. & Song, W.C., 2010. Complement and its role in innate and adaptive immune responses. *Cell Res.,* **20,** 34-50.

Elvington, A., Atkinson, C., Zhu, H., Yu, J., Takahashi, K., Stahl, G.L., Kindy, M.S. and Tomlinson, S., 2012. The alternative complement pathway propagates inflammation and injury in murine ischemic stroke. *J.Immunol.,* **189,** 4640-4647.

Endo, Y., Nakazawa, N., Liu, Y., Iwaki, D., Takahashi, M., Fujita, T., Nakata, M. and Matsushita, M., 2005. Carbohydrate-binding specificities of mouse ficolin A, a splicing variant of ficolin A and ficolin B and their complex formation with MASP-2 and sMAP. *Immunogenetics,* **57,** 837-844.

Endo, Y., Takahashi, M., Kuraya, M., Matsushita, M., Stover, C.M., Schwaeble, W.J. and Fujita, T., 2002. Functional characterization of human mannose-binding lectin-associated serine protease (MASP)-1/3 and MASP-2 promoters, and comparison with the C1s promoter. *Int.Immunol.,* **14,** 1193-1201.

Eng, L.F., Ghirnikar, R.S. and Lee, Y.L., 2000. Glial fibrillary acidic protein: GFAP-thirty-one years (1969-2000). *Neurochem.Res.,* **25,** 1439-1451.

Engel, O., Kolodziej, S., Dirnagl, U. and Prinz, V., 2011. Modeling stroke in mice - middle cerebral artery occlusion with the filament model. *J.Vis.Exp.,* **(47). pii: 2423. doi,** 10.3791/2423.

Fan, R. & Tenner, A.J., 2004. Complement C1q expression induced by Abeta in rat hippocampal organotypic slice cultures. *Exp.Neurol.,* **185,** 241-253.

Farkas, I., Baranyi, L., Ishikawa, Y., Okada, N., Bohata, C., Budai, D., Fukuda, A., Imai, M. and Okada, H., 2002. CD59 blocks not only the insertion of C9 into MAC but inhibits ion channel formation by homologous C5b-8 as well as C5b-9. *J.Physiol.,* **539,** 537-545.

Farrar, C.A., Asgari, E., Schwaeble, W.J. and Sacks, S.H., 2012. Which pathways trigger the role of complement in ischaemia/reperfusion injury? *Front.Immunol.,* **3,** 341.

Farries, T.C., Lachmann, P.J. and Harrison, R.A., 1988. Analysis of the interaction between properdin and factor B, components of the alternative-pathway C3 convertase of complement. *Biochem.J.,* **253,** 667-675.

Fleischmann, J., Golde, D.W., Weisbart, R.H. and Gasson, J.C., 1986. Granulocyte-macrophage colony-stimulating factor enhances phagocytosis of bacteria by human neutrophils. *Blood,* **68,** 708-711.

Fleming, S.D., Shea-Donohue, T., Guthridge, J.M., Kulik, L., Waldschmidt, T.J., Gipson, M.G., Tsokos, G.C. and Holers, V.M., 2002. Mice deficient in complement receptors 1 and 2 lack a tissue injury-inducing subset of the natural antibody repertoire. *J.Immunol.,* **169,** 2126-2133.

Frijns, C.J. & Kappelle, L.J., 2002. Inflammatory cell adhesion molecules in ischemic cerebrovascular disease. *Stroke,* **33,** 2115-2122.

Fujita, T., Matsushita, M. and Endo, Y., 2004. The lectin-complement pathway--its role in innate immunity and evolution. *Immunol.Rev.,* **198,** 185-202.

Fust, G., Munthe-Fog, L., Illes, Z., Szeplaki, G., Molnar, T., Pusch, G., Hirschberg, K., Szegedi, R., Szeplaki, Z., Prohaszka, Z., Skjoedt, M.O. and Garred, P., 2011. Low ficolin-3 levels in early follow-up serum samples are associated with the severity and unfavorable outcome of acute ischemic stroke. *J.Neuroinflammation,* **8,** 185-2094-8-185.

Gibson, C.L., Bath, P.M. and Murphy, S.P., 2005. G-CSF reduces infarct volume and improves functional outcome after transient focal cerebral ischemia in mice. *J.Cereb.Blood Flow Metab.,* **25,** 431-439.

Gibson, C.L. & Murphy, S.P., 2004. Progesterone enhances functional recovery after middle cerebral artery occlusion in male mice. *J.Cereb.Blood Flow Metab.,* **24,** 805-813.

Goldberg, M., Fremeaux-Bacchi, V., Koch, P., Fishelson, Z. and Katz, Y., 2011. A novel mutation in the C3 gene and recurrent invasive pneumococcal infection: a clue for vaccine development. *Mol.Immunol.,* **48,** 1926-1931.

Gorsuch, W.B., Chrysanthou, E., Schwaeble, W.J. and Stahl, G.L., 2012. The complement system in ischemia-reperfusion injuries. *Immunobiology,* **217,** 1026-1033.

Gosset, P., Tillie-Leblond, I., Oudin, S., Parmentier, O., Wallaert, B., Joseph, M. and Tonnel, A.B., 1999. Production of chemokines and proinflammatory and antiinflammatory cytokines by human alveolar macrophages activated by IgE receptors. *J.Allergy Clin.Immunol.,* **103,** 289-297.

Gulla, K.C., Gupta, K., Krarup, A., Gal, P., Schwaeble, W.J., Sim, R.B., O'Connor, C.D. and Hajela, K., 2010. Activation of mannan-binding lectin-associated serine proteases leads to generation of a fibrin clot. *Immunology,* **129,** 482-495.

Hall, E.D. & Braughler, J.M., 1989. Central nervous system trauma and stroke. II. Physiological and pharmacological evidence for involvement of oxygen radicals and lipid peroxidation. *Free Radic.Biol.Med.,* **6,** 303-313.

Halterman, M.W. & Federoff, H.J., 1999. HIF-1alpha and p53 promote hypoxia-induced delayed neuronal death in models of CNS ischemia. *Exp.Neurol.,* **159,** 65-72.

Hamann, G.F., Okada, Y., Fitridge, R. and del Zoppo, G.J., 1995. Microvascular basal lamina antigens disappear during cerebral ischemia and reperfusion. *Stroke,* **26,** 2120-2126.

Hansen, S., Selman, L., Palaniyar, N., Ziegler, K., Brandt, J., Kliem, A., Jonasson, M., Skjoedt, M.O., Nielsen, O., Hartshorn, K., Jorgensen, T.J., Skjodt, K. and Holmskov, U., 2010. Collectin 11 (CL-11, CL-K1) is a MASP-1/3-associated plasma collectin with microbial-binding activity. *J.Immunol.,* **185,** 6096-6104.

Hart, M.L., Ceonzo, K.A., Shaffer, L.A., Takahashi, K., Rother, R.P., Reenstra, W.R., Buras, J.A. and Stahl, G.L., 2005. Gastrointestinal ischemia-reperfusion injury is lectin complement pathway dependent without involving C1q. *J.Immunol.,* **174,** 6373-6380.

Hochreiter-Hufford, A. & Ravichandran, K.S., 2013. Clearing the dead: apoptotic cell sensing, recognition, engulfment, and digestion. *Cold Spring Harb Perspect.Biol.,* **5,** 10.1101/cshperspect.a008748.

Horner, P.J. & Gage, F.H., 2000. Regenerating the damaged central nervous system. *Nature,* **407,** 963-970.

Huber, J.D., Egleton, R.D. and Davis, T.P., 2001. Molecular physiology and pathophysiology of tight junctions in the blood-brain barrier. *Trends Neurosci.,* **24,** 719-725.

Iwaki, D., Kanno, K., Takahashi, M., Endo, Y., Matsushita, M. and Fujita, T., 2011. The role of mannose-binding lectin-associated serine protease-3 in activation of the alternative complement pathway. *J.Immunol.,* **187,** 3751-3758.

Kahle, K.T., Simard, J.M., Staley, K.J., Nahed, B.V., Jones, P.S. and Sun, D., 2009. Molecular mechanisms of ischemic cerebral edema: role of electroneutral ion transport. *Physiology (Bethesda),* **24,** 257-265.

Kainulainen, L., Peltola, V., Seppanen, M., Viander, M., He, Q., Lokki, M.L. and Ruuskanen, O., 2012. C4A deficiency in children and adolescents with recurrent respiratory infections. *Hum.Immunol.,* **73,** 498-501.

Katsura, K., Kristian, T. and Siesjo, B.K., 1994. Energy metabolism, ion homeostasis, and cell damage in the brain. *Biochem.Soc.Trans.,* **22,** 991-996.

Kelly, P.J., Morrow, J.D., Ning, M., Koroshetz, W., Lo, E.H., Terry, E., Milne, G.L., Hubbard, J., Lee, H., Stevenson, E., Lederer, M. and Furie, K.L., 2008. Oxidative stress and matrix metalloproteinase-9 in acute ischemic stroke: the Biomarker Evaluation for Antioxidant Therapies in Stroke (BEAT-Stroke) study. *Stroke,* **39,** 100-104.

Keshi, H., Sakamoto, T., Kawai, T., Ohtani, K., Katoh, T., Jang, S.J., Motomura, W., Yoshizaki, T., Fukuda, M., Koyama, S., Fukuzawa, J., Fukuoh, A., Yoshida, I., Suzuki, Y. and Wakamiya, N., 2006. Identification and characterization of a novel human collectin CL-K1. *Microbiol.Immunol.,* **50,** 1001-1013.

Kimelberg, H.K., 2005. Astrocytic swelling in cerebral ischemia as a possible cause of injury and target for therapy. *Glia,* **50,** 389-397.

King, L.S. & Agre, P., 1996. Pathophysiology of the aquaporin water channels. *Annu.Rev.Physiol.,* **58,** 619-648.

Klein, R.J., Zeiss, C., Chew, E.Y., Tsai, J.Y., Sackler, R.S., Haynes, C., Henning, A.K., SanGiovanni, J.P., Mane, S.M., Mayne, S.T., Bracken, M.B., Ferris, F.L., Ott, J., Barnstable, C. and Hoh, J., 2005. Complement factor H polymorphism in age-related macular degeneration. *Science,* **308,** 385-389.

Krarup, A., Wallis, R., Presanis, J.S., Gal, P. and Sim, R.B., 2007. Simultaneous activation of complement and coagulation by MBL-associated serine protease 2. *PLoS One,* **2,** e623.

Kwan, W.H., van der Touw, W. and Heeger, P.S., 2012. Complement regulation of T cell immunity. *Immunol.Res.,* **54,** 247-253.

Le Friec, G. & Kemper, C., 2009. Complement: coming full circle. *Arch.Immunol.Ther.Exp.(Warsz),* **57,** 393-407.

Lee, B.H., Kwak, S.H., Shin, J.I., Lee, S.H., Choi, H.J., Kang, H.G., Ha, I.S., Lee, J.S., Dragon-Durey, M.A., Choi, Y. and Cheong, H.I., 2009. Atypical hemolytic uremic syndrome associated with complement factor H autoantibodies and CFHR1/CFHR3 deficiency. *Pediatr.Res.,* **66,** 336-340.

Lee, J.M., Grabb, M.C., Zipfel, G.J. and Choi, D.W., 2000. Brain tissue responses to ischemia. *J.Clin.Invest.,* **106,** 723-731.

Lehto, T., Morgan, B.P. and Meri, S., 1997. Binding of human and rat CD59 to the terminal complement complexes. *Immunology,* **90,** 121-128.

Leys, D., Henon, H., Mackowiak-Cordoliani, M.A. and Pasquier, F., 2005. Poststroke dementia. *Lancet Neurol.,* **4,** 752-759.

Liang, D., Bhatta, S., Gerzanich, V. and Simard, J.M., 2007. Cytotoxic edema: mechanisms of pathological cell swelling. *Neurosurg.Focus.,* **22,** E2.

Lin, T.N., He, Y.Y., Wu, G., Khan, M. and Hsu, C.Y., 1993. Effect of brain edema on infarct volume in a focal cerebral ischemia model in rats. *Stroke,* **24,** 117-121.

Lippold, H.J., 1982. Quantitative succinic dehydrogenases histochemistry. A comparison of different tetrazolium salts. *Histochemistry,* **76,** 381-405.

Liu, H., Jensen, L., Hansen, S., Petersen, S.V., Takahashi, K., Ezekowitz, A.B., Hansen, F.D., Jensenius, J.C. and Thiel, S., 2001. Characterization and quantification of mouse mannan-binding lectins (MBL-A and MBL-C) and study of acute phase responses. *Scand.J.Immunol.,* **53,** 489-497.

Livnat, A., Barbiro-Michaely, E. and Mayevsky, A., 2010. Mitochondrial function and cerebral blood flow variable responses to middle cerebral artery occlusion. *J.Neurosci.Methods,* **188,** 76-82.

Lu, J.H., Thiel, S., Wiedemann, H., Timpl, R. and Reid, K.B., 1990. Binding of the pentamer/hexamer forms of mannan-binding protein to zymosan activates the proenzyme C1r2C1s2 complex, of the classical pathway of complement, without involvement of C1q. *J.Immunol.,* **144,** 2287-2294.

Lublin, D.M. & Atkinson, J.P., 1989. Decay-accelerating factor: biochemistry, molecular biology, and function. *Annu.Rev.Immunol.,* **7,** 35-58.

Lundgren, J., Zhang, H., Agardh, C.D., Smith, M.L., Evans, P.J., Halliwell, B. and Siesjo, B.K., 1991. Acidosis-induced ischemic brain damage: are free radicals involved? *J.Cereb.Blood Flow Metab.,* **11,** 587-596.

Lynch, N.J., Willis, C.L., Nolan, C.C., Roscher, S., Fowler, M.J., Weihe, E., Ray, D.E. and Schwaeble, W.J., 2004. Microglial activation and increased synthesis of complement component C1q precedes blood-brain barrier dysfunction in rats. *Mol.Immunol.,* **40,** 709-716.

Martin, R.L., Lloyd, H.G. and Cowan, A.I., 1994. The early events of oxygen and glucose deprivation: setting the scene for neuronal death? *Trends Neurosci.,* **17,** 251-257.

Matsuo, Y., Onodera, H., Shiga, Y., Nakamura, M., Ninomiya, M., Kihara, T. and Kogure, K., 1994. Correlation between myeloperoxidase-quantified neutrophil accumulation and ischemic brain injury in the rat. Effects of neutrophil depletion. *Stroke,* **25,** 1469-1475.

Matsushita, M. & Fujita, T., 1995. Cleavage of the third component of complement (C3) by mannose-binding protein-associated serine protease (MASP) with subsequent complement activation. *Immunobiology,* **194,** 443-448.

Matsushita, M. & Fujita, T., 1992. Activation of the classical complement pathway by mannose-binding protein in association with a novel C1s-like serine protease. *J.Exp.Med.,* **176,** 1497-1502.

Mayilyan, K.R., Arnold, J.N., Presanis, J.S., Soghoyan, A.F. and Sim, R.B., 2006. Increased complement classical and mannan-binding lectin pathway activities in schizophrenia. *Neurosci.Lett.,* **404,** 336-341.

McColl, B.W., Rothwell, N.J. and Allan, S.M., 2007. Systemic inflammatory stimulus potentiates the acute phase and CXC chemokine responses to experimental stroke and exacerbates brain damage via interleukin-1- and neutrophil-dependent mechanisms. *J.Neurosci.,* **27,** 4403-4412.

Meldrum, B., Evans, M., Griffiths, T. and Simon, R., 1985. Ischaemic brain damage: the role of excitatory activity and of calcium entry. *Br.J.Anaesth.,* **57,** 44-46.

Morrison, H., Frye, J., Davis-Gorman, G., Funk, J., McDonagh, P., Stahl, G. and Ritter, L., 2011. The contribution of mannose binding lectin to reperfusion injury after ischemic stroke. *Curr.Neurovasc Res.,* **8,** 52-63.

Mullen, R.J., Buck, C.R. and Smith, A.M., 1992. NeuN, a neuronal specific nuclear protein in vertebrates. *Development,* **116,** 201-211.

Muller-Eberhard, H.J., 1988. Molecular organization and function of the complement system. *Annu.Rev.Biochem.,* **57,** 321-347.

Murray, C.J. & Lopez, A.D., 1997. Mortality by cause for eight regions of the world: Global Burden of Disease Study. *Lancet,* **349,** 1269-1276.

Ohsawa, K., Imai, Y., Kanazawa, H., Sasaki, Y. and Kohsaka, S., 2000. Involvement of Iba1 in membrane ruffling and phagocytosis of macrophages/microglia. *J.Cell.Sci.,* **113 (Pt 17),** 3073-3084.

Ohtsuka, Y., Lee, J., Stamm, D.S. and Sanderson, I.R., 2001. MIP-2 secreted by epithelial cells increases neutrophil and lymphocyte recruitment in the mouse intestine. *Gut,* **49,** 526-533.

Ooboshi, H., Ibayashi, S., Shichita, T., Kumai, Y., Takada, J., Ago, T., Arakawa, S., Sugimori, H., Kamouchi, M., Kitazono, T. and Iida, M., 2005. Postischemic gene transfer of interleukin-10 protects against both focal and global brain ischemia. *Circulation,* **111,** 913-919.

Orsini, F., Villa, P., Parrella, S., Zangari, R., Zanier, E.R., Gesuete, R., Stravalaci, M., Fumagalli, S., Ottria, R., Reina, J.J., Paladini, A., Micotti, E., Ribeiro-Viana, R., Rojo, J., Pavlov, V.I., Stahl, G.L., Bernardi, A., Gobbi, M. and De Simoni, M.G., 2012.

Targeting mannose-binding lectin confers long-lasting protection with a surprisingly wide therapeutic window in cerebral ischemia. *Circulation,* **126,** 1484-1494.

Osthoff, M., Katan, M., Fluri, F., Schuetz, P., Bingisser, R., Kappos, L., Steck, A.J., Engelter, S.T., Mueller, B., Christ-Crain, M. and Trendelenburg, M., 2011. Mannose-binding lectin deficiency is associated with smaller infarction size and favorable outcome in ischemic stroke patients. *PLoS One,* **6,** e21338.

Otto, V.I., Heinzel-Pleines, U.E., Gloor, S.M., Trentz, O., Kossmann, T. and Morganti-Kossmann, M.C., 2000. sICAM-1 and TNF-alpha induce MIP-2 with distinct kinetics in astrocytes and brain microvascular endothelial cells. *J.Neurosci.Res.,* **60,** 733-742.

Paciaroni, M., Caso, V. and Agnelli, G., 2009. The concept of ischemic penumbra in acute stroke and therapeutic opportunities. *Eur.Neurol.,* **61,** 321-330.

Palarasah, Y., Skjodt, K., Brandt, J., Teisner, B., Koch, C., Vitved, L. and Skjoedt, M.O., 2010. Generation of a C3c specific monoclonal antibody and assessment of C3c as a putative inflammatory marker derived from complement factor C3. *J.Immunol.Methods,* **362,** 142-150.

Pangburn, M.K., Pangburn, K.L., Koistinen, V., Meri, S. and Sharma, A.K., 2000. Molecular mechanisms of target recognition in an innate immune system: interactions among factor H, C3b, and target in the alternative pathway of human complement. *J.Immunol.,* **164,** 4742-4751.

Parker, C., 2009. Eculizumab for paroxysmal nocturnal haemoglobinuria. *Lancet,* **373,** 759-767.

Pham, C.T., 2006. Neutrophil serine proteases: specific regulators of inflammation. *Nat.Rev.Immunol.,* **6,** 541-550.

Phillips, A.E., Toth, J., Dodds, A.W., Girija, U.V., Furze, C.M., Pala, E., Sim, R.B., Reid, K.B., Schwaeble, W.J., Schmid, R., Keeble, A.H. and Wallis, R., 2009. Analogous interactions in initiating complexes of the classical and lectin pathways of complement. *J.Immunol.,* **182,** 7708-7717.

Platts, S.H., Linden, J. and Duling, B.R., 2003. Rapid modification of the glycocalyx caused by ischemia-reperfusion is inhibited by adenosine A2A receptor activation. *Am.J.Physiol.Heart Circ.Physiol.,* **284,** H2360-7.

Podack, E.R., Muller-Eberhard, H.J., Horst, H. and Hoppe, W., 1982. Membrane attach complex of complement (MAC): three-dimensional analysis of MAC-phospholipid vesicle recombinants. *J.Immunol.,* **128,** 2353-2357.

Pradhan, V., Rajadhyaksha, A., Mahant, G., Surve, P., Patwardhan, M., Dighe, S. and Ghosh, K., 2012. Anti-C1q antibodies and their association with complement components in Indian systemic lupus erythematosus patients. *Indian.J.Nephrol.,* **22,** 353-357.

Presanis, J.S., Hajela, K., Ambrus, G., Gal, P. and Sim, R.B., 2004. Differential substrate and inhibitor profiles for human MASP-1 and MASP-2. *Mol.Immunol.,* **40,** 921-929.

Ram, S., Lewis, L.A. and Rice, P.A., 2010. Infections of people with complement deficiencies and patients who have undergone splenectomy. *Clin.Microbiol.Rev.,* **23,** 740-780.

Risitano, A.M., 2013. Paroxysmal nocturnal hemoglobinuria and the complement system: recent insights and novel anticomplement strategies. *Adv.Exp.Med.Biol.,* **734,** 155-172.

Rosenberg, G.A. & Yang, Y., 2007. Vasogenic edema due to tight junction disruption by matrix metalloproteinases in cerebral ischemia. *Neurosurg.Focus.,* **22,** E4.

Rossi, D.J., Brady, J.D. and Mohr, C., 2007. Astrocyte metabolism and signaling during brain ischemia. *Nat.Neurosci.,* **10,** 1377-1386.

Rossi, D.J., Oshima, T. and Attwell, D., 2000. Glutamate release in severe brain ischaemia is mainly by reversed uptake. *Nature,* **403,** 316-321.

Rossi, V., Cseh, S., Bally, I., Thielens, N.M., Jensenius, J.C. and Arlaud, G.J., 2001. Substrate specificities of recombinant mannan-binding lectin-associated serine proteases-1 and -2. *J.Biol.Chem.,* **276,** 40880-40887.

Schafer, M.K., Schwaeble, W.J., Post, C., Salvati, P., Calabresi, M., Sim, R.B., Petry, F., Loos, M. and Weihe, E., 2000. Complement C1q is dramatically up-regulated in brain microglia in response to transient global cerebral ischemia. *J.Immunol.,* **164,** 5446-5452.

Schmalstieg, F.C.,Jr & Goldman, A.S., 2010. Birth of the science of immunology. *J.Med.Biogr.,* **18,** 88-98.

Schwaeble, W., Dahl, M.R., Thiel, S., Stover, C. and Jensenius, J.C., 2002. The mannan-binding lectin-associated serine proteases (MASPs) and MAp19: four components of the lectin pathway activation complex encoded by two genes. *Immunobiology,* **205,** 455-466.

Schwaeble, W.J., Lynch, N.J., Clark, J.E., Marber, M., Samani, N.J., Ali, Y.M., Dudler, T., Parent, B., Lhotta, K., Wallis, R., Farrar, C.A., Sacks, S., Lee, H., Zhang, M., Iwaki, D., Takahashi, M., Fujita, T., Tedford, C.E. and Stover, C.M., 2011. Targeting of mannan-binding lectin-associated serine protease-2 confers protection from myocardial and gastrointestinal ischemia/reperfusion injury. *Proc.Natl.Acad.Sci.U.S.A.,* **108,** 7523-7528.

Schwaeble, W.J. & Reid, K.B., 1999. Does properdin crosslink the cellular and the humoral immune response? *Immunol.Today,* **20,** 17-21.

Selman, L. & Hansen, S., 2012. Structure and function of collectin liver 1 (CL-L1) and collectin 11 (CL-11, CL-K1). *Immunobiology,* **217,** 851-863.

Seya, T., Nakamura, K., Masaki, T., Ichihara-Itoh, C., Matsumoto, M. and Nagasawa, S., 1995. Human factor H and C4b-binding protein serve as factor I-cofactors both encompassing inactivation of C3b and C4b. *Mol.Immunol.,* **32,** 355-360.

Silva, M.T., 2009. When two is better than one: macrophages and neutrophils work in concert in innate immunity as complementary and cooperative partners of a myeloid phagocyte system. *J.Leukoc.Biol.,* .

Silver, I.A., Deas, J. and Erecinska, M., 1997. Ion homeostasis in brain cells: differences in intracellular ion responses to energy limitation between cultured neurons and glial cells. *Neuroscience,* **78,** 589-601.

Silver, J. & Miller, J.H., 2004. Regeneration beyond the glial scar. *Nat.Rev.Neurosci.,* **5,** 146-156.

Spera, P.A., Ellison, J.A., Feuerstein, G.Z. and Barone, F.C., 1998. IL-10 reduces rat brain injury following focal stroke. *Neurosci.Lett.,* **251,** 189-192.

Stengaard-Pedersen, K., Thiel, S., Gadjeva, M., Moller-Kristensen, M., Sorensen, R., Jensen, L.T., Sjoholm, A.G., Fugger, L. and Jensenius, J.C., 2003. Inherited deficiency of mannan-binding lectin-associated serine protease 2. *N.Engl.J.Med.,* **349,** 554-560.

Storini, C., Rossi, E., Marrella, V., Distaso, M., Veerhuis, R., Vergani, C., Bergamaschini, L. and De Simoni, M.G., 2005. C1-inhibitor protects against brain ischemia-reperfusion injury via inhibition of cell recruitment and inflammation. *Neurobiol.Dis.,* **19,** 10-17.

Stover, C.M., Schwaeble, W.J., Lynch, N.J., Thiel, S. and Speicher, M.R., 1999a. Assignment of the gene encoding mannan-binding lectin-associated serine protease 2 (MASP2) to human chromosome 1p36.3-->p36.2 by in situ hybridization and somatic cell hybrid analysis. *Cytogenet.Cell Genet.,* **84,** 148-149.

Stover, C.M., Thiel, S., Lynch, N.J. and Schwaeble, W.J., 1999b. The rat and mouse homologues of MASP-2 and MAp19, components of the lectin activation pathway of complement. *J.Immunol.,* **163,** 6848-6859.

Stover, C.M., Thiel, S., Thelen, M., Lynch, N.J., Vorup-Jensen, T., Jensenius, J.C. and Schwaeble, W.J., 1999c. Two constituents of the initiation complex of the mannan-binding lectin activation pathway of complement are encoded by a single structural gene. *J.Immunol.,* **162,** 3481-3490.

Suankratay, C., Zhang, Y., Jones, D., Lint, T.F. and Gewurz, H., 1999. Enhancement of lectin pathway haemolysis by immunoglobulins. *Clin.Exp.Immunol.,* **117,** 435-441.

Takada, F., Seki, N., Matsuda, Y., Takayama, Y. and Kawakami, M., 1995. Localization of the genes for the 100-kDa complement-activating components of Ra-reactive factor (CRARF and Crarf) to human 3q27-q28 and mouse 16B2-B3. *Genomics,* **25,** 757-759.

Takahashi, M., Ishida, Y., Iwaki, D., Kanno, K., Suzuki, T., Endo, Y., Homma, Y. and Fujita, T., 2010. Essential role of mannose-binding lectin-associated serine protease-1 in activation of the complement factor D. *J.Exp.Med.,* **207,** 29-37.

Takahashi, M., Iwaki, D., Kanno, K., Ishida, Y., Xiong, J., Matsushita, M., Endo, Y., Miura, S., Ishii, N., Sugamura, K. and Fujita, T., 2008. Mannose-binding lectin (MBL)-associated serine protease (MASP)-1 contributes to activation of the lectin complement pathway. *J.Immunol.,* **180,** 6132-6138.

Teillet, F., Dublet, B., Andrieu, J.P., Gaboriaud, C., Arlaud, G.J. and Thielens, N.M., 2005. The two major oligomeric forms of human mannan-binding lectin: chemical characterization, carbohydrate-binding properties, and interaction with MBL-associated serine proteases. *J.Immunol.,* **174,** 2870-2877.

Ten, V.S., Sosunov, S.A., Mazer, S.P., Stark, R.I., Caspersen, C., Sughrue, M.E., Botto, M., Connolly, E.S.,Jr and Pinsky, D.J., 2005. C1q-deficiency is neuroprotective against hypoxic-ischemic brain injury in neonatal mice. *Stroke,* **36,** 2244-2250.

Thiel, S., Jensen, L., Degn, S.E., Nielsen, H.J., Gal, P., Dobo, J. and Jensenius, J.C., 2012. Mannan-binding lectin (MBL)-associated serine protease-1 (MASP-1), a serine protease associated with humoral pattern-recognition molecules: normal and acute-phase levels in serum and stoichiometry of lectin pathway components. *Clin.Exp.Immunol.,* **169,** 38-48.

Thiel, S., Petersen, S.V., Vorup-Jensen, T., Matsushita, M., Fujita, T., Stover, C.M., Schwaeble, W.J. and Jensenius, J.C., 2000. Interaction of C1q and mannan-binding lectin (MBL) with C1r, C1s, MBL-associated serine proteases 1 and 2, and the MBL-associated protein MAp19. *J.Immunol.,* **165,** 878-887.

Thomas, A., Gasque, P., Vaudry, D., Gonzalez, B. and Fontaine, M., 2000. Expression of a complete and functional complement system by human neuronal cells in vitro. *Int.Immunol.,* **12,** 1015-1023.

Tomita, M., Holman, B.J., Santoro, C.P. and Santoro, T.J., 2005. Astrocyte production of the chemokine macrophage inflammatory protein-2 is inhibited by the spice principle curcumin at the level of gene transcription. *J.Neuroinflammation,* **2,** 8.

Turner, M.W., 1996. Mannose-binding lectin: the pluripotent molecule of the innate immune system. *Immunol.Today,* **17,** 532-540.

van Beek, J., Elward, K. and Gasque, P., 2003. Activation of complement in the central nervous system: roles in neurodegeneration and neuroprotection. *Ann.N.Y.Acad.Sci.,* **992,** 56-71.

Wagner, E. & Frank, M.M., 2010. Therapeutic potential of complement modulation. *Nat.Rev.Drug Discov.,* **9,** 43-56.

Wagner, S., Lynch, N.J., Walter, W., Schwaeble, W.J. and Loos, M., 2003. Differential expression of the murine mannose-binding lectins A and C in lymphoid and nonlymphoid organs and tissues. *J.Immunol.,* **170,** 1462-1465.

Wallis, R., 2007. Interactions between mannose-binding lectin and MASPs during complement activation by the lectin pathway. *Immunobiology,* **212,** 289-299.

Wallis, R. & Dodd, R.B., 2000. Interaction of mannose-binding protein with associated serine proteases: effects of naturally occurring mutations. *J.Biol.Chem.,* **275,** 30962-30969.

Wallis, R., Dodds, A.W., Mitchell, D.A., Sim, R.B., Reid, K.B. and Schwaeble, W.J., 2007. Molecular interactions between MASP-2, C4, and C2 and their activation fragments leading to complement activation via the lectin pathway. *J.Biol.Chem.,* **282,** 7844-7851.

Wallis, R. & Drickamer, K., 1999. Molecular determinants of oligomer formation and complement fixation in mannose-binding proteins. *J.Biol.Chem.,* **274,** 3580-3589.

Wallis, R., Shaw, J.M., Uitdehaag, J., Chen, C.B., Torgersen, D. and Drickamer, K., 2004. Localization of the serine protease-binding sites in the collagen-like domain of mannose-binding protein: indirect effects of naturally occurring mutations on protease binding and activation. *J.Biol.Chem.,* **279,** 14065-14073.

Walsh, M.C., Bourcier, T., Takahashi, K., Shi, L., Busche, M.N., Rother, R.P., Solomon, S.D., Ezekowitz, R.A. and Stahl, G.L., 2005. Mannose-binding lectin is a regulator of inflammation that accompanies myocardial ischemia and reperfusion injury. *J.Immunol.,* **175,** 541-546.

Wang, J.Y., Shum, A.Y., Chao, C.C., Kuo, J.S. and Wang, J.Y., 2000. Production of macrophage inflammatory protein-2 following hypoxia/reoxygenation in glial cells. *Glia,* **32,** 155-164.

Weiser, M.R., Williams, J.P., Moore, F.D.,Jr, Kobzik, L., Ma, M., Hechtman, H.B. and Carroll, M.C., 1996. Reperfusion injury of ischemic skeletal muscle is mediated by natural antibody and complement. *J.Exp.Med.,* **183,** 2343-2348.

Whaley, K. & Schwaeble, W., 1997. Complement and complement deficiencies. *Semin.Liver Dis.,* **17,** 297-310.

Williams, J.P., Pechet, T.T., Weiser, M.R., Reid, R., Kobzik, L., Moore, F.D.,Jr, Carroll, M.C. and Hechtman, H.B., 1999. Intestinal reperfusion injury is mediated by IgM and complement. *J.Appl.Physiol.,* **86,** 938-942.

Williams, T.J., 1983. Vascular permeability changes induced by complement-derived peptides. *Agents Actions,* **13,** 451-455.

Wirthmueller, U., Dewald, B., Thelen, M., Schafer, M.K., Stover, C., Whaley, K., North, J., Eggleton, P., Reid, K.B. and Schwaeble, W.J., 1997. Properdin, a positive regulator of complement activation, is released from secondary granules of stimulated peripheral blood neutrophils. *J.Immunol.,* **158,** 4444-4451.

Wu, J., Wu, Y.Q., Ricklin, D., Janssen, B.J., Lambris, J.D. and Gros, P., 2009. Structure of complement fragment C3b-factor H and implications for host protection by complement regulators. *Nat.Immunol.,* **10,** 728-733.

Yanamoto, H., Nagata, I., Niitsu, Y., Xue, J.H., Zhang, Z. and Kikuchi, H., 2003. Evaluation of MCAO stroke models in normotensive rats: standardized neocortical infarction by the 3VO technique. *Exp.Neurol.,* **182,** 261-274.

Zeller, J.A., Lenz, A., Eschenfelder, C.C., Zunker, P. and Deuschl, G., 2005. Platelet-leukocyte interaction and platelet activation in acute stroke with and without preceding infection. *Arterioscler.Thromb.Vasc.Biol.,* **25,** 1519-1523.

Zeller, J.A., Tschoepe, D. and Kessler, C., 1999. Circulating platelets show increased activation in patients with acute cerebral ischemia. *Thromb.Haemost.,* **81,** 373-377.

Zhang, M., Alicot, E.M., Chiu, I., Li, J., Verna, N., Vorup-Jensen, T., Kessler, B., Shimaoka, M., Chan, R., Friend, D., Mahmood, U., Weissleder, R., Moore, F.D. and Carroll, M.C., 2006. Identification of the target self-antigens in reperfusion injury. *J.Exp.Med.,* **203,** 141-152.

Zhang, M., Austen, W.G.,Jr, Chiu, I., Alicot, E.M., Hung, R., Ma, M., Verna, N., Xu, M., Hechtman, H.B., Moore, F.D.,Jr and Carroll, M.C., 2004. Identification of a specific self-reactive IgM antibody that initiates intestinal ischemia/reperfusion injury. *Proc.Natl.Acad.Sci.U.S.A.,* **101,** 3886-3891.

Zhang, M., Takahashi, K., Alicot, E.M., Vorup-Jensen, T., Kessler, B., Thiel, S., Jensenius, J.C., Ezekowitz, R.A., Moore, F.D. and Carroll, M.C., 2006. Activation of the lectin pathway by natural IgM in a model of ischemia/reperfusion injury. *J.Immunol.,* **177,** 4727-4734.

Zhao, Y. & Rempe, D.A., 2010. Targeting astrocytes for stroke therapy. *Neurotherapeutics,* **7,** 439-451.

Zhou, W., Patel, H., Li, K., Peng, Q., Villiers, M.B. and Sacks, S.H., 2006. Macrophages from C3-deficient mice have impaired potency to stimulate alloreactive T cells. *Blood,* **107,** 2461-2469.

Zundel, S., Cseh, S., Lacroix, M., Dahl, M.R., Matsushita, M., Andrieu, J.P., Schwaeble, W.J., Jensenius, J.C., Fujita, T., Arlaud, G.J. and Thielens, N.M., 2004. Characterization of recombinant mannan-binding lectin-associated serine protease (MASP)-3 suggests an activation mechanism different from that of MASP-1 and MASP-2. *J.Immunol.,* **172,** 4342-4350.

Books

Longmore, M., Wilkinson, I., Davidson, E., Foulkes, A., Mafi, A., 2010. Oxford Handbook of Clinical Medicine. (8th edition). *Oxford Medicine.,* **10,** 60.